GEOELECTRIC INVESTIGATION OF THE BASEMENT STRUCTURE AND GROUNDWATER POTENIAL OF THE UNIVERSITY OF JOS PERMANENT SITE.

BY

ZUME, JOSEPH TERZUNGWE
B.SC (HONS) PHYSICS

A THESIS SUBMITTED TO THE POSTGRADUATE SCHOOL, AHMADU BELLO UNIVERSITY ZARIA, IN PARTIAL FULFILMENT FOR THE AWARD OF THE DEGREE OF MASTER OF SCIENCE IN APPLIED GEOPHYSICS.

DEPARTMENT OF PHYSICS
FACULTY OF SCIENCE
AHMADU BELLO UNIVERSITY, ZARIA.

JULY, 1999.

DECLARATION

I hereby declare that, the work presented here, is an original work carried out by the author under the supervision of Dr. M.N Umego and prof. C. O. Ajayi.

As far as I know, no part of the work has been submitted elsewhere for the award of any degree.

All excerpts from works of others are duly acknowledged and referenced.

Zume, Joseph Terzungwe
Author
Ahmadu Bello University, Zaria.

23/7/99
Date

DEDICAION

This work is dedicated to my loving wife Blessing, and my two daughters, Ngodoo and Nguveren.

CERTIFICATION.

This thesis entitled: Geoelectric investigation of the basement structure and groundwater potential of the University of Jos permanent site by Zume, Joseph Terzungwe meets the regulations governing the award of the degree master of science (Applied Geophysics) of Ahmadu Bello University, and is approved for its contribution to knowledge and literary presentation.

Dr. M. N. Umego
Chairman, Supervisory Committee — Date 06/8/99.

Prof. C. O. Ajayi
Member, Supervisory Committee — Date 8/9/99

Prof. I. B. Osazuwa
Head, Department of Physics — Date 13/9/99

Prof. S. B. Ojo
Dean, Postgraduate School — Date 15/05/00

ACKNOWLEDGEMENT

I thank God Almighty for his mercies, protection and providence. His unfailing love saw me through this work.

I am most grateful to Dr M.N. Umego who supervised this work. He is indeed, a motivator, a delight to work with. His criticisms and useful suggestions contributed immeasurably to the successful completion of this work.

My sincere appreciation goes to Prof. C. O. Ajayi, who co - supervised this work. His experience in this field was a special asset to me. Sir, I can not thank you enough.

I also wish to express my sincere gratitude to Prof. I. B. Osazuwa, who was instrumental to my enrolment into the geophysics program. Sir your assistance was very much appreciated.

I must not forget the outstanding contributions of Prof. S. B. Ojo and Dr. P. sule, who taught me in the program.

To a special friend, Dr. A. A. Tarhule, I say, God bless you for the moral and financial support I recieved from you while on this study.

I appreciate the contributions made by friends like Ishaku Ziyock, S. O. Ibe, Basil Nwonsu, Mallam Jatau, Dogara Mato, Rose Nwosu(Mrs), Kola Lawal, Leonard Shilgba and Ajibade. May God bless you all.

My special thanks to my dear wife, Blessing, and my two daughters, Ngodoo and Nguveren for enduring hardships just to enable me complete my studies.

The encouragement I enjoyed from Dr. and Mrs Mailumo, Mr and Mrs Adeiyongo can never be forgotten.

I wish to acknowledge the cooperation and sponsorship I recieved from my employer, The University of Jos. My Head of Department, Dr. B. N. Gyang, has been particularly cooperative.

Finally, I remember my late parents,Mr Cyprain and Mrs Mbanengen Zume. Their foresight, love and care has been the cause of my joy today. Daddy and Mummy, it is unfortunate that you did not live long to reap what you sowed but I believe you are happier where you are. ADIEU.

ABSTRACT

A geoelectric investigation employing the conventional vertical electrical sounding (VES) as well as resistivity and electromagnetic profiling was carried out on the permanent site of the University of Jos. Twenty Six VES stations were occupied together with four resistivity Profiles as well as three EM Profiles. The survey was carried out to determine the basement structure and the groundwater potential of the area.

Interpretations of the VES data yielded results that were used to produce geoelectric and geologic sections. These together with the isoresistivity maps, were used to draw certain conclusions. There was good correlation between the profiling (Electrical resistivity and EM) and the VES results.

The results of the study indicate that the study area is underlain by 3 - 5 geoelectric layers. There is a thin superficial layer whose resistivity values range from 15 - 1500 ohm-m. The second, third, fourth and fifth layers have resistivity values ranging from 25 - 200 ohm-m, 201 - 500 ohm-m, 500 - 1000 ohm-m, and above 1000 ohm-m respectively.

The study also reveals that the aquifer system in the area occurs in the weathered and the fractured basement.

From the analysis of the bioelectric/geologic sections, the depth to basement map as well as the aquifer thickness map, the most favorable regions for groundwater exploitation in the area were found to be around VES 13, 10 19, 23, and VESl(in order of preference).

The depth to the basement map produced shows that the bedrock in the study area is undulating being deeper in the northern region. Furthermore, the map seem to suggest that the drainage pattern in the river Dilimi is structurally controlled.

TABLE OF CONTENTS

TABLE OF CONTENTS		PAGE
Title page		i
Declaration		ii
Dedication		iii
Certification		iv
Acknowledgement		v
Abstract		vii
Table of contents		viii
List of tables		xii
List of figures		xiii
List of Appendices		xv
Glossaries		xvi
CHAPTER 1 :	INTRODUCTION	1
1.1	General Introduction	1
1.2	Location and Accessibility	4
1.2.1	Relief and Drainage	6
1.2.2	Climate, Vegetation and Land use	7
1.3	Geology	8
1.3.1	Basement Complex	10
1.3.2	Younger Granites	11
1.3.3	Older Basalts and Old Alluvial Deposits	11
1.3.4	Weathered Zones and Newer Basalts	12
1.3.5	Hydrogeology	12

1.4 Previous Geophysical works. 14
1.5 Aim and scope of the study 16

CHAPTER 2: THEORY AND PRINCIPLES OF THE METHODS USED. . 17
2.1 General Remarks. 17
2.2 Theory of the D.C Resitivity Method. 17
2.2.1 The concept of apparent Resistivity 23
2.2.2 Factors affecting resistivity of Earth materials 24
2.2.3 Electrode layouts 25
2.3 Theory of the EM method 28
2.3.1 The EM 34-3 29

CHAPTER 3: INSTRUMENTATION AND FIELD PROCEDURES. . . 33
3.1 Abem Terameter SAS 300 33
3.2 The Geonics EM 34-3 35
3.3 Choice of Electode Configuration 36
3.4 Electrical Resistivity Data Collection 38
3.5 EM Data Collection 39

CHAPTER 4: INTERPRETATION TECHNIQUES AND DATA PROCESSING 40
4.1 VES Interpretation Method 40
4.1.1 Outline of the Zohdy Method 41
4.1.2 Initial Data Preparation 43
4.1.3 Iterative Procedure 43
4.1.4 Factors Affecting VES Interpretation 47

4.2 EM Interpretation Techniques 49

CHAPTER 5: INTERPRETATION 55
5.1 Introduction 55
5.2 Electrical Resistivity (ER) Profiling 56
5.2.1 Profile 1 58
5.2.2 Profile 2 60
5.2.3 Profile 3 62
5.2.4 Profile 4 62
5.3 Electromagnetic (EM) Profiling 65
5.3.1 Traverse 1 65
5.3.2 Traverse 2 67
5.3.3 Traverse 3 69
5.4 Qualitative Interpretation of VES Around Borehole Locations 71
5.4.1 Borehole No1 (BH.No,1) 71
5.4.2 Borehole No.2 (BH.No.2) 74
5.5 Electrical Resistivity Sounding 74
5.6 The Geoelectric and Geologic sections 78
5.6.1 Profile AA'. 78
5.6.2 Profile BB'. 81
5.6.3 Profile CC' 83
5.6.4 Profile DD' 86
5.7 Maps Production From the Interpreted Data 88
5.7.1 Isoresistivity Map of the surface layer. 88
5.7.2 Isoresistivity Contour Maps at Depth 91
5.7.3 Depth to Basement Map 103

5.7.4 Aquifer Thickness Map 103

CHAPTER 6: DISCUSSIONS, CONCLUSIONS and RECOMMENDATIONS 107

6.1 Discussion of Results 107

6.2 Limitations 109

6.3 Conclussions 110

6.4 Recommendations 111

REFERENCES 114

APPENDIX A 120

APPENDIX B 121

LIST OF TABLES

TABLE		PAGE
3.1	Exploration depth for EM34-3 at various intercoil spacings	35
5.10	Resistivity values for various rock and sediments in the basement complex	77
5.2	Resistivity values used in deriving the geoelectric sections in this work	77

LIST OF FIGURES

FIGURES		PAGE
1.1	Location map of the study area	5
1.2	Geological map of the study area	9
2.1a	Current and Potential distribution within a homogenous Isotropic ground	20
2.1b	A general electrode Configuration	20
2.2a	Wenner configuration	26
2.2b	Schlumberger configuration	26
2.3	Induced current flow (homogenous half space)	30
4.1	Indicated Vs true conductivity curve	50
4.2	Relative response "Vs" Depth	51
4.3	Vertical Dyke, effect of varying dip on profile shape	53
5.1a	Typical field curve	57
5.1b	True resistivity layer model.	57
5.2	Resistivity profile 1	59
5.3	Resistivity profile 2	61
5.4	Resistivity profile 3	63
5.5	Resistivity profile 4	64
5.6	EM traverse 1	66
5.7	EM traverse 2	68
5.8	EM traverse 3	70
5.9a	VES interpretation compared with borehole lithology (VES 5)	72
5.9b	VES interpretation compared with borehole lithology (VES 9)	73
5.10	Geoelectric and Geologic sections for profile AA'	79
5.11	Geoelectric and Geologic sections for profile BB'	82
5.12	Geoelectric and Geologic sections for profie CC'	84

5.13	Geoelectric and Geologic sections for profile DD'	87
5.14a	Isoresistivity contour map at the surface	89
5.14b	Isoresistivity contour map at 1m	92
5.14c	Isoresistivity contour map at 5m	93
5.14d	Isoresistivity contour map at 10m	94
5.14e	Isoresistivity contour map at 15m	96
5.14f	Isoresistivity contour map at 20m	97
5.14g	Isoresistivity contour map at 25m	98
5.14h	Isoresistivity contour map at 30m	99
5.14i	Isoresistivity contour map at 40m	100
5.14j	Isoresistivity contour map at 50m	101
5.14k	Isoresistivity contour map at 60m	102
5.15	Depth-to-basement contour map	104
5.16	Aquifer thickness contour map	105

APPENDIX A

Summay of the VES Interpretation 120

APPENDIX B

Field Curves and Interpreted True Resistivity Layer Models For the VES Measurement 121

GLOSSARIES

ABBREVIATION	DESCRIPTION
D.C	Direct Current
^{o}C	Degree Celcius
EM	Electromagnetic
ER	Electrical Resistivity
VES	VerticalElectricalSounding

CHAPTER 1

INTRODUCTION

1.1 GENERAL INTRODUCTION

Generally speaking, Jos is an area known to be of great geological interest. A lot of geological as well as geophysical works have been carried out in Jos and it's environs. However, the University of Jos in particular has not been surveyed using any of the geophysical methods. Hence, the need for this work.

The main objective of the present study is to attempt to uncover the basement structure as well as locate and evaluate the aquifer underlying the University of Jos permanent Site. This area is of interest for two basic reasons;

(i) There is no available geophysical record on the study area.

(ii) The University is fast expanding, with its population on the increase. However, the water supply to the University community is inadequate to cater for the needs of the growing population.

In the past there has been a general assumption that groundwater is ever abundant and readily exploitable. However, recent studies have shown that special care and skill are needed for its exploration and exploitation. Even though a renewable resource, extra effort is necessary to determine the location(s) for development and the extent of the development in order to avoid over-exploitation which may lead to serious repercussions. It is therefore necessary to employ quick and efficient methods for groundwater exploration especially in these days of scarce resources.

Geophysical studies provide useful information on the possible sites for boreholes. These methods have been used extensively in ground water investigation, geologic mapping and engineering site investigation (e.g. Etu-efeotor *et al.* 1989; Obiakor and chukwudebelu, 1992; Okwueze and Ezeanyim, 1985; Mbipom and Archibong, 1989). The geoelectric methods in particular, have been employed in studies such as, bedrock determination, mapping of superficial deposits, structural mapping, aquifer delineation, saline water mapping, lithological differentiation, and the determination of structural trends etc (Rijo *et al.;* Etu-effeotor and Akpokodge, *1990;* 1977; Olatinwo, 1994). In this survey, the conventional resistivity methods - vertical electrical sounding (VES) and profiling as well as the ground electromagnetic (EM) method were used. The vertical electrical sounding (VES) method, was chosen for this study because it has proved to be an economic, quick and effective exploration tool for groundwater and other purposes in different parts of the world (Ekine and Osobonye, 1996; Zohdy and Jackson, 1969).

The electrical resistivity profiling was embarked upon based on its capability to delineate features such as faults, fractures as well as vertical or near vertical contacts. The delineation of such features is of prime importance in engineering site investigation and geological mapping. Any of the features mentioned above can be a zone of weakness through which impounded water is lost along dam axis or within reservoir floor (Ojo and Olorunfemi, 1995). Foundation failure arising from differential movement in the event of tectonic activity along the linear feature can result in the collapse of civil Engineering

structures such as dams, buildings and roads.

The EM method, on the other hand, was considered appropriate here since it has been found to be highly successful in the Precambrian basement terrains of different regions (Hazell *et al.* 1988, Olurunfemi *et al.* 1995). Moreover, it is hoped that the method will help resolve the problem of equivalence often associated with the conventional resistivity interpretation (Onu and Ajakaiye, 1990). More still, some points on the study area are overlain by dense rocky formations and such points are unsuitable for resistivity surveying, but could be effectively surveyed with the EM method which does not require physical contact with the ground surface (McNeill, 1980).

Palacky *et al.* (1981) applied the HLEM(horizontal loop EM) method in prospecting for groundwater aquifers associated with fracture zones in Precambrian terrains in Upper Volta (Burkina Faso). Palacky and Kiyoshi(1979) also used the EM system for outlining aquifers in Brazil. Amadi and Nurudeen, (1990); Olayinka, (1990), have used the EM34-3 equipment for groundwater investigation in the crystalline basement terrains of different parts of Nigeria.

Many other works have been carried out, both on the D.C. resistivity and electromagnetic methods in different parts of the world for the purposes listed earlier on.

Resistivity method has also been used successfully to determine the saltwater-freshwater interface and the lateral extent of the saltwater intrusion (Etu-Efeotor *et al.*1989; Amadi and Amadi, 1990; Mbipom and Archibong, 1989; Oteri, 1990).

The EM method has also been used by J.O Barongo(1983) to search for Kimberlite pipes in the green - stone belt of western Kenya.

On the study area however, there is little or no available geophysical information. As such, the present study is meant to provide the basic geophysical information on the basement structure and groundwater potential of the area.

Details of the methods used are discussed in subsequent chapters.

1.2 LOCATION AND ACCESSIBILITY

The University of Jos, permanent Site is located just south of Naraguta Village on the northern edge of Jos City. It is bounded by latitudes, 9^0 58" and 9^0 59"N and longitudes 8^0 52" and 8^0 53.5" E (Dar Al Handasah, 1979).

A by-pass road that links the Jos-Bauchi Road to the East, and the Jos - Zaria Road to the West, bound the southern edge of the area. To the North, the Naraguta Village bound it.

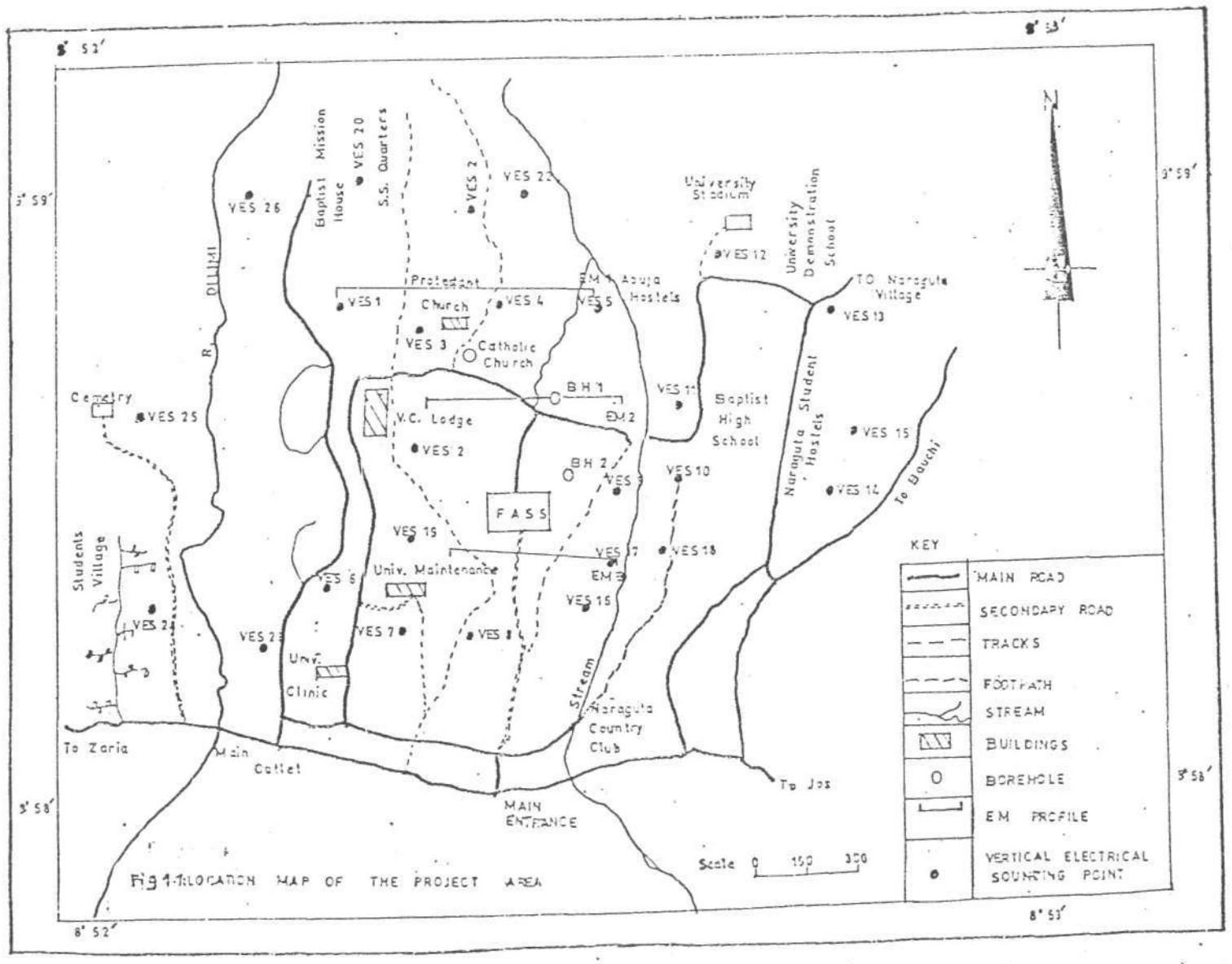


Fig 1: LOCATION MAP OF THE PROJECT AREA

Originally, about 5080 hectares of land was allocated to the University for its development of the permanent Site (Dar Al Handasah, 1979). However, the present area lying largely east of Dilimi River is only a small fraction of the allocated land (Fig. 1.1). The study area is covered by the Federal Survey of Nigeria, sheet 168 Naraguta NE AND 1:100,000 LERE SHEET 147 SE.

The area is easily accessible with the presence of a fine network of main roads, secondary routes, tracks and footpaths that interconnect the various units within the site (Fig: 1.1)

1.2.1. RELIEF AND DRAINAGE

The study area is located in the non-hilly ground, which slopes at various gradients towards the natural drainage of the Dilimi River. The maximum elevation is about 1160m above mean sea level (Ogezi *et al*. 1983). Several small streams traverse the area and flow into the Dilimi River.

The Dilimi River is a perennial river that rises east of Jos and flows through the Jos City and the study area before flowing northeastwards towards Lake Chad. Along the course of the Dilimi and its tributaries, extensive past mining activities have greatly scarred the landscape.

1.2.2 CLIMATE, VEGETATION AND LAND USE

The climate of the study area is similar to that of the entire Jos city. The climate of the Jos Plateau is determined by two main factors:

(i) Its altitude

(ii) Its position across the path of the seasonal migration of the inter-tropical convergence zone (ITCZ)(Ajaegbu *et al.* 1992).

The altitude of Jos makes it experience lower temperatures than elsewhere in Nigeria, except,Perhaps the Obudu Plateau (Ajaegbu *et al.* 1992).

A long-term record of rainfall kept by the University of Jos observatory shows that the study area has a mean rainfall figure of 1568 mm between 1990 and 1997. The rains commence in April and prevail until October, while the dry season starts from November and persist until March. The highest rainfall in the study area is recorded from June-September, having its peak in July.

The highest day temperature of between 29^0C - 35^0C is usually recorded at the end of dry season (around March - early April) just after the harmattan but before the onset of the rainy season.

The lowest temperature of between 14^0C - 18^0C is generally reached in January, at the peak of harmattan or in August, during the rainy season.

During the harmattan months of November - February, the air is usually very dry and the relative humidity low. The mean annual evaporation has been estimated to be about 3,100mm (University of Jos Observatory).

The study area is the usual grassless land typical of the Jos Plateau. The

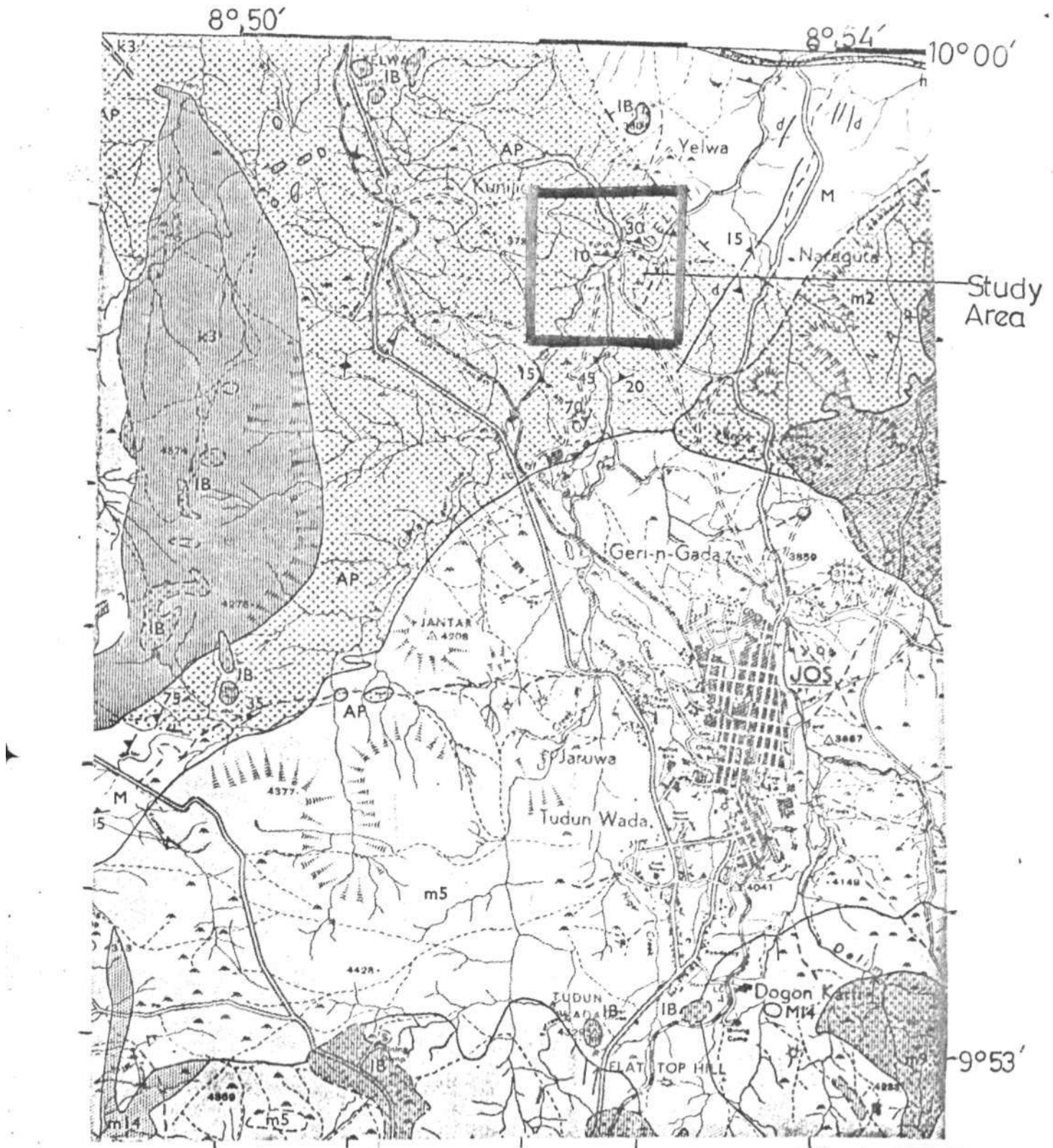
major vegetation found on the study area are; Guava, Mango and other economic trees.

Members of the University community have used the land extensively in cultivation. The major crops grown on the land are maize, rice, cassava, guinea corn, sweet potatoes, acha etc.

1.3 GEOLOGY

Rocks of the Precambrian Basement Complex - composed of gneisses, migmatites, meta-sedimentary and meta-igneous rocks and Pan-African (older) granites underlie the study area. The area is dominated by migmatites, gneisses, applites and pegmatites, which have been sheared and deformed into the "aplo-pegmatitic" granite-gneisses (Macleod *et al.* 1971). Basic dolerite dykes, basaltic lava flows and extensive laterites cover other areas of the permanent site (Ogezi *et al.* 1983).

The geological formations or major rock types within the area, from the youngest to the oldest rocks and their approximate ages are summarized below (Macleod *et al.* 1971).



M Undiffentiated migmatite including veined banded and porphyroblastic gneiss some schist amphibolite etc.
AP Aplo-Pegmatitic Granite gneiss.

Fig·2·1:GEOLOGICAL MAP OF JOS PART OF NARAGUTA SHEET 168 SHOWING THE STUDY AREA·

(i) Present - day stream sediments and alluvium (1 million years youngest).

(ii) Weathered zones of crystalline rocks or regolith (Weathered materials) and newer Basalts of recent age (2 x 10^6 years)

(iii) Older Basalts and older alluvial deposits; Tertiary age(2 million years to 65 million years).

(iv) Dolerite dykes of unknown age, but between 65 million years and 160 million years old.

(v) Younger granites of Jurassic age (about 160 million years.

(vi) Basement Complex gneisses and Migmatites(600 - 3300 million years old): oldest.

1.3.1. BASEMENT COMPLEX

Rocks of the Basement Complex (Ogezi et al. 1983) cover the study area. They are made up of migmatitic and granitic - gneisses, slightly migmatized metasedimentary schists, Meta-igneous rocks and pegmatites.

A geological map published by the Geological Survey of Nigeria (Macleod *et al.* 1971) refer to these rocks as the aplo-pegmatitic granitic - gneiss. All these rocks form good foundation soil. They are impermeable when undisturbed (Mclean and Gribble, 1979). The depths of the weathered part of these rocks differ from place to place, but lies within the range of 3 m to 40 m (Ogezi *et al.* 1983). In some places there is extensive jointing and fracturing of the rocks and

these generally trend North-South, east-west and NNE-SSW. Mafic Dolerite dykes cross cut the Basement Complex up to near the southern edge of the Basement Complex and Younger Granites boundary.

1.3.2. YOUNGER GRANITES

The Younger Granites within the study area are of Jurassic age. They occur at the edges of the watershed. They are technically disturbed and jointed near contacts with the Basement Complex, such as near the permanent site tank tower (Ogezi *et al.* 1983). Hence they sometimes possess good environment for the infiltration of rain water from precipitation. Younger Granite rocks crop out at the eastern and southern flanks of the study area.

1.3.3. OLDER BASALTS AND OLD ALLUVIAL DEPOSITS

Older Basalts, which are of Tertiary age, cover some upper part of the study area, especially, in the extreme northern edge. They are also recognized as flat-topped links protected by latiritic caps. The rocks are weathered, decomposed, and are probably permeable (Macleod *et al.* 1971)

Old alluvial stream deposits are composed of sands, gravels, and sometimes clays. They are deposited only in selected (few) areas of the study area, such as near the students village hostel. These zones are highly permeable.

1.3.4. WEATHERED ZONES AND NEWER BASALTS

The weathered zone of the crystalline rocks is a mixture of coarse - grained materials (quartz grains) with clayey minerals like Kaolinite and probably dicknite (Ogezi *et al.* 1983). The thickness of the zone varies between 7 m to 65 m. In some places, the weathered material forms randomly distributed pockets on the outcrops of the Basement Complex rocks. At locations close to the Dilimi River, blocks of relatively fresh, probably newer basalts, occur (Macleod *et al.* 1971). These may be transported float blocks. Fig 1.2 shows a geological map of the study area.

1.3.5. HYDROGEOLOGY.

The hydrogeology of an area is controlled by factors such as the geology as well as the climate of the region. This is true because the geological formations underlying the area and their structures determine the type of aquifers that would be developed and the means by which they would be recharged, and the climate determines the amount and rate of recharge of the aquifer (Olayinka, 1990).

According to Egboka (1988), groundwater occurrence in the Basement Complex is predominantly confined to shallow water table aquifers that are found in the buried channels, weathered mantle, shear zones and jointed or faulted traces. The weathered mantle is often too thin to trap a significant volume of water during the rainy season. It is often too clayey to be permeable even though the porosity may be high. Dense fractured Basement Complex rocks may be

deeply weathered to produce high yielding aquifers. Also some deep-seated buried channels may have thick sandy layers that could provide veritable aquifers. Olayinka, (1990) also pointed out that the crystalline rocks of the Basement Complex, by virtue of their lithological composition and texture, are generally poor in groundwater content except, however, where there exists fracture systems or where weathering has attained advanced stage that it results in thick permeable product.

Likewise, Hazell *et al.*(1988) suggested that in crystalline terrain, water is stored throughout the saturated part of the weathered zone and transmitted via the basal permeable zone of dislocated rock, and through joints in almost fresh rock. Mica and its decomposition products impede groundwater movement, as of course, do clays. Thus, the most useful crystalline host rocks are low in mica and other ferromagnessian minerals.

Beeson and Jones (1988) stated that the Basement Complex serves as the upland area of many drainage basins, and since it is sometimes highly fractured, a strong possibility of high recharge to the groundwater may exist.

The superficial deposits, which contain partly the products of weathered rocks, and partly alluvial deposits serve as media of infiltration and recharge of aquifers. The areal extent and location of these superficial deposits will encourage or inhibit infiltration. The river valleys and the "fadama" usually contain alluvial materials such as clay and silty products deposited during floods. Their composition and porosity make them good reservoirs of ground water which serve

as source of water for the wells during dry season. Generally, the degree of water productivity of an aquifer depends on the degree of natural water recharge, its physical and chemical properties, climatic conditions, the characteristics of its geometric and hydrologic boundaries, vegetation and human activity (Abdel-Azeez, 1987). The thickness of an aquifer is also an important factor in its degree of water productivity.

In conclusion, it is important to emphasize that even though, groundwater may be contained in crystalline rocks under favorable conditions, location of wells based on the physical and structural states of the rocks as well as the hydrogeological conditions in our area must be preceded by careful geophysical investigations.

1.4 PREVIOUS GEOPHYSICAL WORKS

The earliest known geophysical works carried out on the Plateau area were for mining purposes. The extent of coverage was not more than 500 km^2 (Ajakaiye, 1976). Electrical resistivity and magnetic methods were used to locate the channels of old rivers buried by volcanic/alluvial materials thus leading to a reduction in the in the cost of exploration drilling in the search for tin deposits (Du Preez, 1948; Shaw, 1951).

Aeromagnetic maps (Sheet 168 Naraguta NE and Lere sheet 147 SE) covering the area have also been published by the Federal Geological survey of Nigeria. A comprehensive geophysical survey of the sub-basalt tin deposit in the

area was carried out between 1964 to 1965 under the auspices of the United Nations mineral project and the British Overseas Geological Surveys (Ajakaiye, 1976). Gravity, seismic, resistivity as well as magnetic methods were used in the study (Mason - Smith, 1965).

Extensive regional gravity works have been carried out on the Jos Plateau (Mason - Smith, 1965; Ajakaiye, 1976). The gravity results show that the depth to basement in the area range from 38 to 80 m, and the bedrock is mostly granitic. On the University of Jos permanent site, in particular, there is no available record of any serious geophysical investigations. Most of the works done on this site are geological works. Available records show that Macleod *et al.* (1971), Ogezi *et al.* (1983) as well as students of the Department of Geology and Mining, University of Jos, have, at different times carried out extensive geological mapping of the area. Some of their findings have been cited under section 1.3, "Geology of the area".

Ibe (Personal communication) of the Department of Geology and Mining, University of Jos, revealed that C.A. Kogbe carried out some resistivity soundings in one part of the study area. However, since the work was done on consultancy basis, results of his findings were not made public. There is evidence of extensive past mining activity in the study area but results of geophysical investigations preceding such mining activity could not be found.

Ogezi *et al.* (1983), carried out same preliminary survey of the area in order to access a suitable site for the construction of an earth dam to be used by

the Fisheries and Hydrobiology Unit of the Department of Zoology, University of Jos. Again the survey did not employ any geophysical technique. Thus, the present study will be the first documentation on geophysical activity on the study area.

1.5 AIM AND SCOPE OF THE STUDY

Owing to the fact that there is no concrete geophysical information on the study area, the present work is an attempt to provide a first hand information on the basement structure and ground water potentials of the area.

The objectives pursued to achieve the above aim included:

(i) Production of a geoelectric section at each sounding point in order to determine the subsurface layerings that underlie the study area.

(ii) Production of a depth-to-basement map of the study area from where the basement geometry as well as overburden thickness was inferred.

(iii) Production of isoresistivity maps of the study area at different depths so as to obtain the overall picture of how the layer resistivities vary at depth in the area.

(iv) Production of an aquifer thickness map for the study area.

(v) Recommendation of possible regions for siting boreholes within the area based on (i - iv) above.

CHAPTER 2

PRINCIPLES AND THEORIES OF THE METHODS USED.

2.1 GENERAL REMARKS

The author employing the DC resistivity and the ground EM methods between February and April 1998 carried out geophysical investigations. The instruments used were the ABEM terameter SAS 300 for the DC resistivity survey, and the Geonics EM34-3 for the EM survey.

The Schlumberger electrode configuration was employed in all the VES stations while the Wenner configuration was adopted for the resistivity profiling. The Maximum current electrode separation (AB/2) utilized for the Schlumberger sounding was 135 m while constant electrode separations (a) of 10 m and 20 m were used for the Wenner profiling.

EM profiling was also carried out using coil separations of 10 and 20 m respectively. EM sounding was however not done due to the non-availability of the 40-m cable which makes sounding possible. To make a sounding, readings are taken at the 10, 20 and 40-m intercoil spacing and plotted on a regular scale. The resultant curve is interpreted in terms of the number of subsurface layerings.

2.2 THEORY OF THE D.C. RESISTIVITY METHOD

The electrical resistivity method is one of the most relevant geophysical methods applied for groundwater studies in basement terrains

(Olorunfemi and Fasuyi 1993). In groundwater studies for instance, the relevance of the method is based on the usually significant resistivity contrast between the weathered zone and or fractured column and the resistive fresh bedrock.

In this method, an electric current is introduced into the ground by means of two current electrodes. This sets up a stationary current field, and because of the ohmic potential drop, an electrical potential field is also created. This field gets distorted in the neighborhood of a subsurface zone of anomalous conductivity, and the aim is to search for such anomalous zones in the electrical field with the pair of the potential probes. The assumption made here is that the current flow in the potential measuring circuit is negligible compared with the current flow in the ground, so that the potential electrodes themselves will have no disturbing effect upon the electrical field (Grant and West, 1965).

The purpose of the vertical electrical sounding method is to investigate the change of the formation resistivity with depth. To achieve this purpose it is necessary to arrange measurements in such a way that, at different measurements, the value of the measured potential difference is affected by the formation resistivities at different depth ranges. This may be accomplished by changing the distance between the current electrodes so that the depth range to which the current penetrates is changed. However, the distance between the potential measuring electrodes and their position with respect to the current electrodes also affect the depth range from which information on the formation resistivity is obtained. In the methods employed in this study (Schlumberger and

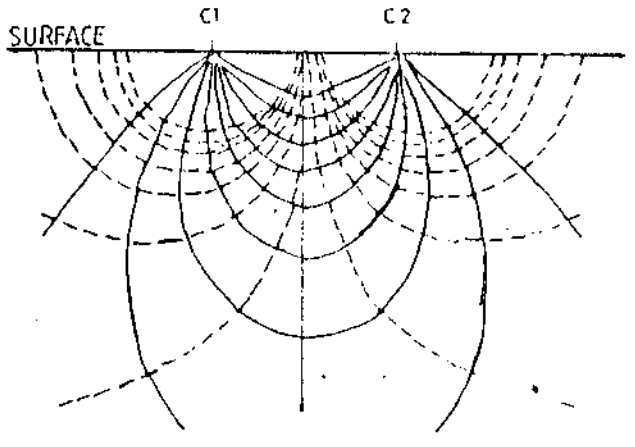
Wenner), the four electrodes are positioned on a straight line, with the two current electrodes on the outside of the potential measuring electrodes. The interpretation of the VES data is based on the assumption that the subsurface consists of a sequence of distinct layers of finite thickness and each of these layers is assumed to be electrically homogeneous and isotropic (Koefoed, 1979), and the boundary planes between subsequent layers are assumed to be horizontal.

These assumptions in the real sense represent only a schematic description of the actual conditions that exist in the subsurface. There are some deviations of the real subsurface conditions from the above assumptions, and these influence the VES measurements and interpretation. These deviations are discussed further in chapter four.

The vertical electrical sounding (VES) is based on the principle that a fraction of the electric current injected into the ground, penetrating below a given depth increases with the separation of the current electrodes. Thus as the current electrodes separation is increased, the depth of penetration will increase. Therefore any anomalous body lying between the ground surface and the last depth of penetration will have great influence on the electrical potential field at depth.

Fig 2.1a shows the current and potential distribution within a homogeneous isotropic ground in a vertical plane through the current electrodes.

The figure suggests that the depth of penetration of current increases with increasing electrode distance.



——— Current Distribution Lines

— — — — Equipotential Lines

FIG 2·1a Current and Potential Distribution within a Homogenous isotropic Ground Through the Current Electrodes·

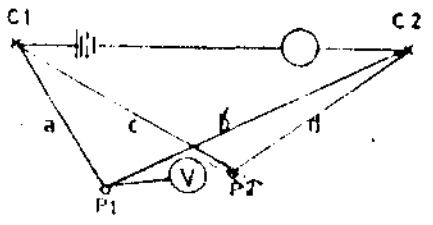


FIG 2·1b A General Electrode Configuration (After Atlas Copco, Abem)

The principle underlying the resistivity method is embodied in Ohm's law. Ohm's law gives the relationship between current

density (ampere/m^2) and the electric field intensity E (volts/m) as

$$\bar{j} = \sigma\bar{E} \qquad \text{---} \qquad (2.1.0)$$

where σ is the conductivity of the medium. Also E is the gradient of a scaler potential U (Volts). i.e

$$\bar{E} = -\nabla U \qquad \text{----------} \qquad (2.1.1)$$

putting (2.1.1) in (2.1.0)

$$\bar{j} = -\sigma\nabla U \qquad \text{----------} \qquad (2.1.2)$$

From divergence condition,

$$\nabla.\bar{j} = 0 \qquad \text{---------} \qquad (2.1.3)$$

Thus, from (2.1.2)

$$\nabla.\bar{j} = -\nabla.(\sigma\nabla u) = 0 \qquad \text{--------} \qquad (2.1.4)$$

or

$$\nabla\sigma.\nabla U + \sigma\nabla^2 U = 0 \qquad \text{----------} \qquad (2.1.5)$$

Since σ is constant for a homogeneous medium, the first term in (5)

varnishes hence,

$$\nabla^2 U = 0 \qquad \text{----------} \qquad (2.1.6)$$

Applying boundary conditions, (2.1.6) can be solved for specific cases.

For instance, for a single current electrode at the surface of a homogeneous ground,

(2.1.6) is expressed in spherical polar co-ordinates as:

$$\frac{1}{r^2}\frac{\partial}{\partial r}(r^2\frac{\partial u}{\partial r})+\frac{1}{r^2\sin\theta}\frac{\partial}{\partial\theta}(\sin\theta\frac{\partial u}{\partial\theta})+\frac{1}{r^2\sin^2\theta}(\frac{\partial^2 u}{\partial\phi^2}) = 0 \quad \text{----------} \quad (2.1.7)$$

For the single current source, there is complete symmetry of current flow with respect to the θ and ϕ directions and the derivatives with respect to these directions are zero. Thus (2.1.7) becomes;

$$\frac{d}{dr}(r^2\frac{du}{dr}) = 0 \qquad \text{----------} \qquad (2.1.8)$$

Equation(2.1.8) can be solved further to arrive at

$$\rho = 2\Pi r(\frac{U}{I}) \qquad \text{-------} \qquad (2.1.9)$$

Or

$$U = \frac{I\rho}{2\pi}(\frac{1}{r}) \qquad \text{---------} \qquad (2.2.0)$$

Thus generally, the potential difference between two arbitrarily located points on the surface of a homogeneous isotropic ground is given by the

expression:

$$\Delta U = \frac{I\rho}{2\pi}\left(\frac{1}{r_1} - \frac{1}{r_2} - \frac{1}{r_3} + \frac{1}{r_4}\right) \quad \text{----------} \quad (2.2.1)$$

Where ρ is the resistivity, I is the current and r_1, r_2, r_3, and r_4, are the inter-electrode distances as shown in fig 2.1b .

From (2.2.1) the apparent resistivity can be solved for as;

$$\rho_a = \frac{\Delta u}{I} \cdot \frac{2\pi}{\left(\frac{1}{r_1} - \frac{1}{r_2} - \frac{1}{r_3} + \frac{1}{r_4}\right)} \quad \text{-----} \quad (2.2.2)$$

The result is independent of the position of the electrodes and is not affected when the current and the potential electrodes are interchanged.

2.2.1. THE CONCEPT OF APPARENT RESISTIVITY

Most resistivity techniques define a response function called apparent resistivity, ρ_a which can be estimated from surface measurements. These apparent resistivities are usually functions of a variable that is related to the depth of current penetration (Bowen, 1986).

The apparent resistivity is equal to the true resistivity only when the subsurface is homogeneous. In practice, this condition is difficult to obtain, however, the subsurface is assumed to be divided into thin strata with each stratum regarded as completely homogeneous and isotropic (Koefoed, 1979). This is a convenient way of representing a response of the actual distribution of lateral

resistivities in the subsurface on the basis of surface measurements. If the electrodes are laid out along a profile and their separations are increased systematically, the change in the apparent resistivity will be a function of electrode spacing (as defined in eqn(2.2.2).

2.2.2 FACTORS AFFECTING RESISTIVITY OF EARTH MATERIALS.

Of all the physical properties of earth materials, resistivity shows the largest range of variation.

The great variability in the resistivities of the various rock types is caused by such factors as mineralogical composition, density, porosity, pore size and shape, water content and quality, temperature as well as structure and texture of rocks(Telford et al. 1976). There are no fixed limits. Igneous and metamorphic rocks yield values ranging from 10^2 to 10^8 Ohm-m,sediments also fall within this range. Clays have typical resistivity values ranging from 10^0 to10^1 Ohm-m while sands have a range between 10^2 to 10^3 Ohm-m.

In porous formations,resistivity is affected more by water content and quality than by the resistivity of the actual rock material. In the aquifers which are composed of unconsolidated materials,resistivity decreases with the degree of saturation and the salinity of the ground water.

Clays have a lower resistivity than permeable alluvial aquifers because they have minerals within them which conduct electric current through their

matrix(Bowen,1986).

2.2.3 ELECTRODE LAYOUTS

A number of different conventional surface configurations are used for the current and potential electrodes placement. In many arrangements, both sets of electrodes are laid out along a line. The current electrodes are usually placed on the outside of the potential electrodes. The most commonly used configurations are the Schlumberger, Wenner, and the Dipole arrangements.

In the Schlumberger arrangement, four electrodes are positioned symmetrically along a straight line, the current electrodes are displaced outward while the potential electrodes, in general, are left in the same position. However, when the ratio of the distance between the current electrodes to that between the potential electrodes becomes too large, the potential electrodes are also displaced outwards so as to obtain a measurable potential difference between the potential electrodes. The Schlumberger arrangement is highly suitable for vertical electrical sounding. Fig 2.2b shows this arrangement. In the Wenner array, the electrode

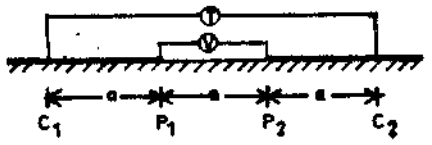


Fig. 2.2a Wenner Configuration

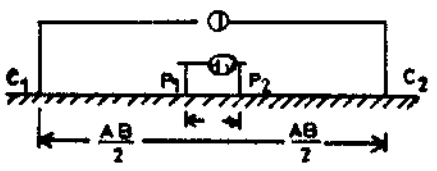


Fig. 2.2b Schlumberger Configuration

spacings are fixed, and the array of electrodes is moved laterally along a profile with constant separation. This electrode configuration is more effective in electric profiting. It is inadequate for exploration objectives requiring depth control which can only be achieved through expanding the geometry of the electrode configuration. The Wenner array is illustrated in fig 2.2a.

Data collected from both Schlumberger and the Wenner electrode configurations are reduced using certain mathematical relationships. In the Wenner configuration, the electrodes are Uniformly, spaced along a line, hence, from (2.2.2)

$$r_1 = r_4 = 1 \text{ and } r_2 = r_3 = 2a$$

Thus, the apparent resistivity is given by

$$\rho_a = 2\pi a\frac{U}{I} \qquad \text{--------} \quad (2.2.3)$$

Where a = distance between the electrodes
I = Current passed through the ground
U = Potential difference measured.

In the Schlumberger configuration, the array is often used symmetrically, the apparent resistivity is thus, given by

$$\rho_a = \frac{\pi l}{2}[(\frac{L}{l})^2-1].\frac{U}{I} \qquad \text{----} \quad (2.2.4)$$

Where

L = half the current electrodes Separation

l = half the potential electrodes Separation.

2.3 THEORY OF THE EM METHOD

Geoelectric prospecting techniques in which a controlled time-varying magnetic field is used as power source are usually referred to as EM techniques.

The EM technique involves the propagation of time varying low frequency E-M fields in the earth. There is a close analogy between the transmitter, receiver and the buried conductor which comes within the path of the applied EM field and a trio of electrical circuits are coupled by EM induction. Generally, inductive coupling is used. However, in some E-M systems, the source energy is introduced into the ground by direct contact, while the detector receives each signal by induction.

EM fields in the ground induce electric currents in any subsurface conductor present; the induced current flows in closed loops normal to the direction of the EM field. The induced current produce secondary EM fields which distort the primary field at that point. The resultant field is picked up with the aid of search coils; a difference in amplitude / intensity and phase can be diagnostic of the presence of a conductor.

EM fields depend on the magnetic permeability, and the conductivity of earth materials. The theory behind EM fields is that they satisfy Maxwell's equation. The fields are time dependent and are harmonic if sinusoidal or transient if stable for a short time. They alternate exponentially.

A commonly used criterion for the penetration of EM waves is the "Skin depth, d. This is the distance in which the signal is reduced to 1/e of its original

value. Skin depth is defined by:

$$d = \sqrt{\frac{2}{\mu_0 w \sigma}} \qquad \text{-----} \qquad (2.2.5)$$

Where ω = Angular frequency
σ = Conductivity
μ_o = Permeability of free space

When an EM field encounters a conductor, the conductor becomes the source of its secondary field, which differs in phase from the primary field but has the same frequency. A suitable detector will hence be energized by both fields simultaneously (Telford et al., 1976). The existence of the secondary fields, showing the presence of a subsurface conductor can be established with respect to the primary field by a change of amplitude and / or phase in the normal detector signal. Some EM systems measure both quantities while some measure one or the other.

2.3.1 THE EM34-3

This EM technique of geophysical prospecting was primarily developed for the delineation of sheet-like metallic conductors, which are often concentrated within faults and fracture zones.

Recently, the application of this method to ground water prospecting has become popular, especially in the Precambrian basement terrains where it has proved to be highly successful.

The technique, which is direct, may be applied to the location of sites with

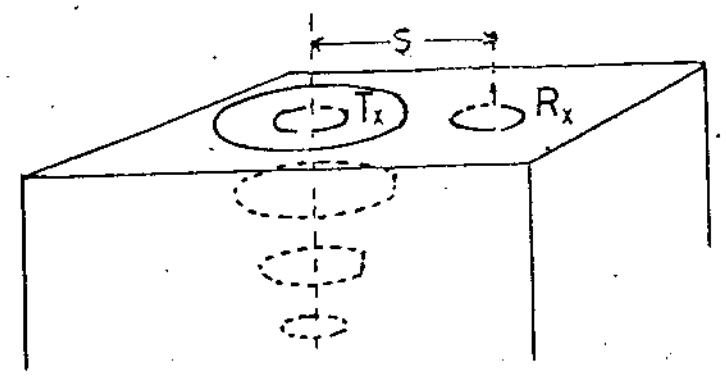


FIG. 2.3
EM 34-3
INDUCED CURRENT FLOW (HOMOGENOUS HALFSPACE)

appreciably thick overburden, or to the mapping of geological structures such as faults and fracture zones (Palacky et al.,1981).

The EM 34-3 instrument is composed of a transmitter coil, T_x energized with an alternating current at an audio frequency, and a receiver coil, R_x which is kept at a fixed distance, S from the transmitter coil (Fig 2.3).

If both the transmitter and receiver are placed on the earth (assumed uniform) as shown in fig 2.3, the time varying magnetic field arising from the alternating current in the transmitter coil induces very small currents in the earth. These small currents generate a secondary magnetic field, H_s which is sensed, together with the primary field, H_p by the receiver coil (McNeill, 1980a). In general this secondary magnetic field is a complicated function of the intercoil spacing, S, the operating frequency, f, and the ground conductivity, σ. The secondary magnetic field is shown to be:

$$\frac{H_s}{H_p} \approx \frac{iw\mu_o\sigma s^2}{4} \qquad \text{------} \qquad (2.2.6)$$

Where
H_s = Secondary magnetic field at the receiver coil
H_p = Primary magnetic field at the receiver coil
$\omega = 2\pi f$
μ_o = Permeability of free space
σ Ground conductivity (mho/m)
S = Inter coil spacing
$i = (-1)^{1/2}$

The ratio of the secondary to the primary magnetic field is now linearly proportional to the terrain conductivity, a fact which makes it possible to construct

a direct reading, linear terrain conductivity meter by simply measuring this ratio. Given $_{Hs/Hp}$ the apparent conductivity indicated by the instrument is defined from equation (2.2.6) as

$$\sigma_a = \frac{4}{w\mu_o s^2}\left(\frac{H_s}{H_p}\right) \qquad \text{---------} \qquad (2.2.7)$$

The units of conductivity are the mho/meter or more conveniently, the millimho/meter.

CHAPTER 3

INSTRUMENTATION AND FIELD PROCEDURE

3.1 ABEM TERAMETER SAS 300

The ABEM Terameter SAS system consists of a basic unit called the Terameter SAS 300, which can be supplemented as desired with the SAS 2000 Booster. SAS stands for signal averaging system - A system whereby consecutive readings are taken automatically and the results are averaged continuously. The continuously updated running average is presented automatically on the display. This continues until the operator is satisfied with the stability of the result. SAS results are more reliable than those obtained using single - shot systems. The SAS 300 (Basic unit) can be used for self-potential (SP) and resistivity surveys.

The SAS 2000 Booster supplements the SAS 300 in situations where the voltage and/or current must be increased. The booster is usually slaved to the SAS300, but can also be used separately in special applications such as charge - potential studies and double-dipole surveys.

The Terameter SAS 300 can operate in two modes; namely, the resistance and the voltage modes. However, only the resistance mode was used by the author in this work and that is what will be discussed here. In the resistivity-surveying mode, the instrument comprises a battery powered, deep - penetrating resistivity meter with an output sufficient for a current electrode separation of 2000 meters under good surveying conditions. Discriminatory circuitry and

programming separates DC voltages, self-potentials and noise from the incoming signal. ? V/I is calculated automatically and displayed in digital form in Kilo-ohms, ohms or milli ohms. The overall range for this instrument extends from 0.5 milli ohms to 1999 kilo-Ohms.

In the voltage-measuring mode, the SAS 300 measures the natural DC potentials. The result is displayed in volts or millivolts. The overall range extends from 0.01mv to 500v.

The Terameter SAS 300 contains three main units, all housed in a single casing: The transmitter, the receiver and the microprocessor. The electrically isolated transmitter sends out well defined and regulated signal current. The receiver discriminates noise and measures voltages correlated with transmitted signal current (resistivity surveying mode) and also measure uncorrelated DC potentials with the same discrimination and noise rejection (Voltage measuring mode). The microprocessor monitors and controls operations and calculates results.

To make a measurement with SAS 300, the cycle selector is kept at a fixed position, either 1, 4 or 16. The 16-cycle position gives the best averaging but it is time consuming. Therefore the 4-cycle position was used in nearly all the stations, except where the difference between readings (kept at 4 cycles or 16) was negligibly small, then the 1 cycle position was used. This condition shows that the ground is homogeneous to some extent. Selecting the number of cycles and pressing the measure button gives a reading automatically.

3.2 THE GEONICS EM43-3

The EM equipment developed by Geonics limited, Canada, comprises a portable transmitter and a receiver. The instrument, which is two-man portable, has the two coils flexibly connected by a cable. The intercoil spacing is measured electronically so that the receiver operator simply reads a meter to accurately set the coils to the correct spacing which can be 10, 20, or 40 meters so as to directly vary the effective depth of exploration.

Table 3.1 shows the exploration depths for EM34-3 at various inter coil spacings (McNeill, 1980).

Table 3.1: EM34-3 responses at different intercoil spacings

Intercoil spacing (m)	Exploration Depths(m)	
	Horizontal Dipole Mode	Vertical Dipole Mode
10.0	7.5	15.0
20.0	15.0	30.0
40.0	30.0	60.0

The instrument is calibrated to read terrain conductivity in Millimhos/m.

To measure terrain conductivity, the transmitter operator stops at the measurement station; the receiver operator moves the receiver (coil backward or forwards until his meter indicates the correct intercoil spacing and he reads the

terrain conductivity from a second meter. The coils are normally carried with their plane vertical (horizontal dipole mode) since in this configuration the measurement is relatively insensitive to mis-alignment of the coils. In the event that the greater depth of penetration resulting when the two coils are in the vertical dipole mode (plane of the coils horizontal) is desired, more care must be taken with intercoil alignment. This is because this mode is more sensitive to coil misalignment (McNeill, 1980).

3.3 CHOICE OF ELECTRODE CONFIGURATION

There are several electrode configurations that could be employed in the electrical resistivity survey. However, the Schlumberger and the Wenner electrode configurations were adopted in this study.

In comparing the Wenner and Schlumberger configurations, it is noted that in both of these configurations, the distance between the current electrodes predominantly controls the depth of current penetration. With equal values of the current electrode spacing, the depth of penetrations reached in the two configurations are, thus, nearly equal. However, the voltage difference between the potential electrodes is in these conditions considerably larger in the Wenner configuration than in that of Schlumberger, because the distance between the potential electrodes is larger in the Wenner configuration. This tends to make the reading accuracy of the voltage better in the Wenner configuration than it is, for comparable depth of penetration, in the Schlumberger configuration (Koeffoed,

1979).

There is another consideration, however, which is in favor of the Schlumberger configuration, and which, definitely outweighs the disadvantage of the smaller measuring accuracy. One of the assumptions on which the interpretation of resistivity sounding measurements is based is that each of the subsurface layers is electrically homogeneous. In practice however, this differs in that inhomogeneities of relatively small lateral extent occur close to the surface in many areas. These inhomogeneities distort the pattern of electrical current flow in their surroundings, and consequently, falsify the measured potential difference, if they lie close to the potential electrodes. This falsification of the measured potential difference occurs, both in the Schlumberger and the Wenner configurations. However, in the Wenner configuration the potential electrodes are displaced for each measurement making the effect of near-surface inhomogeneities erratic and difficult to account for, in interpretation (Koefoed, 1979; Kunetz, 1966). In the Schlumberger configuration, on the other hand, the position of the potential electrodes is kept constant throughout a series of measurements so that similar errors occur on all the measurements. Hence, as long as the dimensions of the near-surface inhomogeneity are small compared with the distance between the current electrodes, the relative error that they produce in the measured potential difference is the same for all measurements. This predictable aspect of the errors in the Schlumberger configuration makes it far easier to account for them in the interpretation, hence the choice of the Schlumberger electrode

configuration.

Other factors that make the Schlumberger configuration advantageous are;- The potential electrodes are usually not moved or, if moved at all, they are moved a minimum number of times during a given sounding, only the current electrodes are moved. This makes the soundings less cumbersome.

The Schlumberger electrode configuration also saves time and manpower. A minimum of three people can effectively carry out measurements with this electrode arrangement on the field, unlike other electrode configurations.

The Wenner array was used for the resistivity profiling for the following advantage. Since the whole array is expanded along a traverse about the centre point, the fall-off in potential gradient with increasing spacing, a, is automatically partly compensated for by the increase in potential electrode Separation (Beck, 1981).

3.4 ELECTRICAL RESISTIVITY DATA COLLECTION

Twenty-six vertical electrical soundings (VES) were carried out with a maximum current electrode separation of 270 m. The potential electrode separation MN was expanded from time to time in order to obtain satisfactory readings. The maximum potential electrode separation reached was 9 m. At least two readings were repeated with the same value of AB as the value of MN was gradually increased.

The VES points were selected in such a way as to ensure their uniform

distribution over the entire area. However, some sounding points were slightly shifted and others omitted where dense rocky formations and built up areas were encountered.

Taking additional resistivity measurements using the Wenner configuration followed up the results of the Schlumberger soundings.

Four profiles of lengths 630 m, 520 m, 450 m and 420 m respectively were traversed. Along each profile, constant electrode spacings "a" of 10 m and 20m were used in order to study the lateral variation of resistivity along those profiles.

3.5 EM DATA COLLECTION

It was intended that both EM sounding and profiling would be carried out on the study area, so as to compare results obtained using this method and those from electrical resistivity. However, due to the non-avalaibility of the 40-m cable, only EM profiling was done.

Three (3) EM profiles were taken around the central region of the study area. Two of the profiles were taken to coincide with two of the resistivity profiles while the third was run across a newly drilled borehole. The profiles were of length 710 m, 700 m and 500 m respectively.

Along each profile, intercoil separations of 10 m and 20 m were used and measurement of the terrain conductivity were made both in the horizontal dipole mode (plane of the coils vertical) and the vertical dipole mode (plane of the coils horizontal).

CHAPTER 4

INTERPRETATION TECHNIQUES AND DATA PROCESSING

4.1 VES INTERPRETATION METHODS

There are at least two main approaches to computerized interpretations of VES data. One approach (Zohdy, 1975) assumes that nothing is known about the number of subsurface layers, their thicknesses, or resistivities. This approach has advantages when a survey is being made in an area where absolutely no geologic information is available.

In the second approach, some rudimentary geologic information is available. In this situation, it is usually desirable to obtain an interpretation which has the same number of layers as there are distinct lithological units as opposed to the first approach where the number of layers is often equal to the number of input data points (Rijo *et al.*, 1977).

In the 1970s, several computerized interpretation methods of vertical electrical sounding (VES) were developed. These methods may be grouped into two categories. The first group relies on the transformation of a VES curve into its corresponding resistivity transform (or Kernel function) curve using forward filters such as those developed by Gosh (1971) and Koefoed (1979). The resistivity transform curve is interpreted using methods based on Pekeris (1940) and Koefeod's (1979) formulae.

In the present study, a new iterative procedure is used based on Zohdy and

Bisdorf, (1989), in which a layering model is obtained directly from a digitized sounding curve. The method does not require a preliminary guess (from curve matching) for the number of layers, their thicknesses, or their resistivities; and it does not require extrapolation of the first and last branches of the sounding curve to their respective asymptotes. The number of layers is equal to the number of digitized points, and the layer boundaries are spaced uniformly on a logarithmic depth scale. For field sounding curves, this method provides a theoretical curve that fits the observed curve as closely as possible and produces a corresponding, well-behaved layering model (with no extremely thin layers of un-usually high or usually low resistivities). The resulting solution can be accepted, simplified, or modified to satisfy known geologic information using other equivalent layering models (Zohdy, 1989).

4.1.1. OUTLINE OF THE ZOHDY METHOD

The iterative procedure used in the interpretation of all the Schlumberger VES curves in which a layering model is obtained directly from a digitized sounding curve follows from Zohdy (1989). The outline of the method is as follows:

The study of Schlumberger theoretical sounding curves for horizontally stratified, laterally homogenous, and isotropic media shows that regardless of the number of layers or resistivity distribution with depth, the following properties are observed.

(1) Computed apparent resistivities are always positive.

(2) The form of a sounding curve follows the form of the true resistivity - depth curve. As the true resistivities increase (or decrease) with greater depth, the apparent resistivities increase (or decrease) with greater electrode separation. This is particularly the case with layers whose thicknesses increase logarithmically with depth.

(3) The maximum change in apparent resistivity always occurs at an electrode spacing that is larger than the depth at which the corresponding change in true resistivity occurs. This means that a sounding curve is "out of phase" with the resistivity-depth curve and is always shifted to the right of the resistivity-depth curve.

(4) The amplitude of a sounding curve is always less than or equal to the amplitude of the true resistivity - depth curve. The apparent resistivity asymptotically approaches the true resistivity at electrode spacings that are very small with respect to the thickness of the first layer or very large with respect to the depth to an infinitely thick last layer.

(5) In a multilayer model, if the true resistivity of a thick layer is changed, the apparent resistivity along a corresponding segment of the sounding curve also changes accordingly. Furthermore, the maximum change in apparent resistivity is approximately equal to the net change in true resistivity.

4.1.2 INITIAL DATA PREPARATION

A field Schlumberger sounding curve, unlike a theoretical curve, is composed of several overlapping segments. The segmented Schlumberger field curve is processed and reduced to a continuous curve prior to its interpretation in terms of a horizontally stratified model. (Zohdy, 1989).

The processed Schlumberger sounding curve is digitized at a logarithmic interval equal to the sampling interval of the filter to be used in calculating the theoretical curve. The purpose of digitizing the sounding curve is to speed up the computations of the succession of theoretical sounding curves used in the itera tive procedure.

A sampling interval of six points per decade (logarithmic cycle) is considered commensurable with the electrode spacing intervals used in the field and is considered optimal for defining the form of a sounding curve.

When a processed field Schlumberger sounding curve is digitized, it is ready for interpretation by the iterative method.

4.1.3. ITERATIVE PROCEDURE

The iterative procedure relies on the following initial assumptions:

(i) The number of layers in the model equals the number of digitized points on the observed curve. The assumption remains unchanged throughout the iterative process.

(ii) The depths of the model layers are equal to the digitized electrode

spacings which are equally spaced on the logarithmic depth scale.

(iii) The true resistivities of the model are equal to apparent resistivities.

Depth determinations are done iteratively as follows:

(a) It is assumed that the digitized electrode spacings are equal to the depths and that the apparent resistivities are equal to the true resistivities at those depths.

(b) A theoretical sounding curve is calculated for this multilayer model by convolution.

(c) The root-mean-square (rms) percent is computed from the equation:

$$rms\ percent = \frac{\sqrt{\sum_{j=1}^{N}\left(\frac{\overline{\rho_{oj}}-\overline{\rho_{cj}}}{\rho_{oj}}\right)^2}}{N}\times 100 \quad ----- \quad (4.1)$$

Where ρ_{oj} = jth 'observed' apparent resistivity

ρ_{cj} = jth calculated apparent resistivity

N = Number of digitized apparent resistivity poinst (with j = 1 to N

(d) All the depths are multiplied by 0.9 to decrease the layer depths by 10% (This is to ensure that the layers are as thin as possible for isotropic conditions to hold).

(e) Steps (b) and c are repeated and a new rms percent is computed.

(f) The new rms is compared with the previous one. If the new rms percent is less than the previous one, then the newly computed shallower depths are now more in phase and closer in position with respect to the true, but unknown, depths than the previously assumed depths.

(g) Steps (d), (b), (c) and (f) are repeated until the rms percent is minimum. A minimum, is detected when the rms percent increases as the depths are shifted too far to the left.

Resistivity determinations are also done iteratively through the following processes:

(a) At each digitized electrode spacing on the observed and calculated curves, if the computed apparent resistivity, at jth spacing, is less (or greater) than the corresponding observed apparent resistivity, the corresponding true resistivity of the jth layer is increased (or decreased) so that the calculated apparent resistivity will rise (or fall) and approach the observed resistivity. The amplitude of a layer resistivity is adjusted iteratively as:

$$\rho_{i+1}(j) = \frac{\rho_i(j) \times \rho_o(j)}{\rho_{ci}(j)} \quad \text{------} \quad (4.2)$$

Where:

i = number of iteration

j = jth layer and jth spacing

$\rho_i(j)$ = jth layer resistivity at the ith iteration

ρ_{ci} (j) = Calculated apparent resistivity at the jth spacing for the ith iteration, and

$\rho_o(j)$ = Observed apparent resistivity at the jth spacing.

The ratio of observed to calculated apparent resistivity is multiplied by the corresponding layer resistivity to adjust it to a higher or lower value.

(b) A new rms percent is calculated using the adjusted layer resistivities.

(C) A new rms percent is computed and compared with the previously obtained one in (b) above.

(d) Steps (a), (b) and (c) are repeated until a match is found to the observed curve or until another condition is met to terminate the iterative process.

The iterative process is terminated when any one of the following conditions is met: a prescribed minimum rms percent (less than 2 percent for field data) is obtained; a slowness in further improvement in fit is detected; a maximum number of iterations (30) is reached; or the rms percent increases instead of decreasing. The average number of iterations is about 10. (Zohdy, 1989).

4.1.4 FACTORS AFFECTING VES INTERPRETATION

Effect of Anisotropy

As discussed earlier on in chapter 2,there are some deviations of the real subsurface conditions from the assumptions made in resistivity interpretation. One assumption made is that the geoelectric layers must be isotropic. However, in reality geological formations may be electrically anisotropic. This phenomenon is quite common in formations that are rich in clays or shale. In such conditions the electrical resistivity is the same in all directions along a layer, but has a higher value in the direction perpendicular to the stratification.

Another condition, which may arise, is the fact that geological formations may consist of an alternation of two different facies made up of quite thin beds. Current will then flow more readily in the direction along the strata than in the perpendicular direction. This condition is referred to as pseudoanisotropy. Exactly the same laws as in the condition of true anisotropy describe the electrical field in this condition of pseudoanisotropy.

It is important to note that in an anisotropic medium the Laplace's equation does not hold. Generally, anisotropy of a subsurface layer cannot be detected by means of resistivity sounding measurement.

Effect of Continuous Change of the Resistivity

One other assumption underlying the usual procedures of VES interpretation is that the resistivity in each of the layers is constant. This

assumption represents an approximation to the situation occurring most frequently in the subsurface. However, there are also situations in which the resistivity changes with depth in a continuous and more or less regular manner over an appreciable depth range. One of such situations is found where hard granitic or basaltic rock is overlain by a layer of weathered granite or basalt in which the degree of weathering, and hence the electrical conductivity gradually decreases with increasing depth.

The Effect of Slope on the Boundary Plane

Another assumption underlying the theory of resistivity interpretation is that the boundary planes between the resistivity layers are horizontal. In practice however,this assumption is hardly ever fully satisfied. It is therefore important to gain an impression of the order of magnitude of the influence upon the measurements of a slope of a boundary plane. Such an impression may be gained by restricting the consideration of a simple case: that of a two-layer structure with a boundary plane sloping at a constant angle.

Effect of Vertical Contact Planes

Mathematically, this case is to a certain extent a special case of the sloping boundary discussed above. Vertical contact planes in an otherwise homogenous ground can be used as an approximation in studying the influence of faults upon measurements.

All the factors discussed above can impose serious limitations on VES interpretation.

4.2 EM INTERPRETATION TECHNIQUES

The theoretical expressions for the EM 34-3 response at low induction numbers depend on the inequality

$WS^2 \ll 2\mu_o\sigma$ (McNeill, 1980). Given this condition, the simplifying assumptions can be made that induced current flow is horizontal, there is no interaction between different conductive beds and hence that secondary field contributions at the ground surface from conductors can be added directly (McNeill, 1980). Furthermore, under the same constraints by which the instrument is designed, the depth of penetration is limited only by the intercoil spacing. It can be said that the depth of penetration is "source" or "geometry" dependent rather than "skin depth" limited since it is now controlled by the fall-off with distance of the bipolar transmitter field.

The response of the EM 34-3 to conductivity changes is presented in four ways as follows:

(a) LINEARITY RESPONSE

At high conductivity values the indicated conductivity is no longer linearly proportional to the actual conductivity. This effect is however more severe for the vertical dipole mode of operation as shown in fig. 4.1 which illustrates indicated "vs" true ground

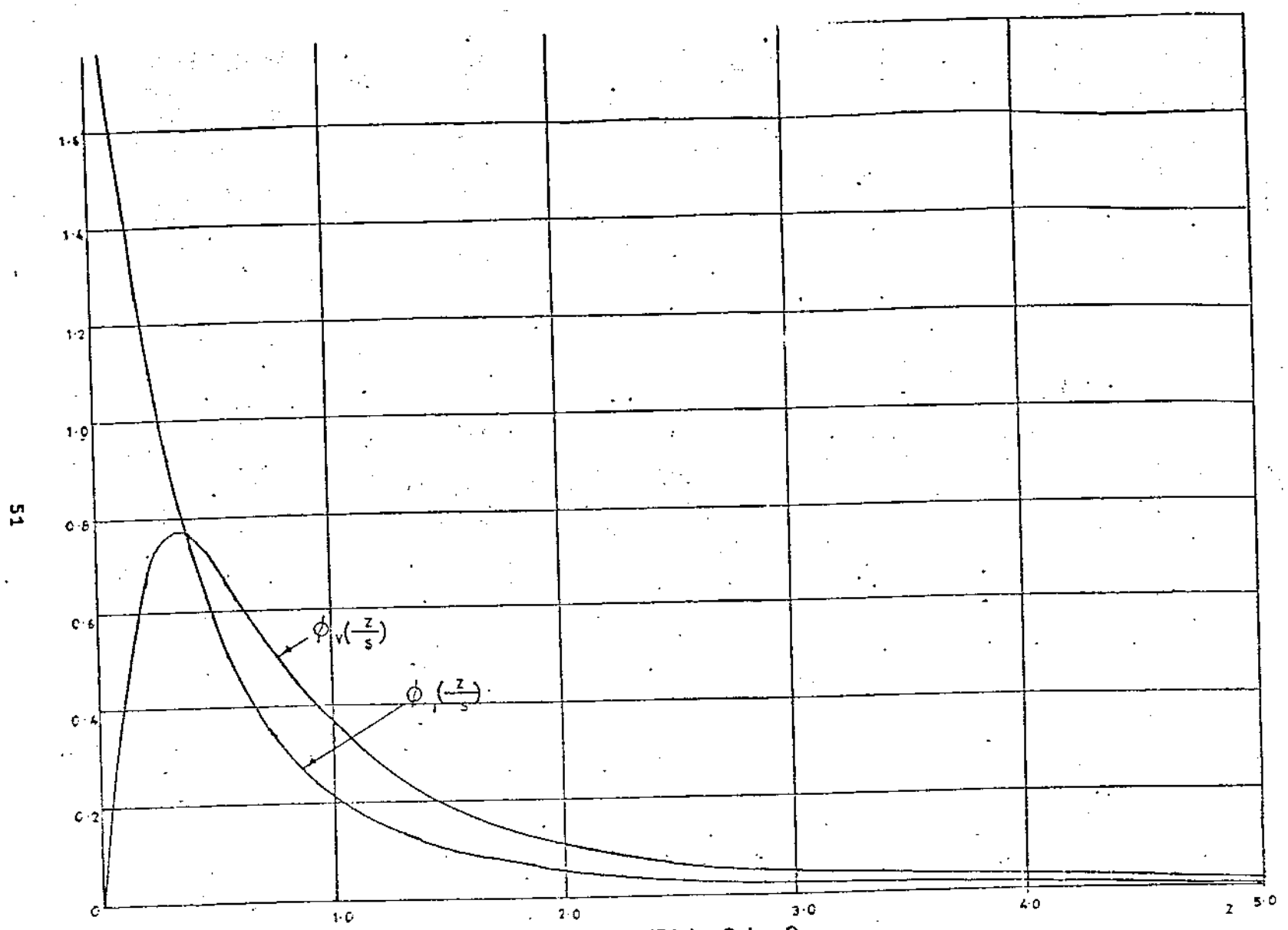


FIG. 4.2 EM 34-3
RELATIVE RESPONSE VS DEPT

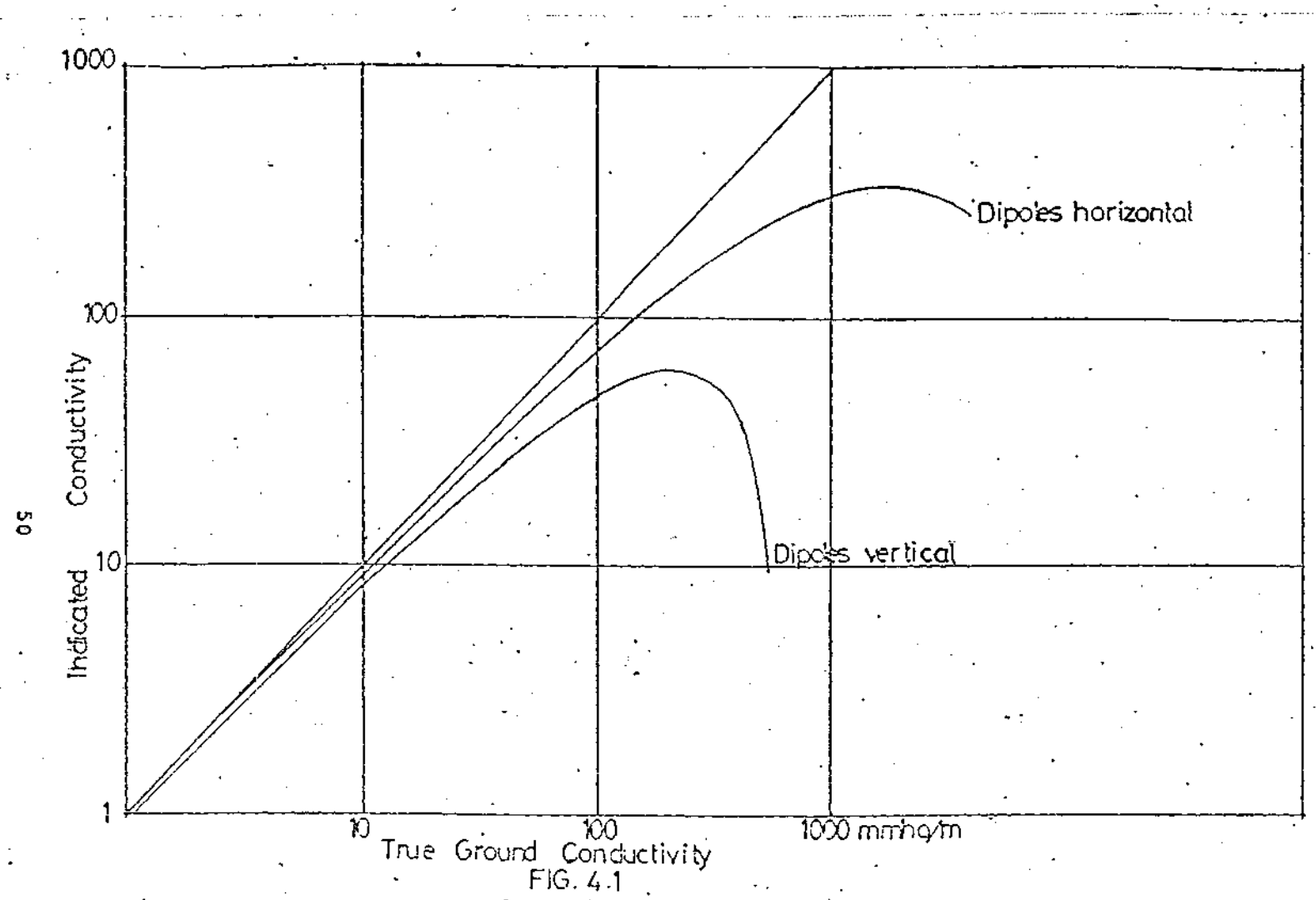


FIG. 4.1

EM 34-3

INDICATED VS TRUE CONDUCTIVITY

conductivity for both operating configurations.

The curves indicate that for ground conductivity in excess of 700 mho/m, the indicated conductivity in the vertical dipole mode falls to zero, and in fact for greater conductivity it becomes negative.

(b) RELATIVE RESPONSE WITH DEPTH.

It is possible to calculate the relative response from material at different depths for either coil configuration. Fig 4.2 shows the results for the EM 34-3. The X-axis is the depth divided by the intercoil spacing. The great difference in the response to near surface material from the two coil configurations is important; the horizontal dipole mode will be relatively sensitive to variations in the near surface material whereas the vertical dipole mode will be relatively insensitive to such changes. This fact is very useful in the interpretation of EM sounding and profiling data.

(c) DIKE - LIKE RESPONSE

When employed in the vertical dipole mode the EM 34-3 operates as a quadrature - phase horizontal loop instrument and as such is capable of detecting dike-like targets of low conductivity - thickness product in resistive ground. To yield a characteristic response the target must, of course, have a thickness that is substantially less than

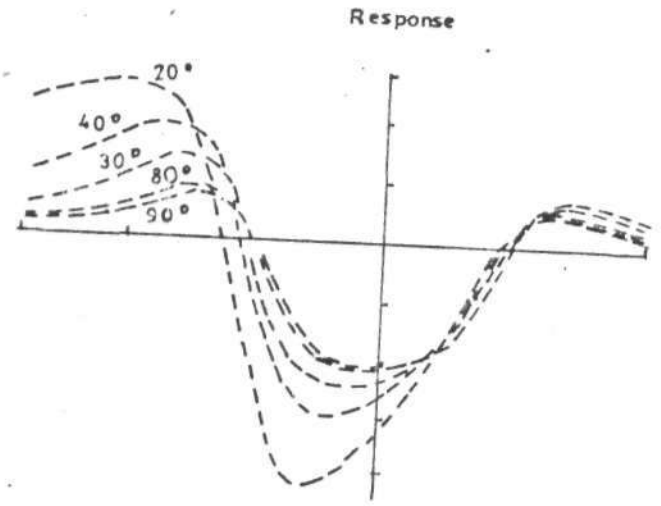


FIG. 4.5

EM 34-3

VERTICAL DYKE

Effect of varying dip on profile shape

the intercoil spacing (McNeill, 1980).

In general, for horizontal conductive layers, increased conductivity and/ or thickness results in a positive response or anomaly. However, dike-like conductive bodies produce relatively negative anomalies with a shape, which is diagnostic of dip (fig 4.3).

CHAPTER 5

INTERPRETATION

5.1 INTRODUCTION

Interpretation of geophysical data entails expressing in geological terms the information acquired from geophysical field measurements. Quantitative interpretation of geophysical data is more meaningful with the availability of reliable and abundant geological controls. Consequently, a meaningful qualitative interpretation of the data obtained in the form of horizontally stratified layers of different geoelectric characteristics require abundance of reliable stratigraphic control (Ako, 1982). Such controls are often obtained from borehole data. Fortunately, two boreholes are located within the study area and as such, the interpretation presented in this work was based on the borehole information as well as the resistivity of earth materials presented in tables 5.1 and 5.2.

Two geophysical techniques namely; the D.C. resistivity and the electromagnetic (EM) methods were employed for this study.

The assumption made for the resistivity interpretation was that each layer of rock in the area was electrically homogenous and isotropic.

The data analysis for the vertical electrical sounding was performed using Zohdy's new method for the automatic interpretation of Schlumberger and Wenner sounding curves (Zohdy and Bisdorf, 1989).

This method was used to obtain the equivalent n- layer model from the

apparent resistivity curve of each sounding as typified by fig.5.1a. The resulting true resistivity layer models from the application of this method is illustrated in fig.5.1b. The true resistivity model at each sounding were used to produce geoelectric sections along four profiles (figures 5.10 - 5.14).

The geoelectric sections were used for the interpretation of the VES data instead of discussing the individual soundings. Such interpretation can give a comprehensive picture of the subsurface configuration of the geoelectric layers underlying the study area since the sounding points were evenly distributed in the area. A discussion of each interpreted section as well as the deduced geologic sections is provided in the later part of this chapter.

The geologic sections were derived based on lithologies observed in the two boreholes found in the area (locations shown on fig.1.1) as well as the resistivity values of earth materials shown in Table 5.2.

Results of the electrical resistivity profiling as well as the EM profiling are also discussed below.

5.2 ELECTRICAL RESISTIVITY (ER) PROFILING

The results of the resistivity sounding were extended by taking additional resisitivity measurements using the Wenner electrode configuration with electrode spacings a = 10 m and 20 m respectively along four traverses Viz.; Profile 1, Profile 2, Profile 3, and Profile 4. The purpose of the resistivity profiling was to investigate the lateral variation in resistivity and also to investigate, at the depths

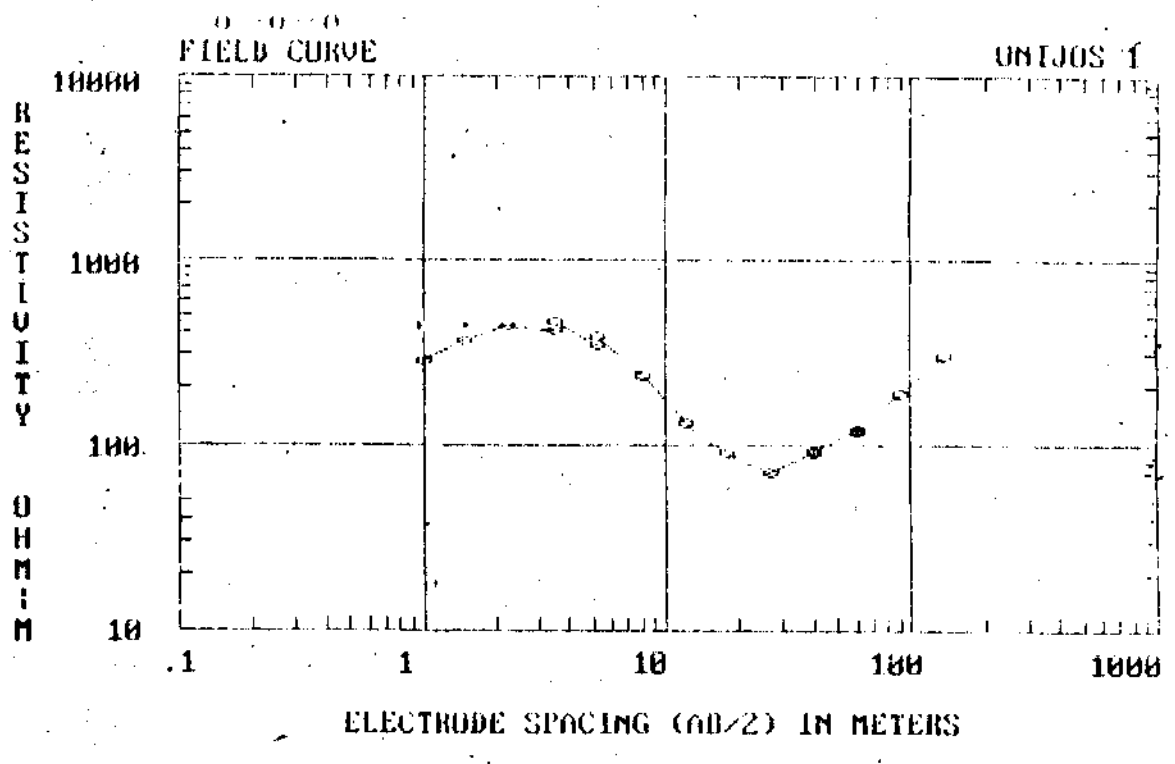


Fig. 5.1a Typical Field Curve

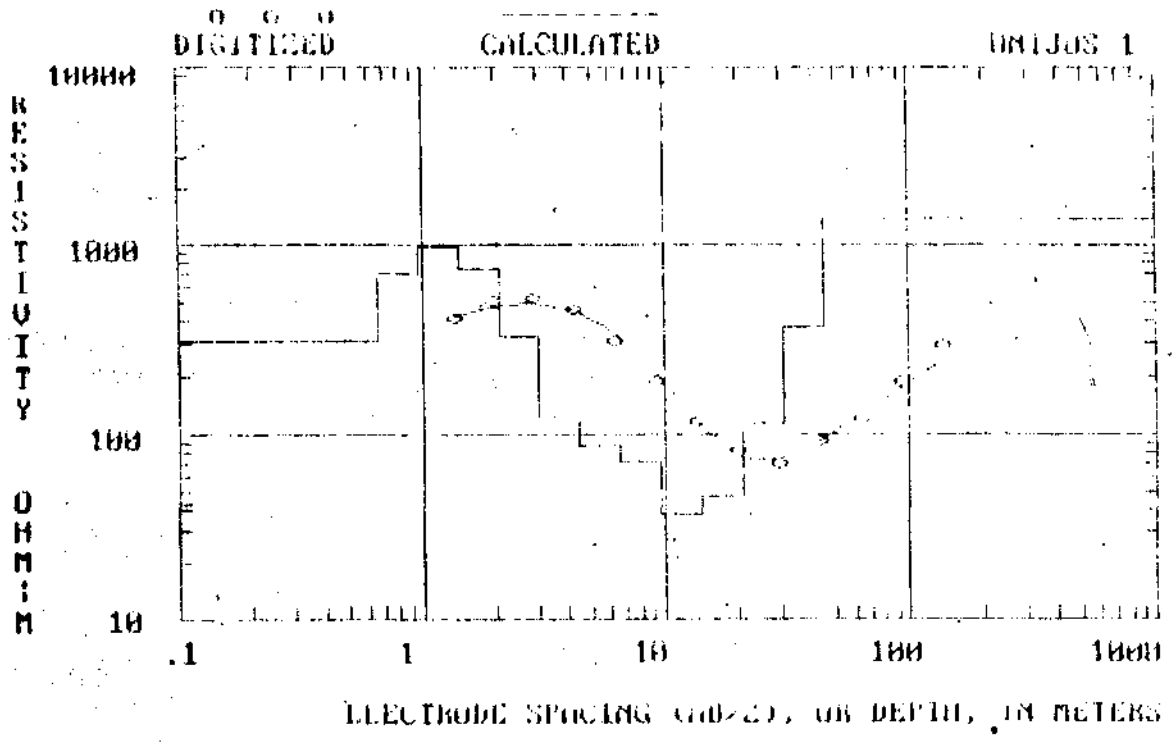


Fig. 5.1b True resistivity layer model

chosen, the areas along those Profiles that are probably weathered or fractured. Such areas are more favorable to groundwater occurrence in a basement terrain.

The four profiles were occupied randomly around the central region of the study area.

These Profiles were of lengths 630m, 520m, 450m, and 420 m respectively.

Generally, linear geological features such as veins, dikes, faults, buried channels e.t.c, have certain significances in mineral exploration, groundwater investigation, engineering site investigation as well as geological mapping. The delineation of such features by the geophysical method involves the running of profiles at an angle, preferably orthogonal to the strike of the feature for maximum resolution (Ojo *et al., 1995*). In this study however, the resistivity profiling was carried out mainly for groundwater studies. Results of the resistivity profiling measurements are shown in figures 5.2 - 5.5.

5.2.1 PROFILE 1

Figures 5.2 (a) and (b) show the results of the ER profiling measurements made on profile 1 for electrode separations (a) of 10 m and 20 m respectively.

The interesting features on fig. 5.2a are the low resistivity values. (55 - 105 ohm-m) indicated between distance 50-100 m, 350-400 m and between 520-560 m from the beginning of the profile. These low resistivity values would indicate that the layer is weathered at these points and may contain some considerable amount of water (Onu & Ajakaiye, 1990). The moderately high resistivity values

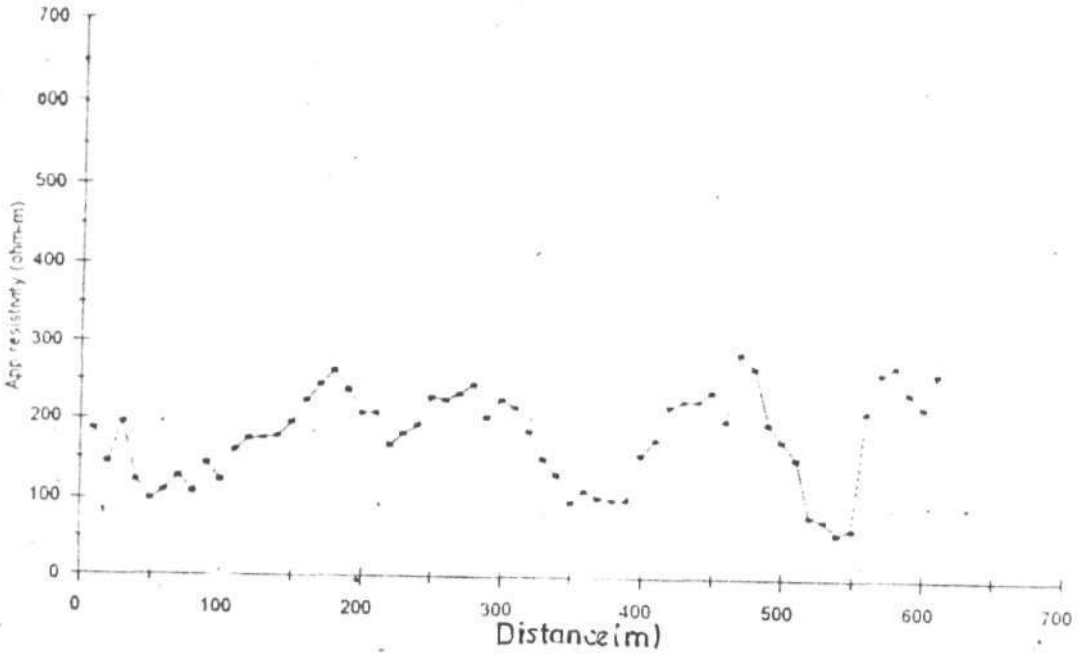


Fig. 5.2a a = 10m

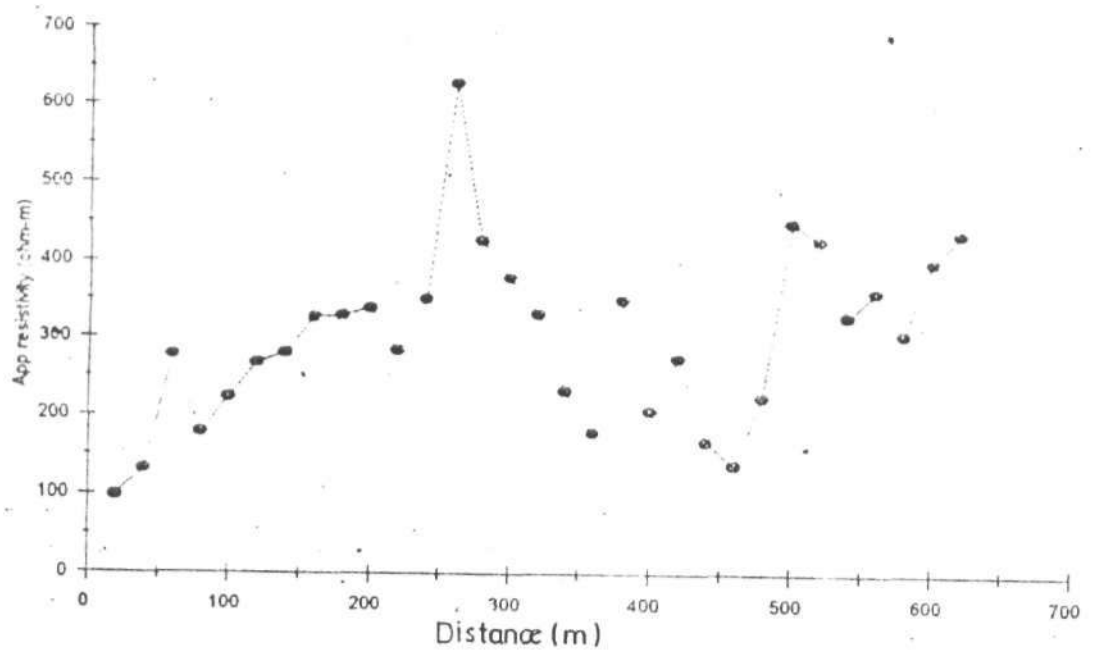


Fig. 5.2b a= 20m

Fig. 5.2 Resistivity profile 1

(200-300 ohm-m) occur between the start of the profile and 40 m, 100 to 350 m, 400 to 500 m and beyond 550 m on the profile. The resistivity range suggests a weathered material, though, of lesser degree of weathering as delineated by resistivity sounding.

The curve for a = 20 m (fig 5.2b) follows almost the same pattern as for a = 10 m, though the resistivity values at this depth are appreciably higher. At this depth one would think that the resistivity values are affected by the coarseness of particles in the moderately weathered region.

5.2.2 PROFILE 2

The curves for profile 2 using the same set of electrode separation as in profile 1 are shown in figure 5.3(a) and (b). Both curves exhibit a similar pattern with lower resistivities (less than 100 ohm-m to 280 ohm-m) occurring between 10 m and 100 m and between 250 m - 450 m from the beginning of the profile. Higher resistivity values (360 to 500 ohm-m) occur around the center of the profile (between 120-250 m) and beyond 450m. This suggests that the geoelectric layer at this depth is composed of rocks that are only moderately weathered. Again the resistivity values for fig. 5.3b are higher than in fig.5.3a. This difference in the resistivity values is interpreted to be due to the degree of weathering which reduces with depth.

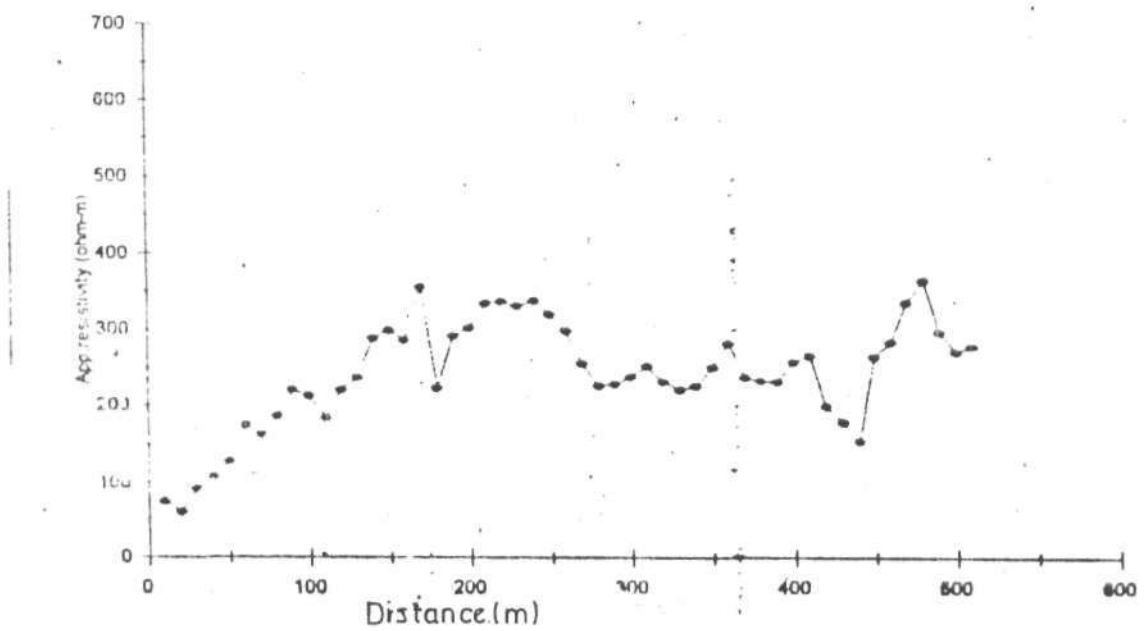


Fig 5.3a a = 10m

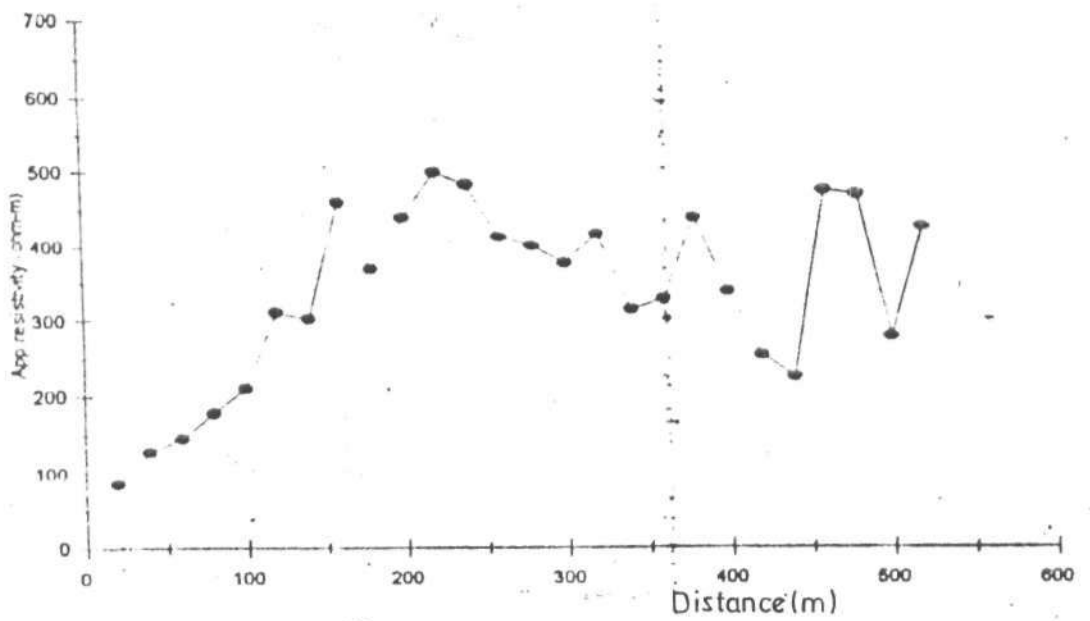


Fig 5.3b a = 20m

Fig 5.3 Resistivity Profile 2

5.2.3 PROFILE 3

Figures 5.4 (a) and (b) present the curves for profile 3. Both curves are generally characterized by low resistivities (0 - 200 ohm-m). However, there are some spikes (between 100 and 150 m and around the 230-m position) on the 10-m electrode separation. Such spikes could be due to lithological inhomogeneities (Ako et al, 1978).

A common feature on the two curves are the very low (near zero) resistivities observed between 280 m and 330 m (fig. 5.4a) and between 300 m - 380 m from the start of the profile (fig 5.4b). These very low resistivity values suggest the presence of a clay regolith.

5.2.4 PROFILE 4

Curves for profile 4 are shown in figures 5.5(a) and (b). Like in profile 3, the two curves follow a similar pattern. The curves reveal an area of large lateral extent of uniform low resistivity values except, for the spike around the 350-m point in both cases.

The range of resistivity values suggests that the formation is of identical rock type, perhaps with varying degree of weathering or compaction at depth. Such formations are more favorable to groundwater occurrence.

Thus, results of the resistivity profiling have shown that,within the depths of 10 m and 20 m probed, the profiles are underlain by the weathered basement rocks.

The degree of weathering however, differs from place to place along those

LIBRARY

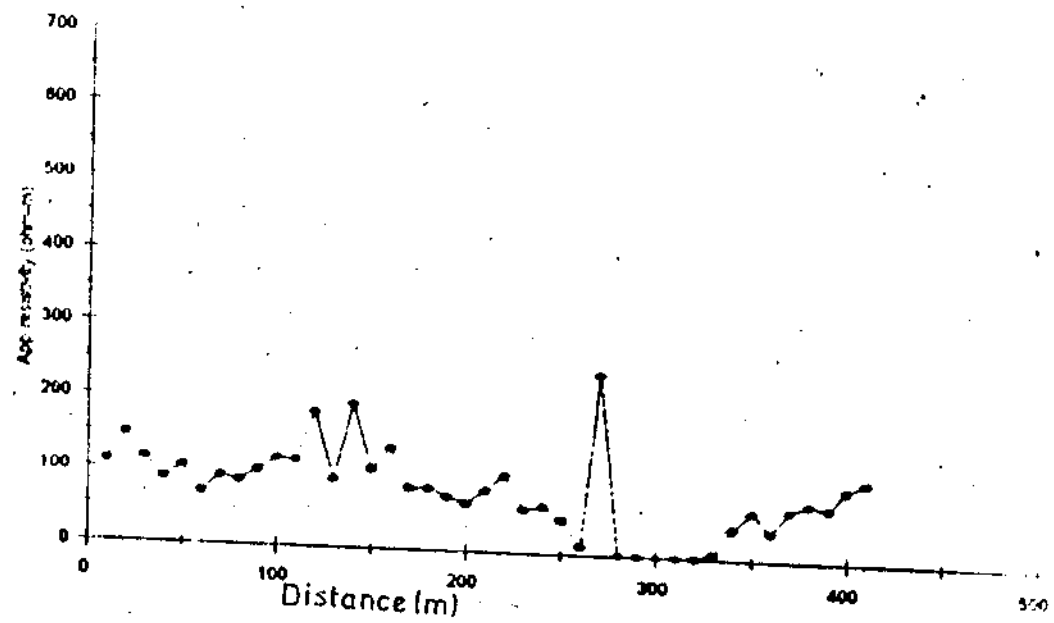


Fig. 5.4a a = 10m

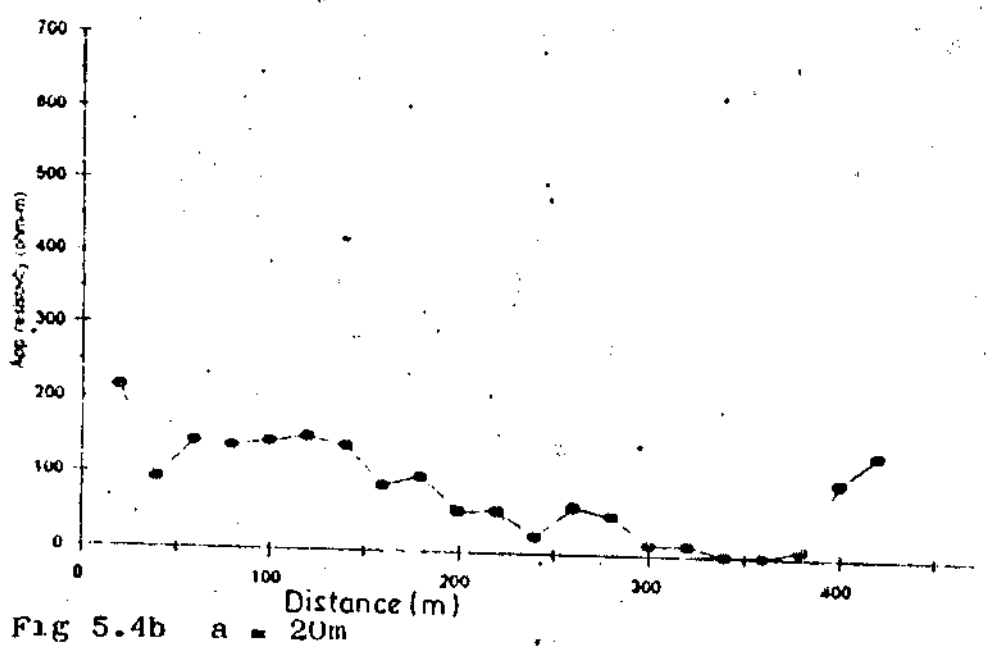


Fig 5.4b a = 20m

Fig 5.4 Resistivity Profile 3

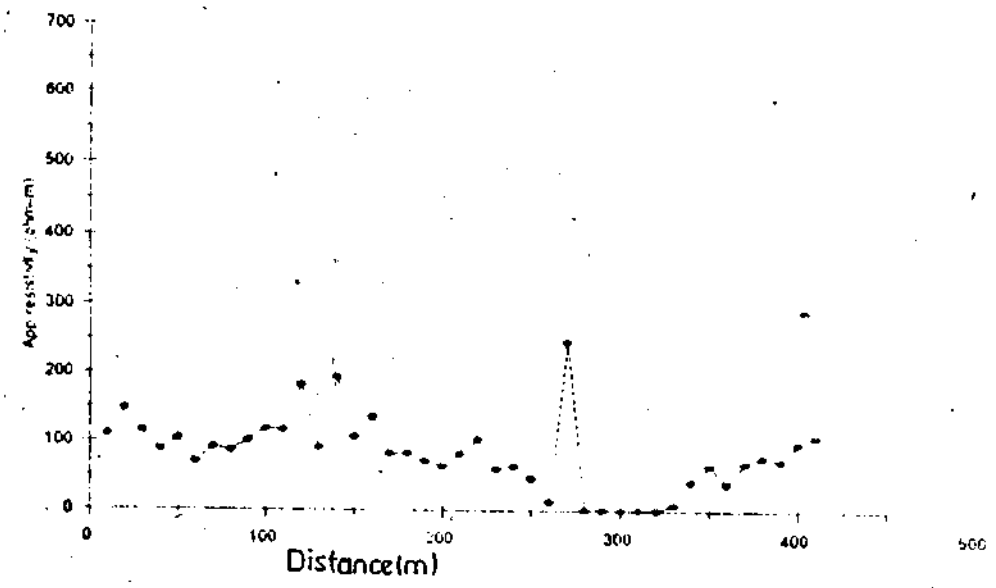


Fig. 5.5a a = 10m

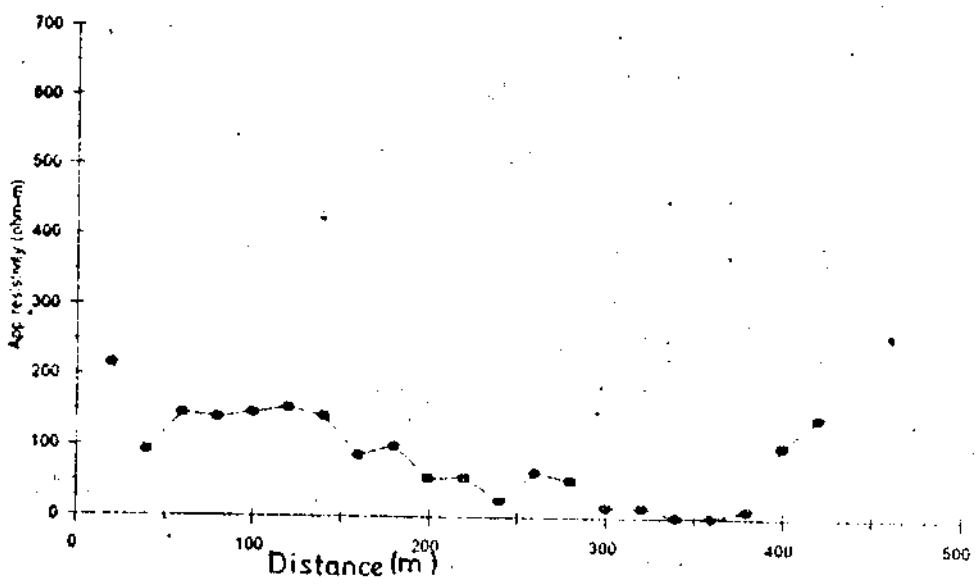


Fig. 5.5b a = 20m

Fig 5.5 Resistivity profile 4

profiles. This is in fairly good agreement with the VES results.

5.3 ELECTROMAGNETIC (EM) PROFILING.

EM measurements were made along three traverses of lengths 710 m, 700 m and 500 m respectively. Two of the profiles were also the resistivity profiles. Coil separations, S = 10 m and S = 20 m were used and measurements were made in the horizontal (plane of the coils vertical) as well as the vertical (plane of the coils horizontal) dipole modes. The results of the EM profiling are presented in figures 5.6 - 5.8.

5.3.1 TRAVERSE 1

Figures 5.6(a) and (b) show EM curves for traverse 1, for S = 10 and 20 m respectively. This traverse was chosen to coincide with the resistivity profile 1 for the purpose of comparison. On each graph, both horizontal (σ_H) and vertical (σ_V) dipole curves are presented.

The EM conductivity values for S = 10 m vary from 3.0 - 11.0 mmho/m along the profile. The conductivity range for S= 20 m is much less at 0 - 8.6 mmho/m. In both cases, there is no indication of an anomalous zone on the profiles. However, in (a), the σ_V Curve shows some slight variations in amplitude, which may be an effect of irregularities in the thickness of the overburden (Ako, *et al.*, 1978). Moreover, the σ_v Curve at S = 20 m (fig 5.6b) indicate zero - conductivity values around the 340 m position and between 400 -

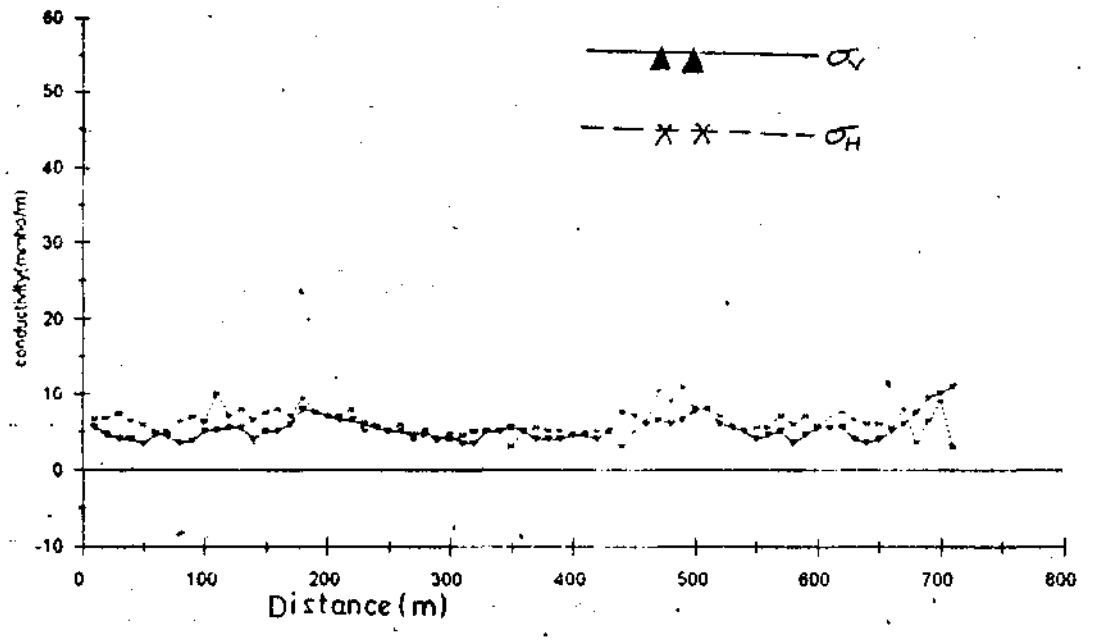


Fig. 5.6a S = 10m

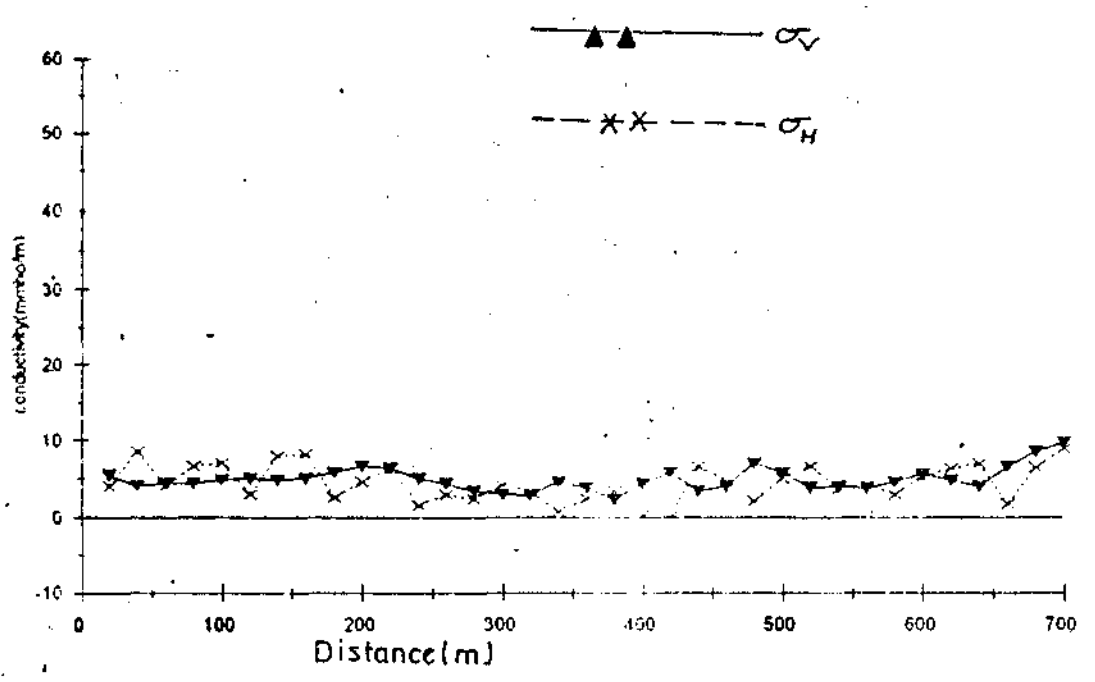


Fig. 5.6b S = 20m

Fig. 5.6 EM Traverse 1

- 420 m from the beginning of the profile. These zero conductivity zones indicate deep weathering zones and as such, are favorable regions for groundwater occurrence.

There is some reasonable agreement between the EM and th resistivity profiles on this traverse.

5.3.2 TRAVERSE 2

Traverse 2 was taken near a borehole with the borehole serving as a control. It is interesting to note that the maximum EM amplitude on this traverse occur just about the position of the borehole.

The EM curves obtained on traverse 2 are shown in figs 5.7 (a) and (b). A careful examination of the two curves reveal a similar pattern. The conductivity values for S = 10 m (fig 5.7 (a) vary from - 2.0 to 43.0 mmho/m whereas those for S= 20m range from - 1.9 to 26 mmho/m. Both curves show a strong positive anomaly at about 100 m(borehole position) from the beginning of the profile. Such high amplitude EM anomalies indicate large weathering thickness, and may be favorable for ground water occurrence (Olorunfemi *et al.,1995*). Moreover, the indicated anomaly is close to BH.NO.1 which has a yield of 2.0 litres/sec. VES 5 taken close to the borehole has also indicated a large weathered layer thickness.

The most interesting feature on the curves is the negative anomaly which occurs at about 310 m from the start of the profile. This negative feature has a

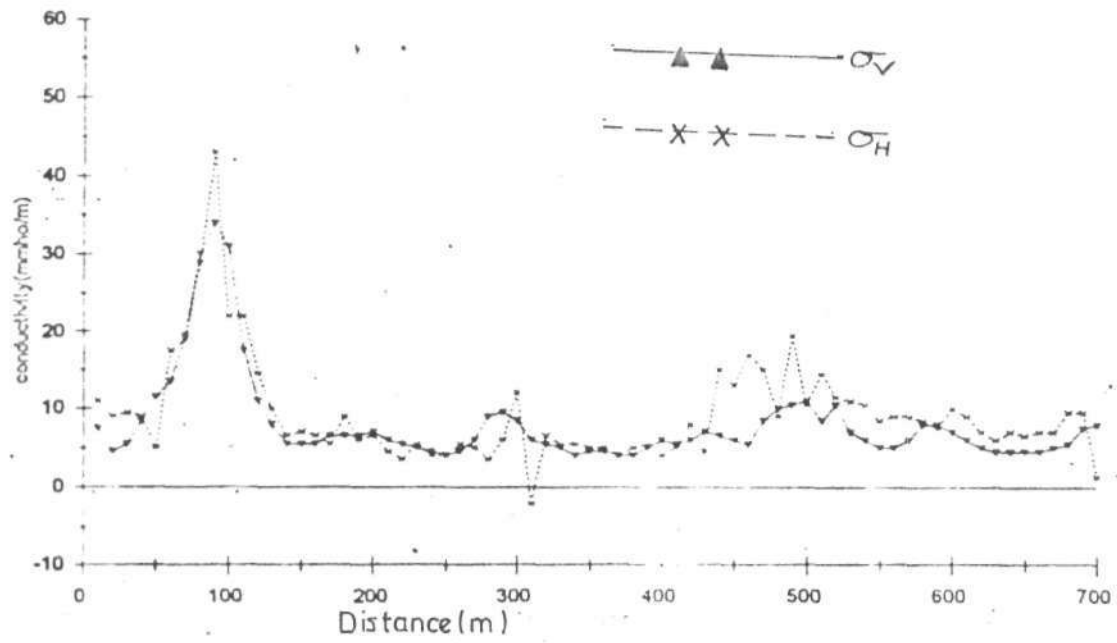


Fig. 5.7a S = 10m

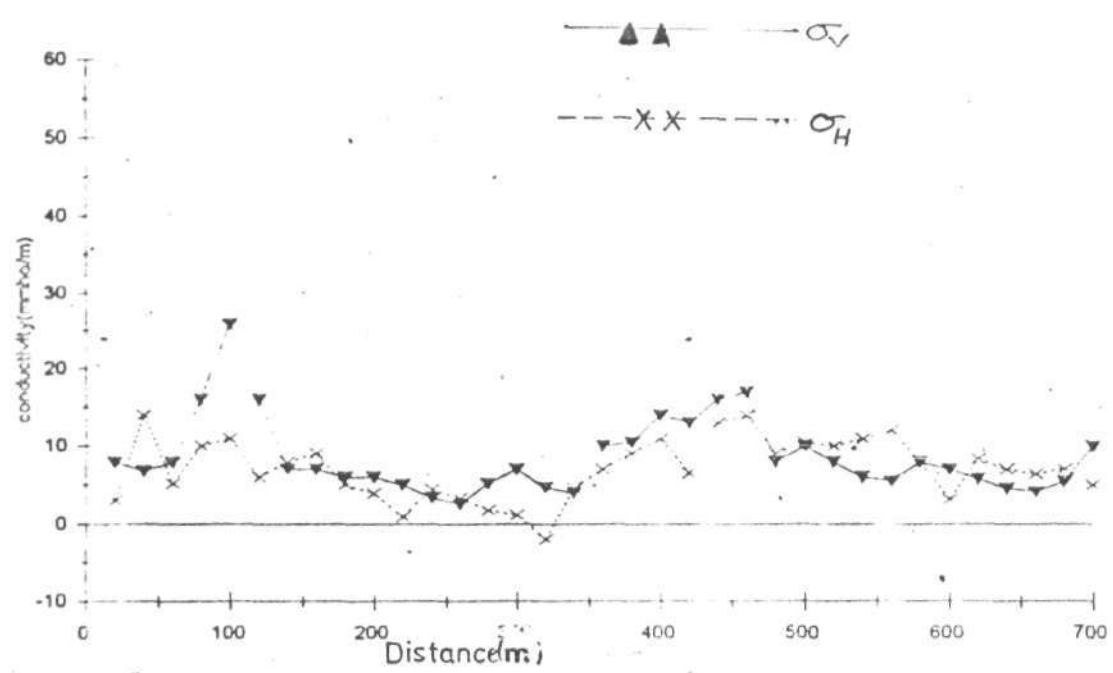


Fig. 5.7b S = 20m

Fig. 5.7 EM Traverse 2

positive shoulder on the left of the anomaly suggesting a dipping fracture zone or basement step, and perhaps a suitable site for a water borehole (Hazell, *et al.*, 1988; Palacky *et al.*, 1981 and Carel De Rooy *et al.*, 1993).

5.3.3 TRAVERSE 3

Figures 5.8(a) and (b) show EM curves obtained on traverse 3. The EM conductivity values for S = 10 m range from O - 48 mmho/m along the profile while those for S = 20 m vary from -2.4 to 52 mmho/m. In Fig 5.8a, there are three anomalous conductivity zones. These occur at 100 m, 170 m and beyond 450 m from the begining of the profile. The high amplitudes indicated at these locations are suggestive of large weathering thickness.

In Fig 5.8b, there is a wide variation in the range of EM amplitudes which suggests varying degrees of weathering thickness. Negative anomalies occur at about 160 m and 480 m from the beginning of the profile. The negative anomalies indicate fracture zones saturated with water. Such negative features are absent in fig.5.8a which shows that the causative body lies below the depth of 15 m probed with the horizontal dipole mode.

The trough-like anomaly, conspicuous at about 410 m is suggestive of a fractured basement (Olorunfemi and Fasuyi, 1993).

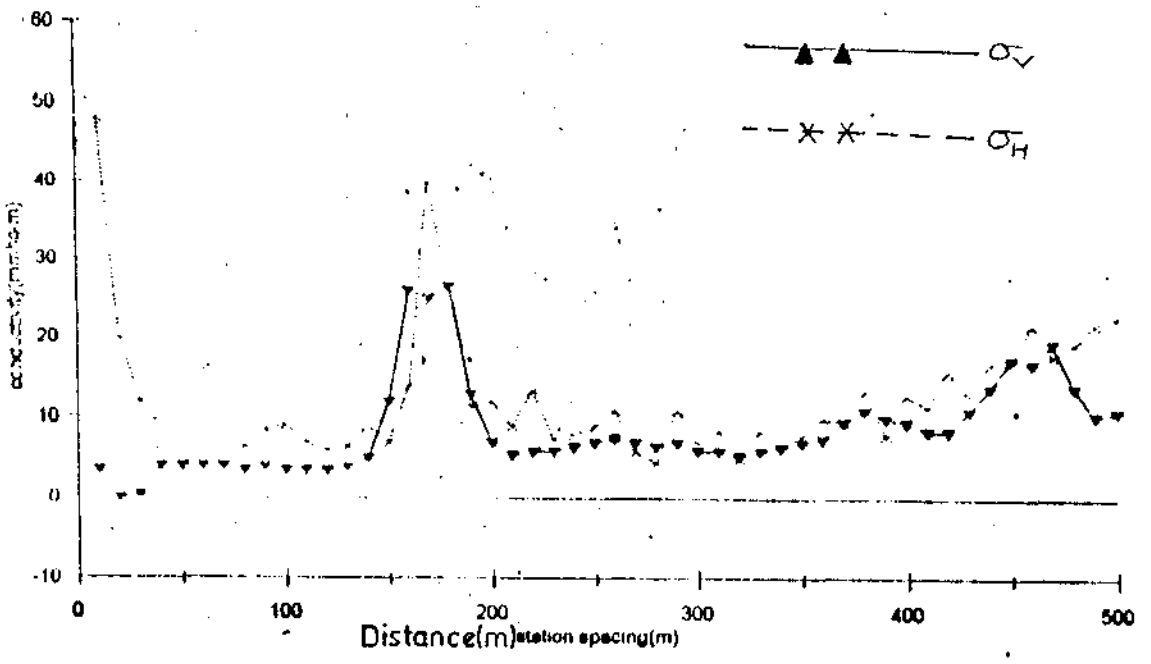


Fig. 5.8a S = 10m

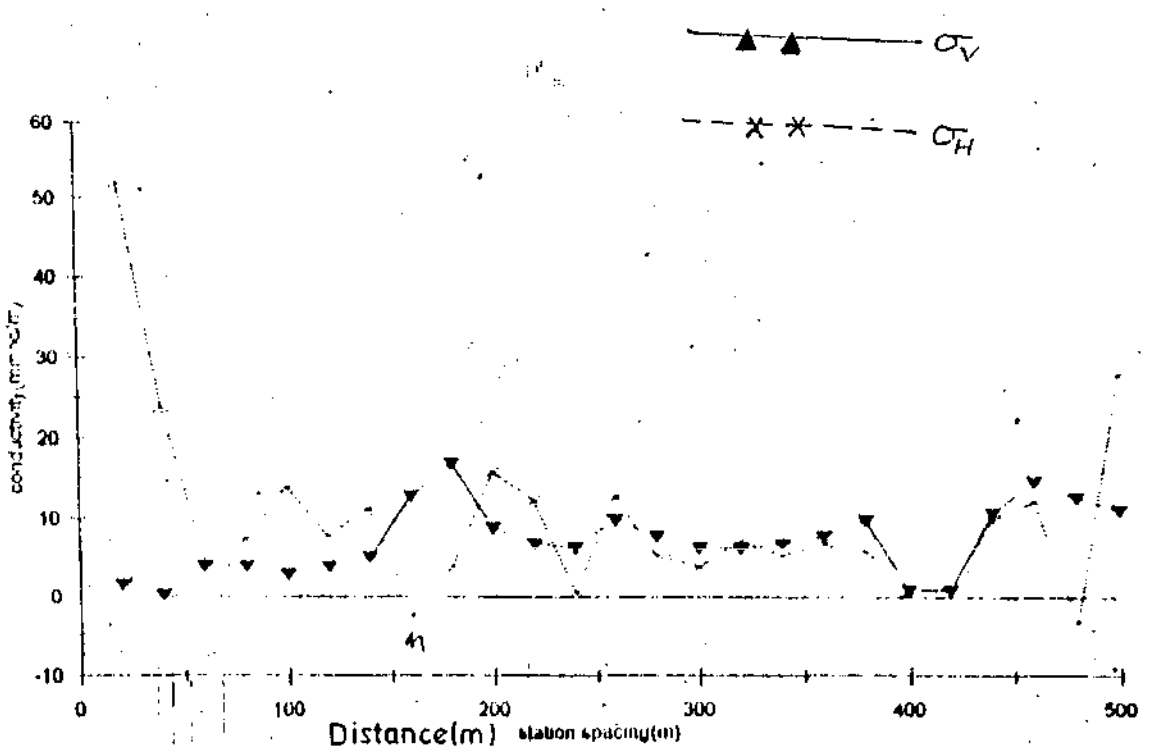


Fig. 5.8b S = 20m

Fig 5.8 EM traverse 3

5.4 QUALITATIVE INTERPRETATION OF VES AROUND BOREHOLE LOCATIONS.

Two boreholes are located within the study area. In order to correlate results of the vertical electrical sounding with the borehole lithologies a sounding was made near each of the boreholes.

It is proper to note that distinguishing between the different geoelectric layers is much easier for the n-layer models since small resistivity contrasts are easily picked. However, this is more pronounced at shallow depths. On the other hand, it is not possible to distinguish these small resistivity contracts through the borehole lithology. This is due to the possibility of increasing compactness with depth, saturation, coarseness or clay contents of individual formation. All the same, great care was taken in examining both the curves and the lithologic logs. The boreholes are designated as BH No 1 and BH No 2 respectively. The comparison is shown in figures 5.9(a) and (b).

5.4.1 BOREHOLE NO 1 (BH. NO1)

VES 5 was made near borehole No. 1. The result of the resistivity - depth plot on this VES point was correlated with the borehole lithology(5.9a). The sounding curve shows a five - layer geoelectric structure. The first layer has a resistivity of 320 ohm-m. This moderately high resistivity value could be due to weathered laterite. Underlying this first layer is a lower resistivity zone of 70 ohm-m. The third layer has a resistivity value of 376 ohm-m while the forth layer

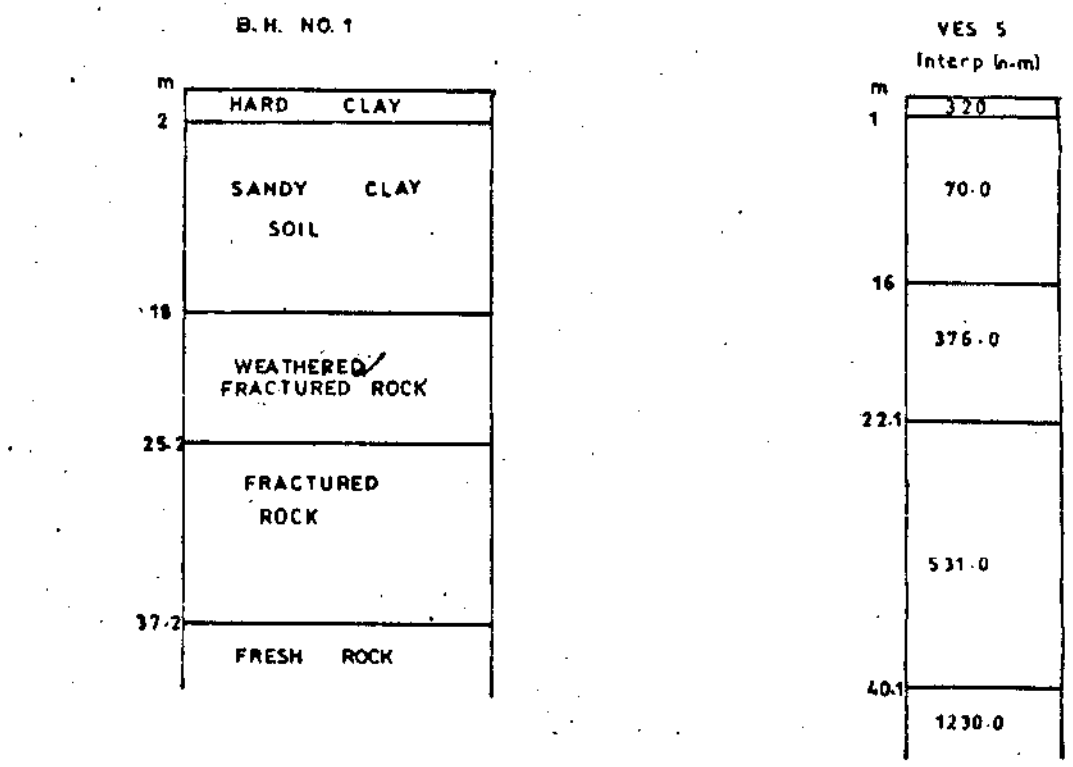


Fig. 5.9a VES Interpretion Compared with Borehole Lithology (VES 5)

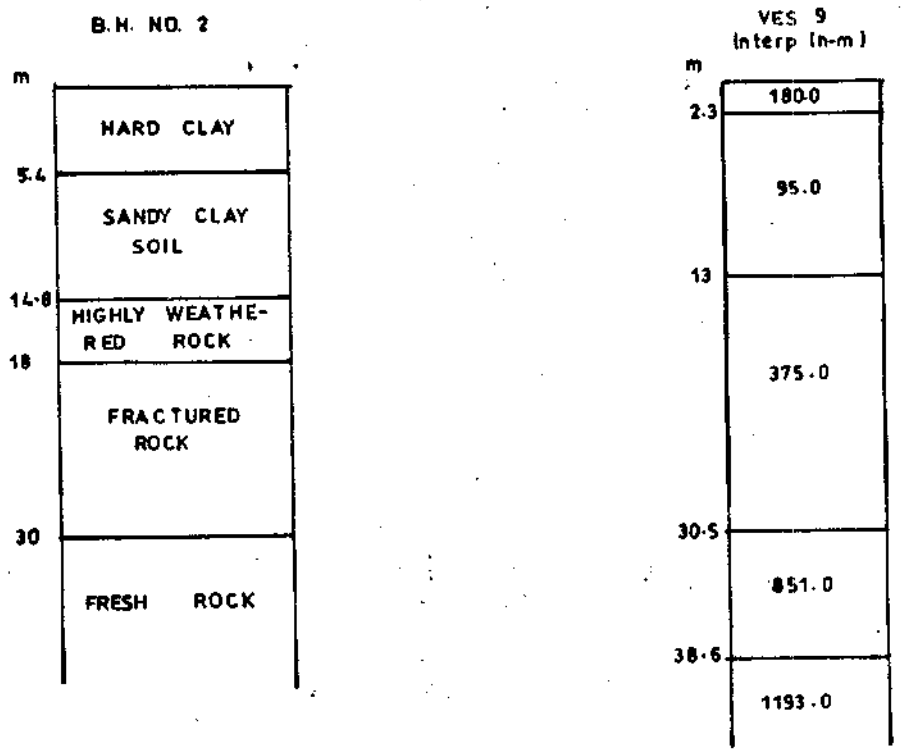


Fig. 5.9b VES Interpretion Compared with Borehole Lithology (VES9)

has a resistivity of 531 ohm - m. The last layer has a resistivity value of 1230 ohm-m. Comparing the resistivity results with the borehole lithology (fig 5.9a) shows that the second layer is supposedly whitish clayey sand,however, based on the resistivity ranges given in table 5.2, this layer is interpreted to be the weathered basement. The third layer is also interpreted to be a weathered layer though of lesser degree of weathering.The forth and the last layer are the fractured and the fresh basement rocks respectively. Result of the VES interpretation shows that the depth to the basement around VES 5 is 40.1m whereas, that obtained from the borehole lithology gives 37.2m.

5.4.2 BOREHOLE No.2. (BH. No.2).

VES 9 was taken close to BH. No.2 for the purpose of comparison of results. The sounding curve also indicates a 5-layer geoelectric structure. This is in fairly good agreement with the borehole lithology (Fig.5.9b). The first geoelectric layer has a resistivity of 181.0 ohm-m. A low resistivity layer of 95.0 ohm-m underlies this layer. The borehole lithology as well as the given resistivity ranges show that the first layer is composed of sandy clay. The second layer is taken to be the weathered basement. Thicknesses of these layers also correlate well. The third, 4th and 5th layers also correlate well with the borehole data.

5.5 ELECTRICAL RESISTIVITY SOUNDING

Based on Zohdy's method, the field curves for the study area were observed

to be generally of 3, 4 and 5 - layer types. These are of different shapes and characteristics depending on the formation layering. The Zohdy program produces a multi-layered model, which is then reduced to an equivalent 3, 4, or 5-layer model by considering the overall shape of the plot when a curve is fitted to the multi-layer model.

Most of the VES curves obtained are observed to have apparent resistivity values that decrease with increasing electrode spacing. Thus, in line with Sarma et al (1962), this is thought to be due to the following factors:

(1) Increasing water saturation of the formations towards the water table.

(2) Decreasing particle size from loose sand at the surface to fine silty sands and clays at depth.

(3) Increasing salinity (as the case may be) of formation water with depth.

However, for the study area the first two factors are the most likely to be responsible for this observation. Most of the curves are characterized by a final segment of positive gradient rising at an angle of about 45^0 to the horizontal axis indicating an infinitely resistive substratum.

Some of the curves show signs of minor distortion due to sudden jumps in values of apparent resistivity. This failure of the apparent resistivity curve (segments) to tie in with each other within the accepted error limit is for two reasons (Koefoed, 1979). The first is that the measurements are, in fact, made

with a symmetrical electrode configuration in which the ratio of the potential measuring electrode spacing to the current electrode spacing has a finite value (This ratio is referred to as the "eccentricity" of the configuration). Changing the distance between the measuring electrodes entails a change in the eccentricity of the configuration. The second reason is the occurrence of near-surface inhomogeneities in the ground. These inhomogeneities affect the current distribution pattern, and the relative change in the current density, which they cause, depends on the position of the measuring points with respect to the inhomogeneity. Hence the relative error in the measured potential difference changes when the electrodes are displaced. Such effects of the near - surface inhomogeneities are also apparent on the iso-resistivity maps. Other causes of such distortions may include; errors in measurement, current leakages, effect of topography etc. Great care was taken on the field to minimize these errors. In all the soundings, smoothening of the field curve was done manually as required by Zohdy, before running the program so as to overcome distortion effects. As a control, the soundings made close to the two existing boreholes were interpreted and their geoelectric sections displayed side by side with the borehole logs for comparison.

A summary of the VES interpretation is presented in Appendix A. The remaining VES curves (field and interpreted) are shown in Appendix B.

TABLE 5.1: Resistivity values for various rocks and sediments in the Basement Complex (Compiled from Olatinwo (1994); Ajayi and Hassan (1988); Shemang (1990).

ROCK TYPE	RESISTIVITY RANGE (OHM - M)
Dry sandy soil	> 250
Dry soil	> 300
Dry clay	> 150
Sandy clay	100 – 200
Laterite(fresh)	> 500
Basement Rock(fresh)	> 1000
Weathered basement	80 – 200
Fadama loam	30 – 90
Sand/Gravel with water	80 – 300

Table 5.2: Resistivity values used in deriving the geoelectric sections in the present work.

ROCK TYPE	RESISTIVITY RANGE(OHM - M)
Sandy clay and sandy silt	100 – 200
Fresh laterite	> 500
Weathered laterite	201 – 500
Weathered basement(fine)	30 – 200
Weathered basement(coarse)	201 – 500
Fractured basement	501 – 1000
Fresh basement	>1000

5.6 THE GEOELECTRIC AND GEOLOGIC SECTIONS

The geoelectric and geologic sections presented in this section are based on individual interpretations for each of the VES stations.

The geoelectric sections provide different resistivity boundaries for each profile. These geoelectric subdivisions were then assigned suitable lithological units based on borehole information as well as their characteristic resistivities to produce the geologic sections.

Geoelectric sections were derived along four profiles and designated AA', BB', CC', and DD' (figures 5.10 - 5.14). A brief description of each of the resulting geoelectric as well as geologic sections is presented below.

5.6.1. PROFILE AA'

FIG 5.10a shows the net geoelectric section obtained for the VES stations along profile AA'. The corresponding geologic section is shown in figure 5.10b.

The section suggests that the subsurface along the profile is made up of five geoelectric layers. The thickness of the first layer varies from 0.8 - 2 m with the thinnest part between VES 16, 17, 18 and 14, and it increases around VES 7 and 23. The resistivity of this layer ranges from 100 - 1200 ohm-m with an average of 530 Ohm-m.

The second layer has a resistivity value that ranges between 45 - 200 ohm-m. An examination of the whole profile reveal that this layer has the lowest

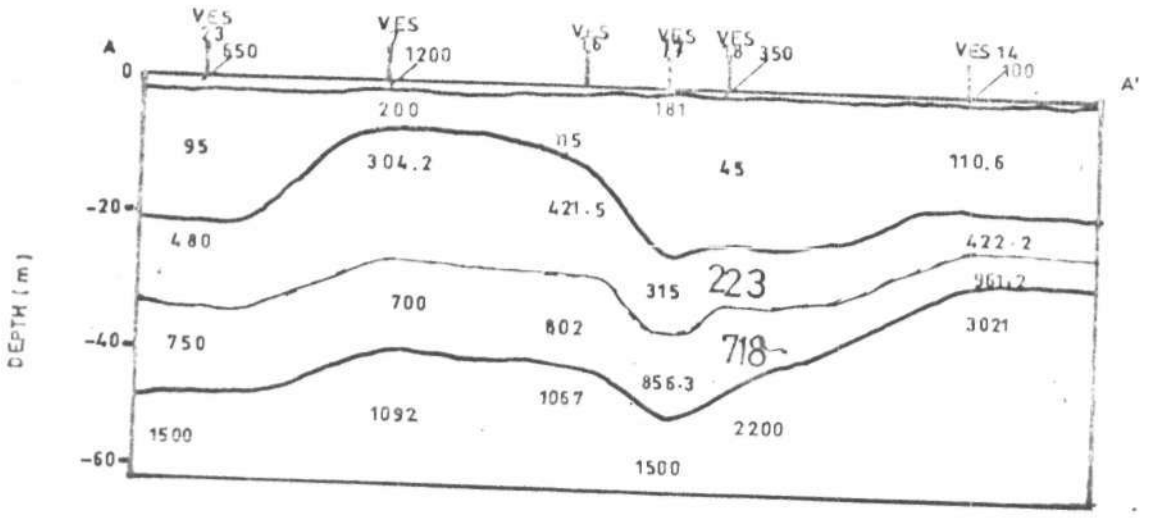


Fig 5.10a Geoelectric section

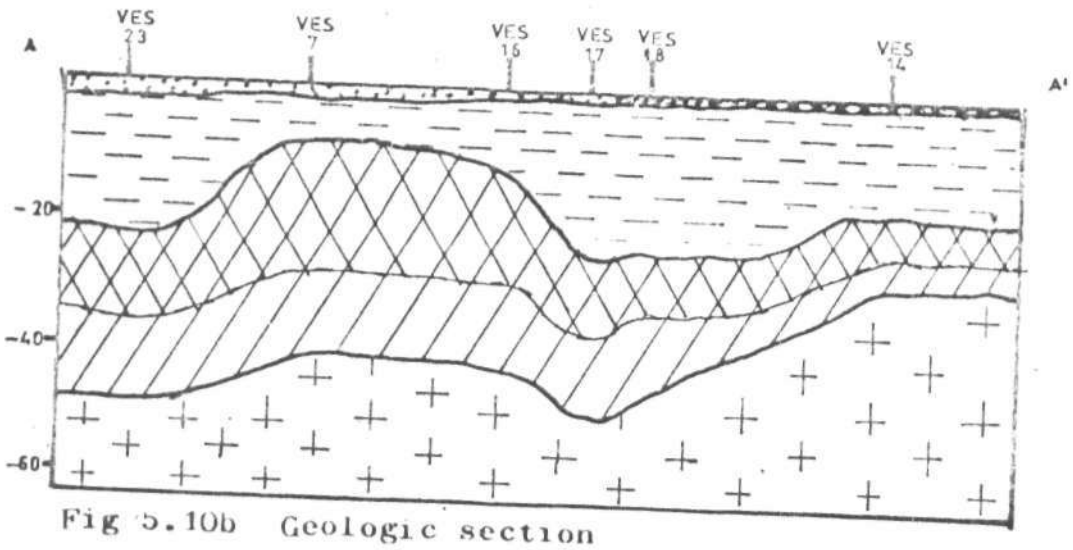


Fig 5.10b Geologic section

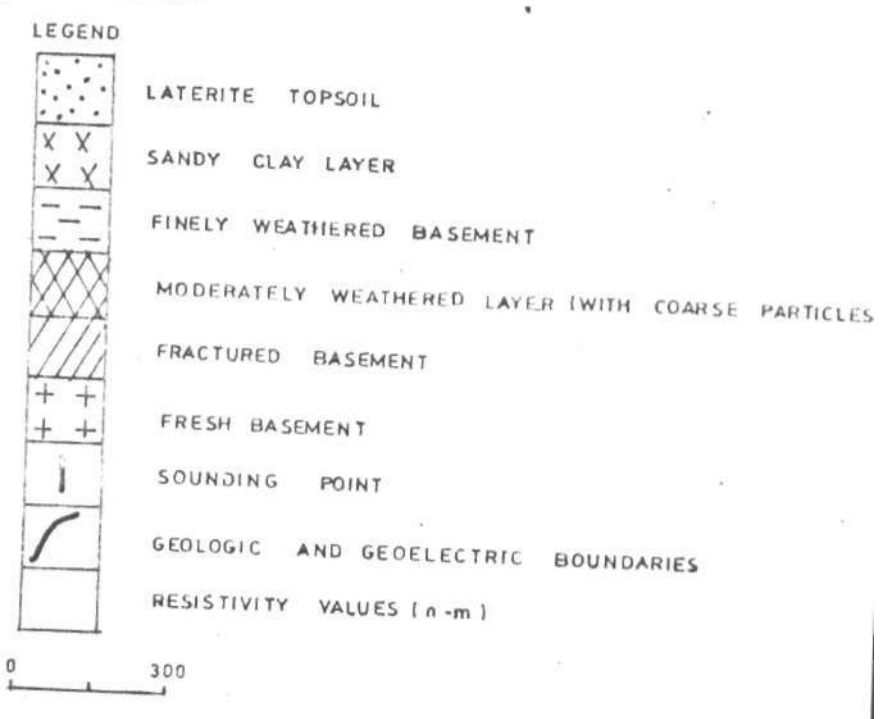


Fig 5.10 Geoelectric and Geologic sections for profile AA'

resistivity range and as such, is likely the most conductive layer under the profile.The thickness of this layer varies from 6.0 to 15.0 m.

The third layer on the section has resistivities that vary from 304.2 to 480 ohm-m. The thickness of the layer ranges from 7.0 to 21.0 m around VES 14 and VES 7 respectively.

The fourth layer on the profile has resistivity values in the range of 700 - 855.3 ohm-m. The thickness of this layer varies from 5 - 14 m, thinning out towards VES 14.

The fifth layer, and perhaps, the deepest layer under the profile, has relatively high resistivity values throughout the length of the profile. Its resistivity range from 1092 to 3021 ohm-m. This layer is of infinite thickness.

Figure 5.10b shows the geologic section corresponding to the geoelectric section along profile AA', The figure suggests that the first layer (top soil) may contain two different rock types. The high resistivity zone (300 - 1200) of the layer occuring between VES 23 and VES 18 is considered to be lateritic (depending on its degree of weathering). On the other hand, the fairly low resistivity value of 100 ohm-m found around VES 14 is probably a sandy clay horizon based on Table 5.2.

The figure also suggests that the second layer with a range of resistivity values between 45 and 200 ohm-m is the weathered basement. The low resistivity value of 45 ohm-m around VES 18 is suggestive of a weathered clay basement.

The third layer whose resistivity range between 304.2 - 480 ohm-m is still

weathered but is probably composed of coarse particles. Since the weathered basement constitutes the major component of the aquifer system in the Basement C omplex, the second and the third layers are taken as the aquifer layers for the study area.

The forth layer (resistivity range 700 - 961ohm - m) is probably fractured, though, form the range of its resistivity values, the fractures may be dry.

The fifth layer whose resistivity values range from 1092 to 3021 ohm-m is considered to be the fresh basement.

5.6.2. PROFILE BB'

The geoelectric section derived for the VES stations along Profile BB' is shown in fig. 5.11a. The section reveals a subsurface layering that varies from a 3-layer case around VES 13 to a 5-layer case along the remaining length of the profile.

The first layer on the profile has resistivity that ranges between 100 to 613 ohm-m while its thickness varies from 0.7 to 3.0 m. The thinnest part of this layer occurs around VES 5. The second layer which runs throughout the profile is of variable thickness from 13.0 to 36.0m being thickest around ves 13. The resistivity of this layer varies from 70 to 191.3 ohm-m. The third layer which is absent around VES 13, has a variable resistivity of between 300 to 450 ohm-m and its thickness varies from 7.0 to 16.5m.

A fourth layer underlies the entire profile. Its resisivity ranges from 501 to 1000

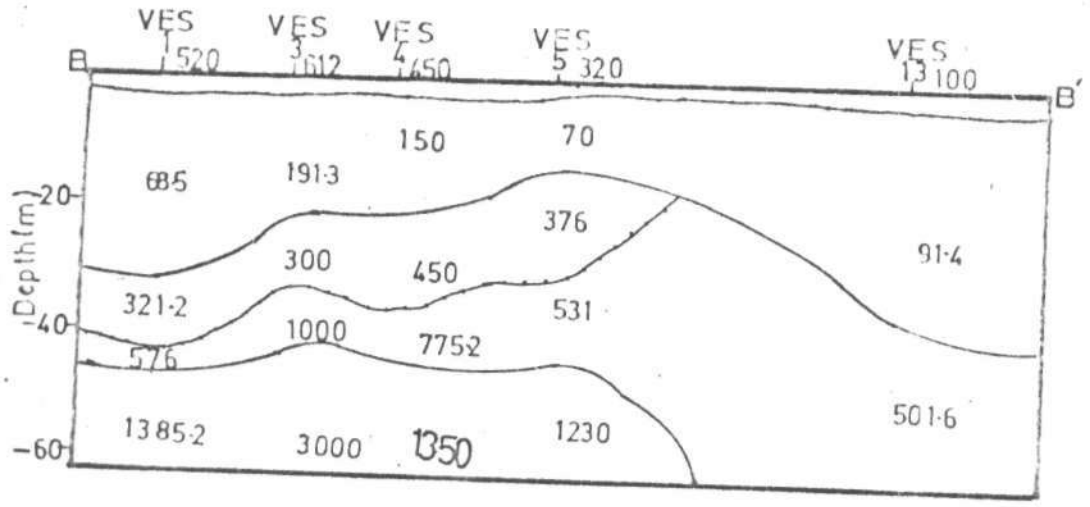


Fig 5.11a Geoelectric section

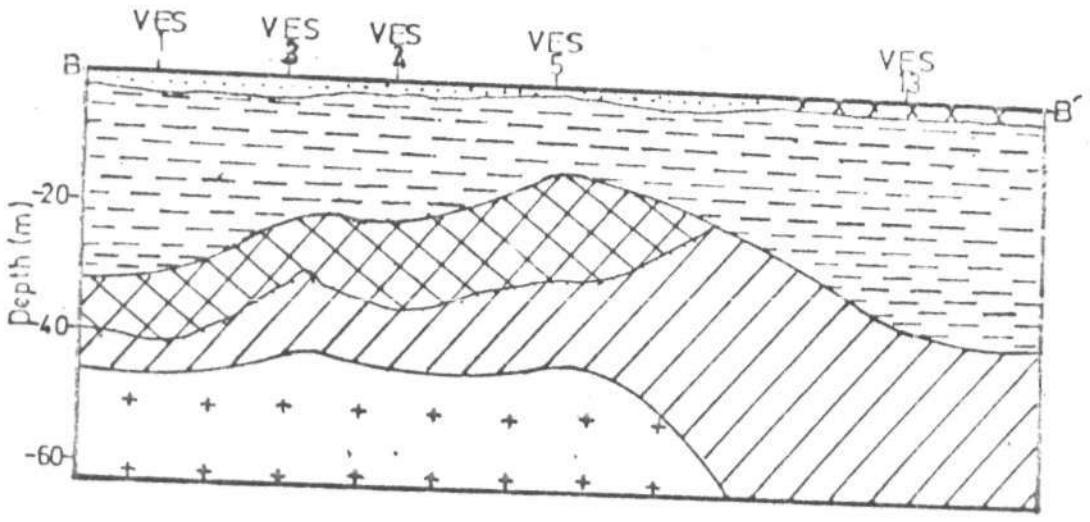


Fig 5.11b Geologic section

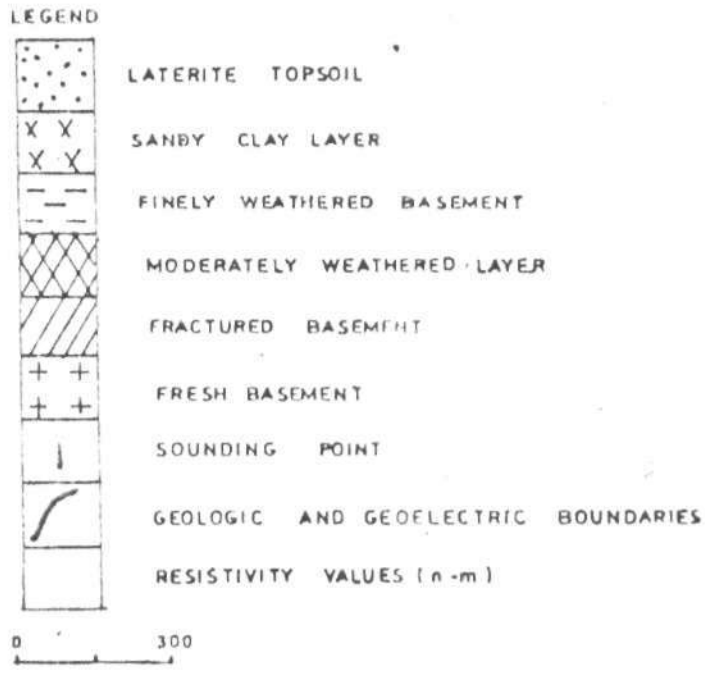


Fig 5.11 Geoelectric and Geologic section for profile BB'

ohm-m while it ranges in thickness from 5.0 to 25.5m. The fifth layer which is also absent around VES 13 has high resistivity values ranging from 1230 - 3000 ohm-m. This layer is of infinite thickness.

The deduced geologic section for Profile BB' is shown in fig 5.11b. The top soil here is composed of two soil types as in the case of Profile AA. The area between ves 1 and ves 5 where the resistivity values range from 320 - 613 is interpreted to be a weathered lateritic layer. The second zone is probably a zone of sandy clay owing to its resistivity value of 100 ohm-m. This zone occurs around VES 13.

The second layer on this Profile is interpreted to be the finely weathered basement based on its resistivity values of between 70 - 191.3 ohm-m.

Directly below the weathered basement is the third layer whose resistivity values range from 300 - 450 ohm- m. This layer is believed to be weathered also but is of lesser degree as compared to the second layer. This layer is absent around VES 13.

Underlying the weathered basement is a layer thought to be the fractured basement. The resistivity range for this layer suggests that the fractures may be saturated around VES 1. The fifth layer is the weathered basement (resistivity ranges between 1230 to 3000 ohm - m).

5.6.3. PROFILE CC'

Figure 5.12a shows the geoelectric section for Profile CC'. Apart from the

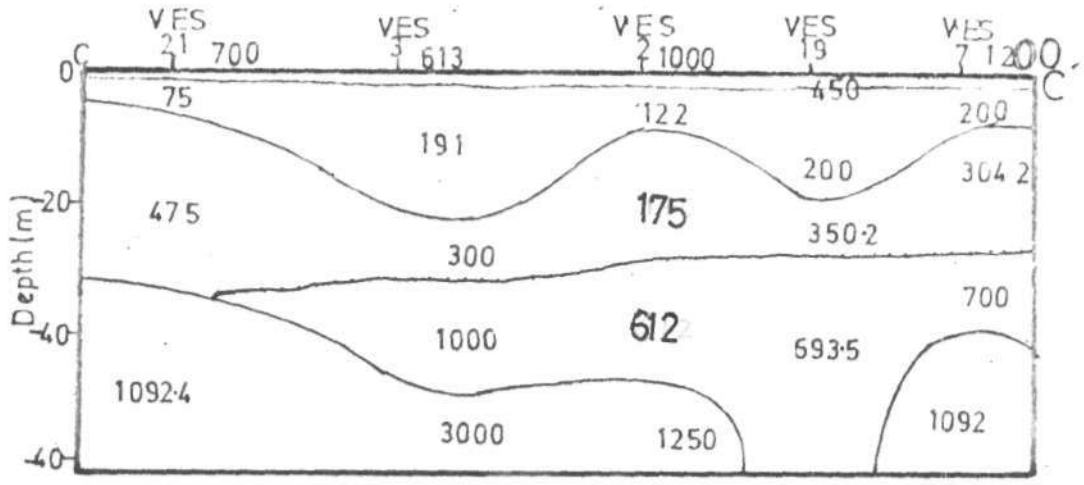


Fig.5.12a Geoelectric section

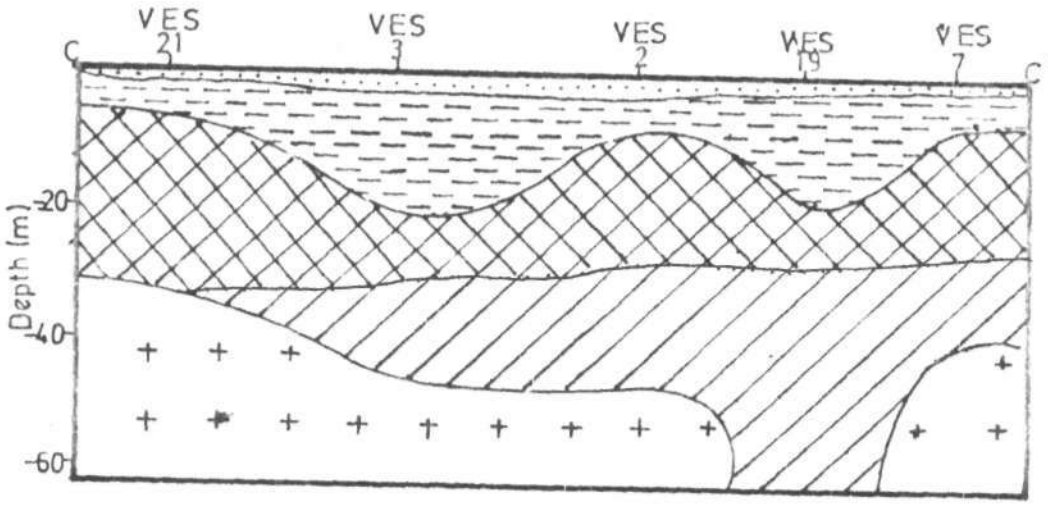
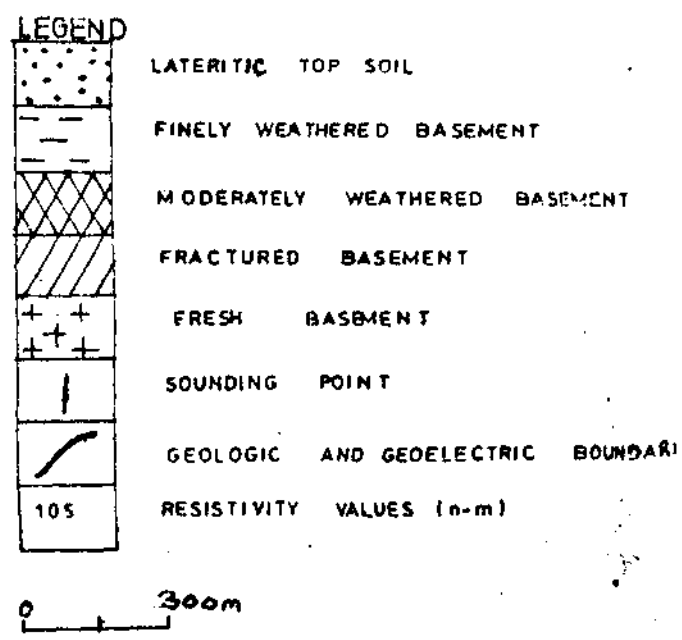


Fig.5.12b Geologic section

Fig. 5.12 Geoelectric and Geologic sections for profile CC′



layerings around VES 19 and 21 which are made up of 4 - layers, the remaining stations are made up of five geoelectric layers.

The first layer is a very thin layer of variable thickness (1.0 - 2.5m). The resistivity of the first layer varies from 450 - 1200 ohm-m. The second layer is of higly variable thickness (5.0 - 21.0m). The thickest point of this layer is observed around VES 3 while the thinnest area is around VES 21. The third layer has a resistivity range of between 300 - 475 ohm-m while its thickness varies from 8.0 - 27.0 m. The fourth layer which is absent around VES 21 varies in thickness from 9.0 - 18.0 m around VES 3, 2 and 7, being of infinite thickness around VES 19. The resistivity of this layer ranges from 693.5 - 1000 ohm-m. The fifth layer, which is the last layer, and absent only around VES 19 has high resistivity values that range from 1092 - 3000 ohm-m.

The deduced geologic section corresponding to the geoelectric section on Profile CC' is shown in fig. 5.12b. The figure suggest that the top layer is made up of the same lithological unit. The high resistivity values of between 450 - 1200 ohm-m is suggestive of a lateritic topsoil, depending on the degree of weathering.

The second and the third layers have resistivity ranges that are suggestive of a weathered basement. The only difference may be in the degree of weathering. Underlying the weathered basement is a layer thought to be fractured based on its resistivity range of 300 - 1000 ohm-m.

Below the fractured layer lies a layer of high resistivity (above 1000ohm-m).

This layer is probably the fresh basement.

5.6.4 PROFILE DD'

The geoelectric section for this profile is shown in fig.5.13a. The section shows a 3-layer case around VES 10 and 13, the remaining VES stations on the profile show 5 - geoelectric layers.

The resistivity of the first layer ranges from 32 - 300ohm-m. Its thickness is highly variable with the thickest points observed at VES 10. The layer is thinnest around VES 16.

The second layer has a resistivity that ranges from 91.4 - 115 ohm-m. The thickness of the layer goes from 11.1 - 33.5 m. The third layer has a resistivity of between 325 - 421.5 ohm-m and it is absent around VES 10 and 13. The thickness of this layer varies from 10.0 - 17.0 m. Directly below the third layer is a fourth layer which is absent around VES 10. The resistivity of this layer ranges from 501 - 802 ohm - m, while its thickness vary from 1.5 around VES 13 to 12m around VES 8. The fifth layer underlies VES 8 and 10. This layer has a high resistivity range of between 1067 - 1750 ohm-m.

The geologic section derived for Profile DD' is shown in fig 5.13b. The section suggest that the top layer is made up of three lithological units. The restivity values observed around VES 8 and 13 is suggestive of sandy clay formations. The top soils at VES 16 and 10 is likely to be weathered laterite and wet clays respectively. This is evident from the range of their resistivity values.

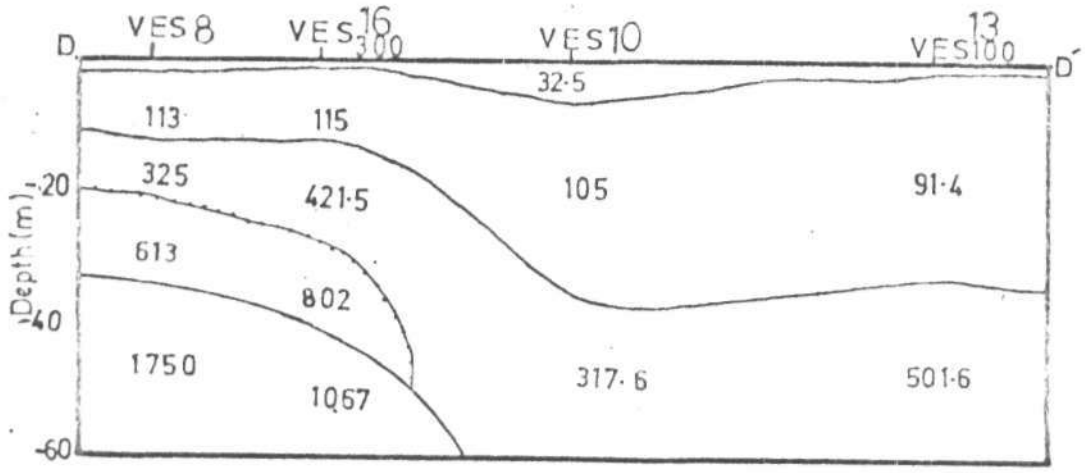


Fig. 5.13a Geoelectric section

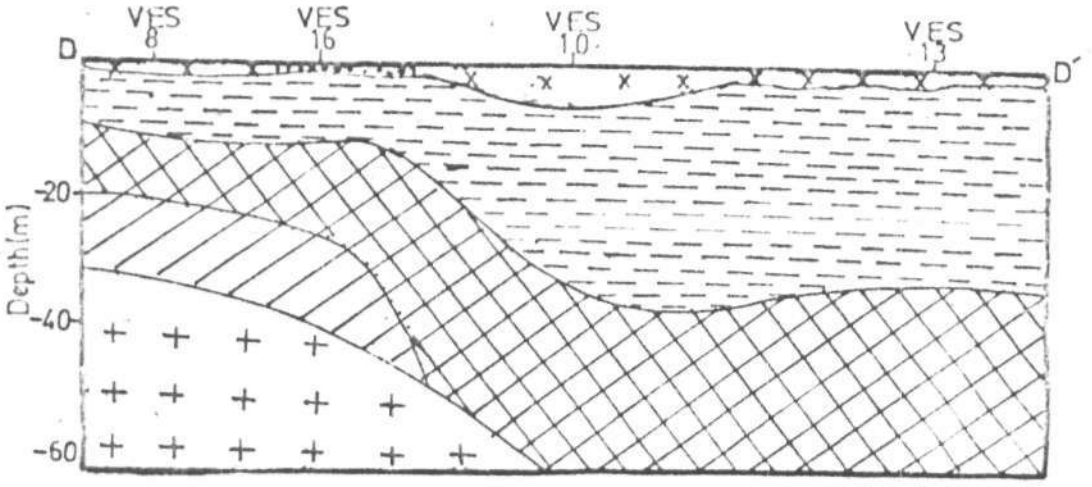


Fig. 5.13b Geologic section

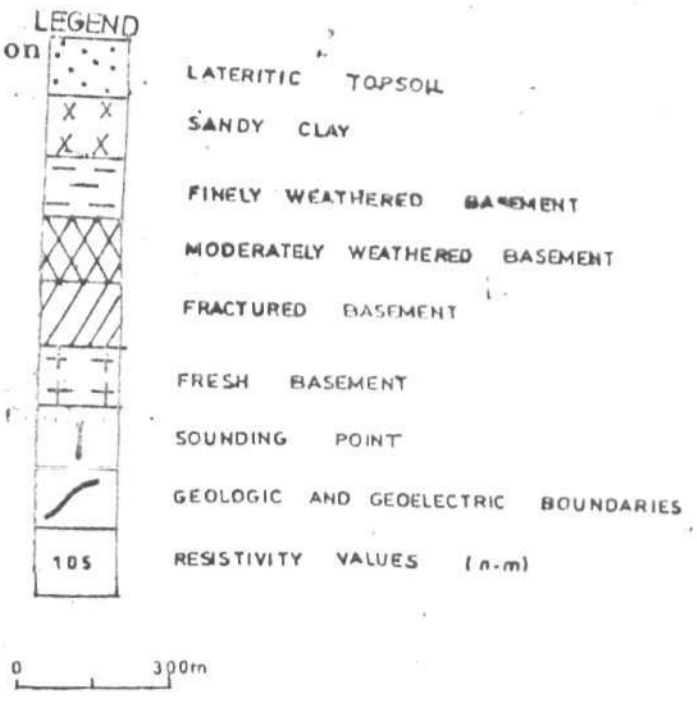


Fig.5.13 Geoelectric and Geologic sections for profile DD'

The second layer is the saturated weathered layer on this profile. This is clear from the resistivity values (91.4 - 422 ohm-m) encountered on the layer.

Underlying the saturated layer is the fractured basement. The fresh basement is encountered under ves 8 and 16 (resistivity greater than 1000 ohm-m). This layer is absent around VES 10 and 13.

5.7 MAPS PRODUCED FROM THE INTERPRETED DATA

Contour maps were produced from the interpreted resistivity data for all the ves stations established. This was done in order to study specific aspects such as the degree of weathering and fracturing of the subsurface rocks, as well as other structures within the study area. These maps include; isoresistivity maps at various pre-selected depths, a depth to basement contour map, and an aquifer thickness map for the area. Details of the maps are discussed below.

5.7.1 ISORESISTIVITY MAP OF THE SURFACE LAYER

The resistivity map of the surface layer was produced by contouring the resistivity values obtained for the surface layer at all the 26 VES locations. The map was contoured using a contour interval of 100 ohm-m. This map is shown in fig 5.14a. A close examination of the map shows that the resistivity values of the surface layer in the study area range from 15 ohm-m around VES 10, to 1500 ohm-m around VES 7, 2 and 26. The surface layer around VES 10 was interpreted to be made up of wet clay soil due to its very low resistivity value, while the high

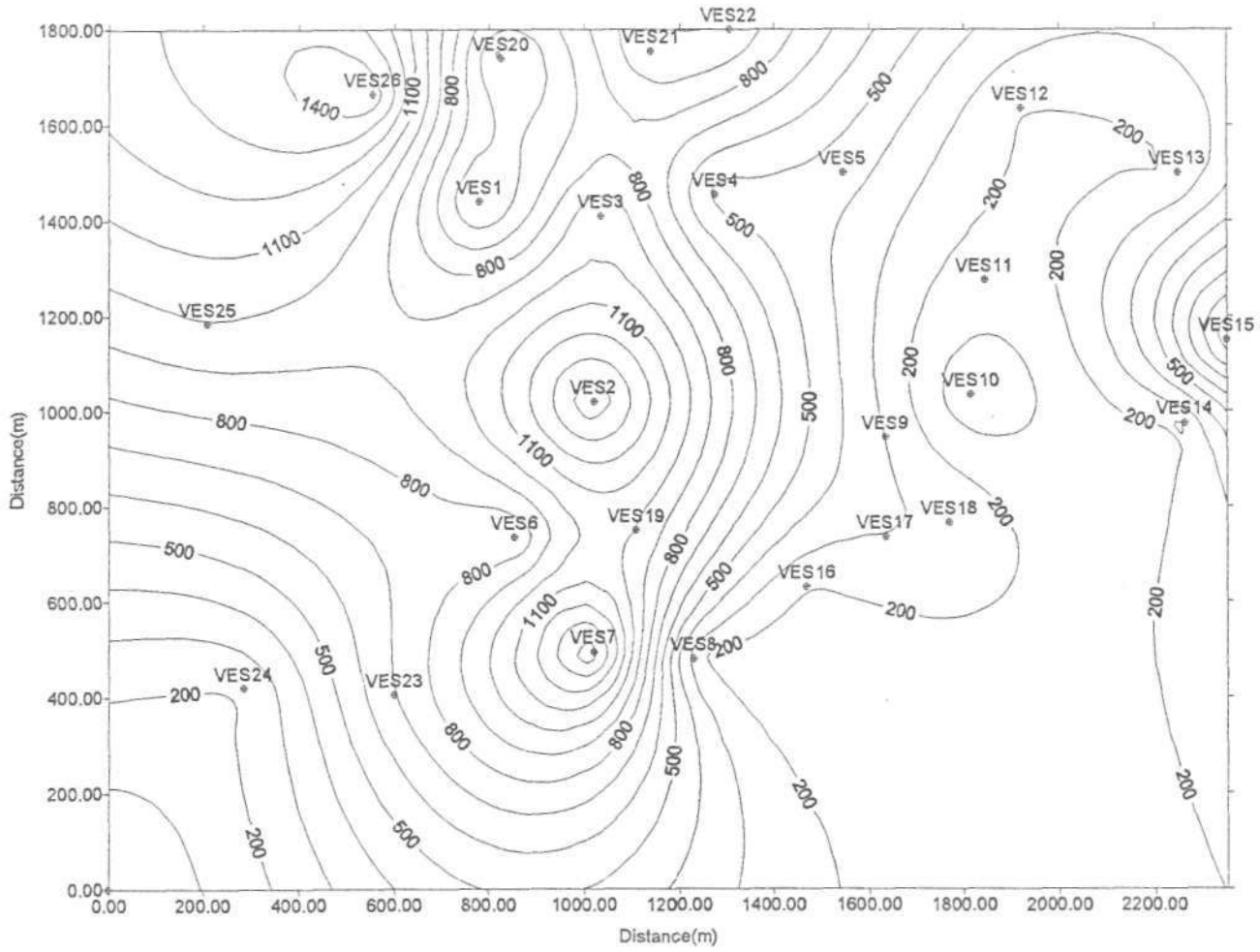


Fig 5.14a Isoresistivity Contour Map of Unijos at the Surface

resistivity values around ves 7, 2 and 26 are suggestive of a fresh lateritic topsoil. This is based on the resistivity ranges given in table 5.2.

Generally, lower resistivity values are observed around the north eastern corner of the map trending in the N - S direction except for the resistivity high around VES 15. This was interpreted to be made up of clay and sandy clay soils. High resistivity values are observed mostly in a north - south direction around the central and north - western regions of the map.

Three major anomalous zones are observed on this map. These anomalies are in the form of contour closures around some VES stations.

One of such anomalous zones is encountered around the north - eastern part of the map and trends in a NE - SW direction (around VES 10, 11, 13, etc). This zone is associated with low resistivity values of between 15 and 200 ohm-m. This resistivity range may be due to the fact that the top soil in this zone is composed mostly of Clays and Sandy clays.

Another anomalous zone on the map is found around VES 24, 4, 1, 15 etc. This zone is of medium resistivity which ranges between 300 - 450 ohm-m. This moderately high resistivity range could be due to weathered laterites at the surface.

The third anomalous zone is seen around VES 25, 26, 2, 15, 7 and 20. The resistivity range is from 1000 ohm-m and above. This is interpreted to be due to fresh lateritic top. Field evidence show that the laterites around these areas are still fresh.

5.7.2 ISORESISTIVITY CONTOUR MAPS AT DEPTH

The isoresistivity contour maps at depths corresponding to 1.0, 5.0, 10.0, 15.0, 20.0, 25.0, 30.0, 40.0, 50.0, and 60.0 respectively, are shown in figures 5.14 b - k. The idea behind the production of these maps is to investigate the extent of weathering, and of course, fracturing(evident on the VES curves) about these depths. Some of the VES curves(see Appendix) show evidence of weathering at shallow depths(low resistivity values),as such, the isoresistivity map at 1 m was meant to see if there is the possibility of water saturation at this depth.

The maps were produced by contouring the interpreted resistivity value at each VES station for any particular depth taken.

The isoresistivity contour map at 1m (fig.5.14b) depth shows a trend that is similar to the surface contour except that the resistivity values are considerably reduced at this depth. Generally, resistivity values at this depth range from 15 ohm-m to 1200 ohm-m. The map suggests that the eastern(VES 9,10,11,14), north - eastern(VES 5,12 and 13), and the southern(VES 7,8,16,17,18)parts of the study area may be saturated at this depth(based on the resistivity values). There is a progressive increase in resistivity towards the top left corner of the map in a NNW – SSE trend.

The isoresistivity contour map at 5 m depth is shown in fig. 5.14c. At this depth, almost all the VES stations show relatively low resistivity values ranging from about 30 ohm-m to a maximum of 350 ohm-m. It is clear from the resistivity values at this depth that the degree of weathering is high. Such zones of strong

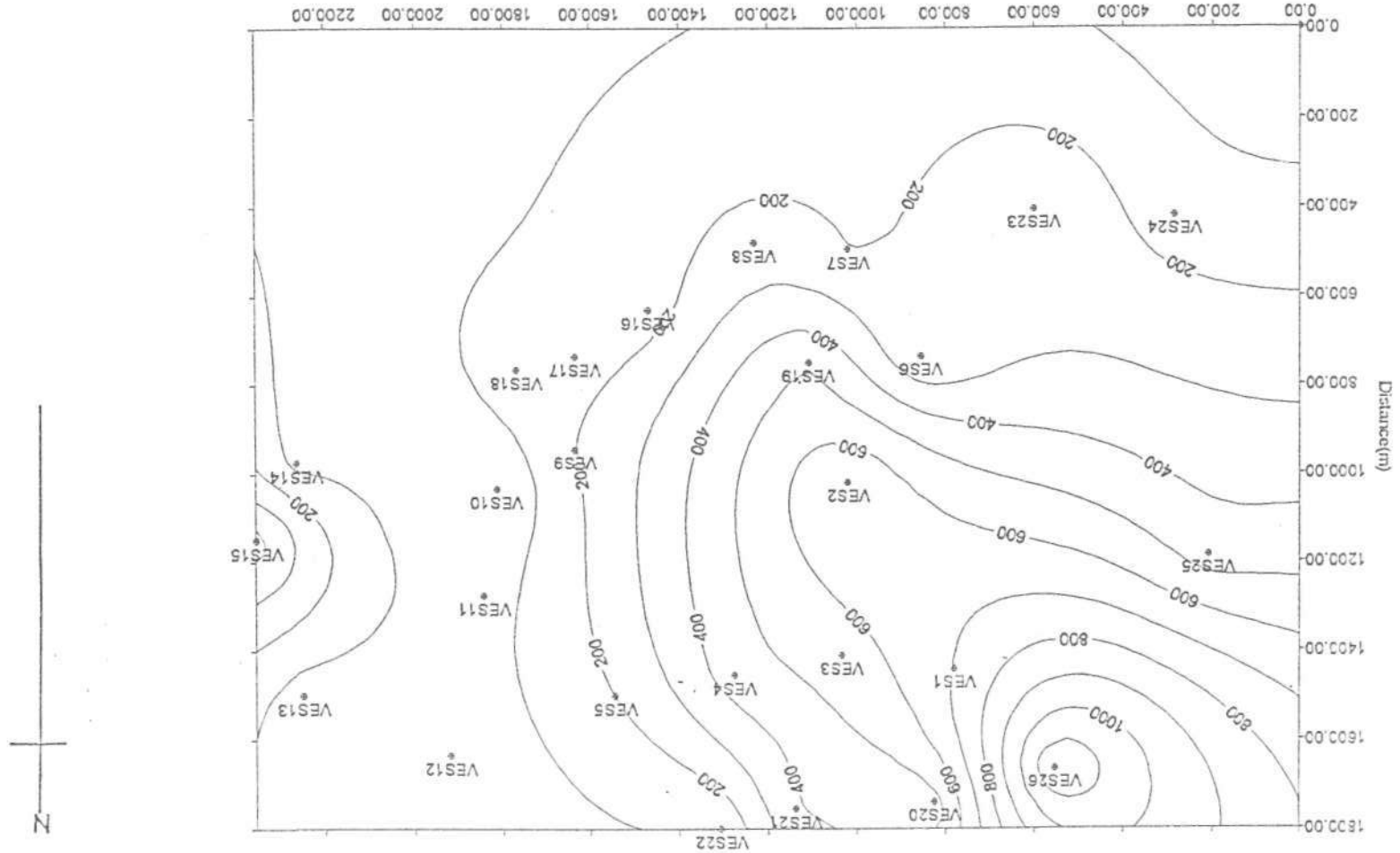


Fig. 5.14b: Isoresistivity Contour Map at 1 m Depth.

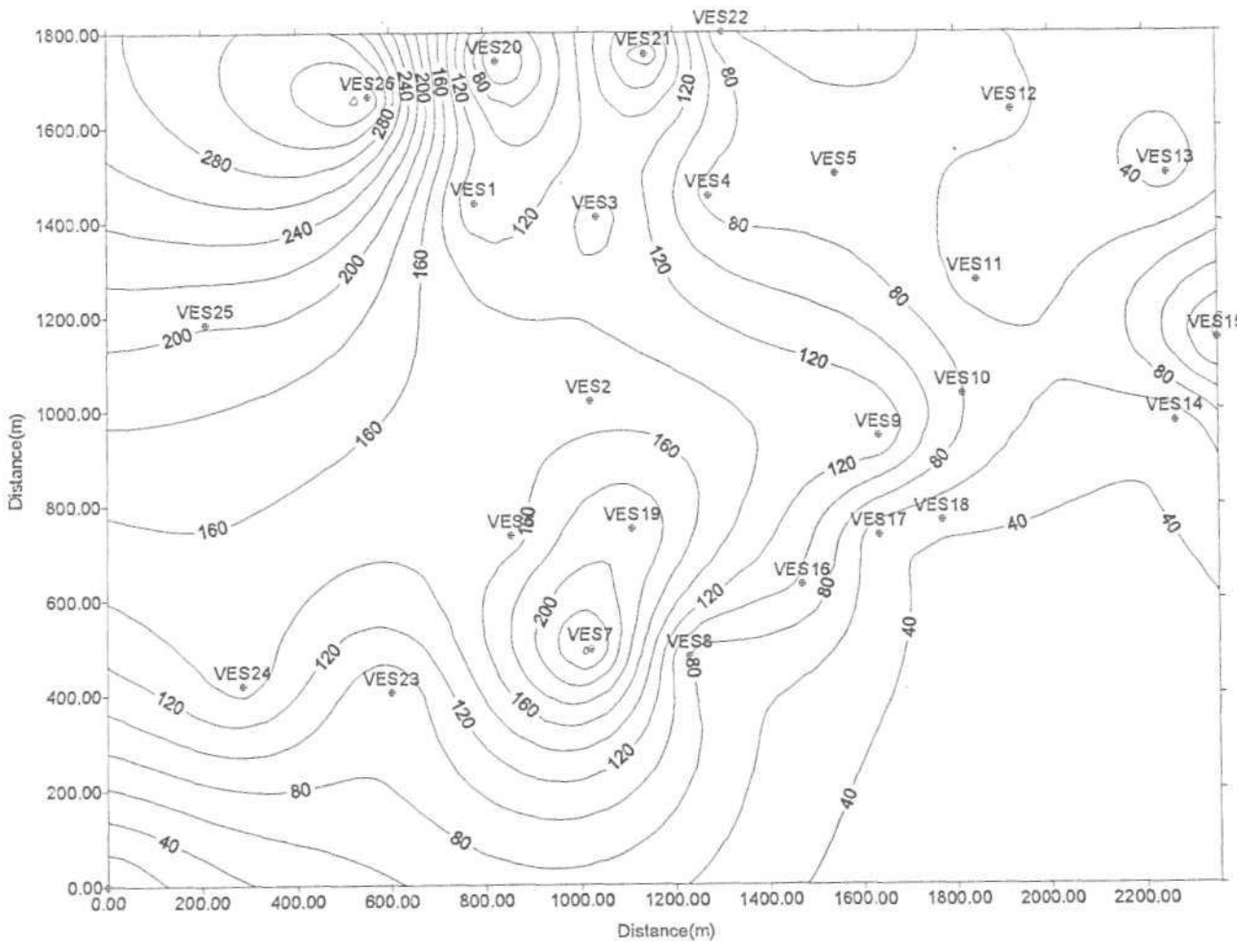


Fig. 5.14c: Isoresistvity Contour Map at 5 m Depth.

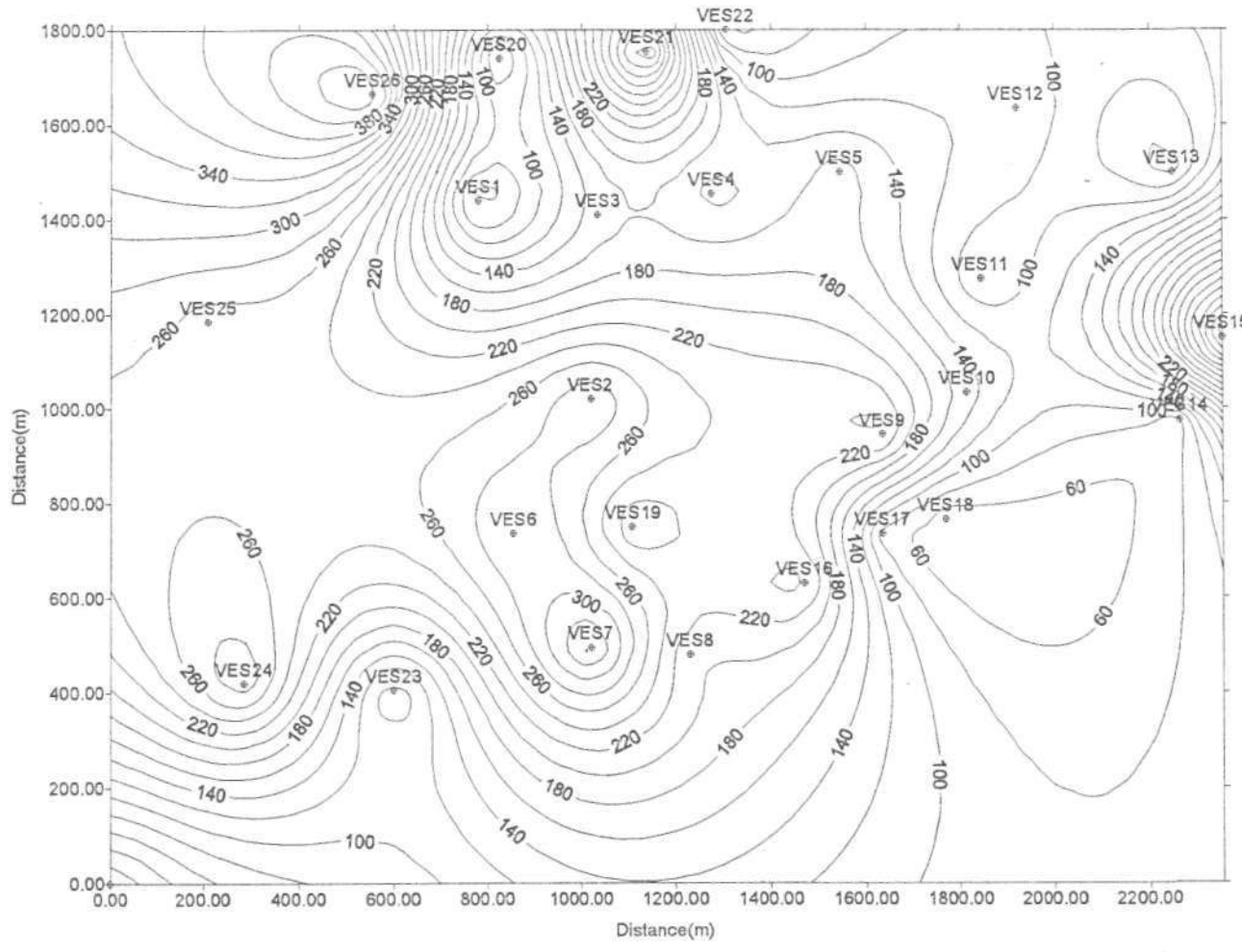


Fig. 5.14d: Isoresistvity Contour Map at 10 m Depth.

weathering are more favorable to groundwater occurrence in the Basement Complex areas.

The contour maps at 10 and 15 m depths (figs 5.14d and e) show a similar trend with that at 5 m. Comparison of those maps show a progressive increase in the resistivity values with depth, which suggests an increase in the coarseness of particles within the weathered region. The contour map at 20 m(fig 5.14f) almost exhibit a similar pattern with the ones discussed above. However, the resistivity values recorded around VES 15, 6 and 24 fall within the range for a fractured basement(Table 5.2), and is interpreted as such. The remaining VES stations on this horizon show resistivity values that are suggestive of a weathered basement, though, of varying degrees of weathering. The maps at 25 and 30 m,(fig.5.14g & h) show a similar pattern with a progressive increase in resistivity values. Figure 5.14g shows a range of resistivity values(120 - 820 ohm - m)that are suggestive of weathered and fractured basements. In figure 5.14h, the resistivity value of 1200 ohm - m recorded at VES 14 and VES 8 is indicative of the fresh basement rocks being encountered at these points.The remaining VES staions are fractured at this depth(From their resistivity values). The contour maps at 40, 50 and 60 m generally show a resistive subsurface at these depths. Apart from VES 10 and 19, the resistivity values at these depths range from 1000 ohm - m and above which suggests that the fresh basement has been hit at these depths.

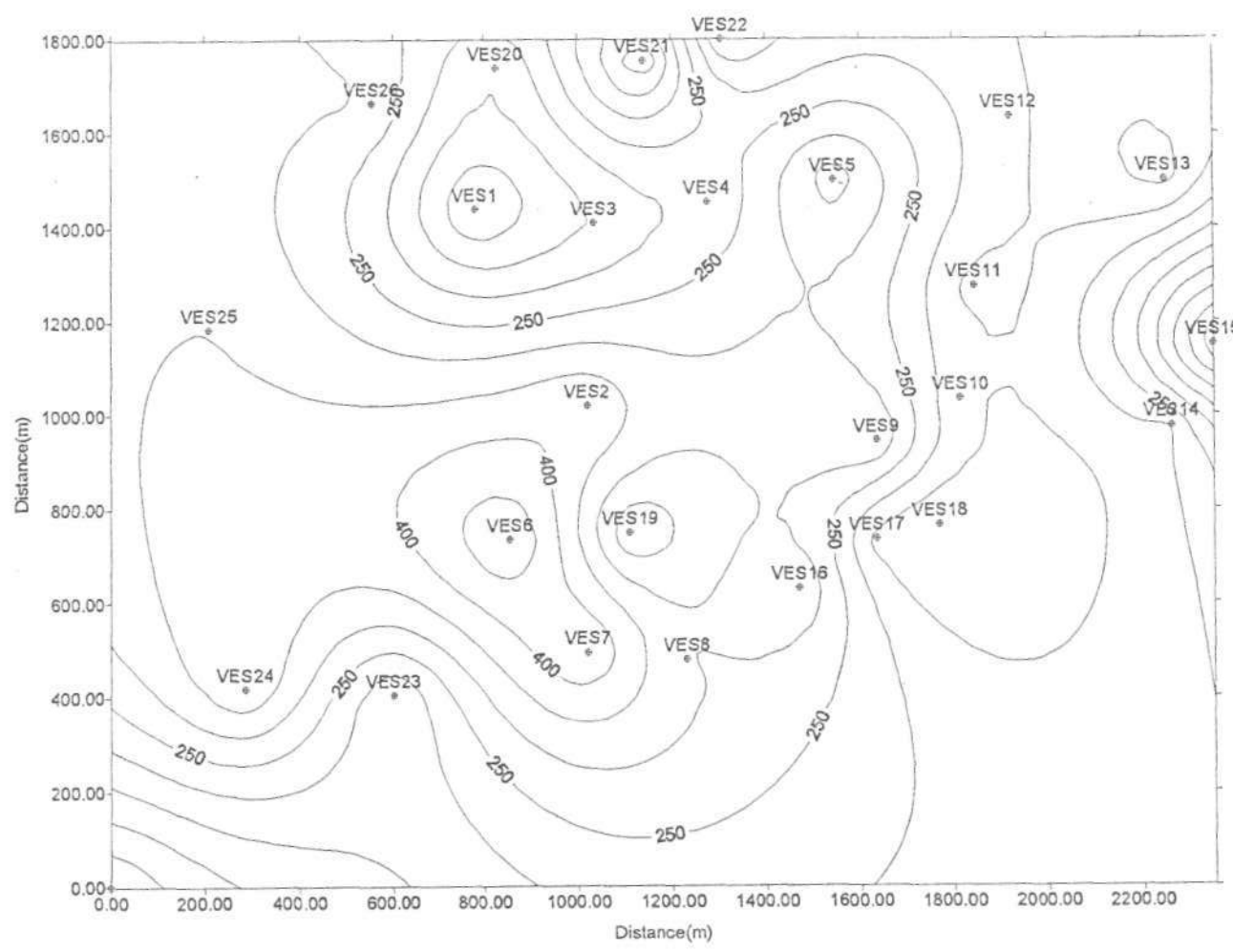


Fig. 5.14e: Isoresistivity Contour Map at 15 m Depth.

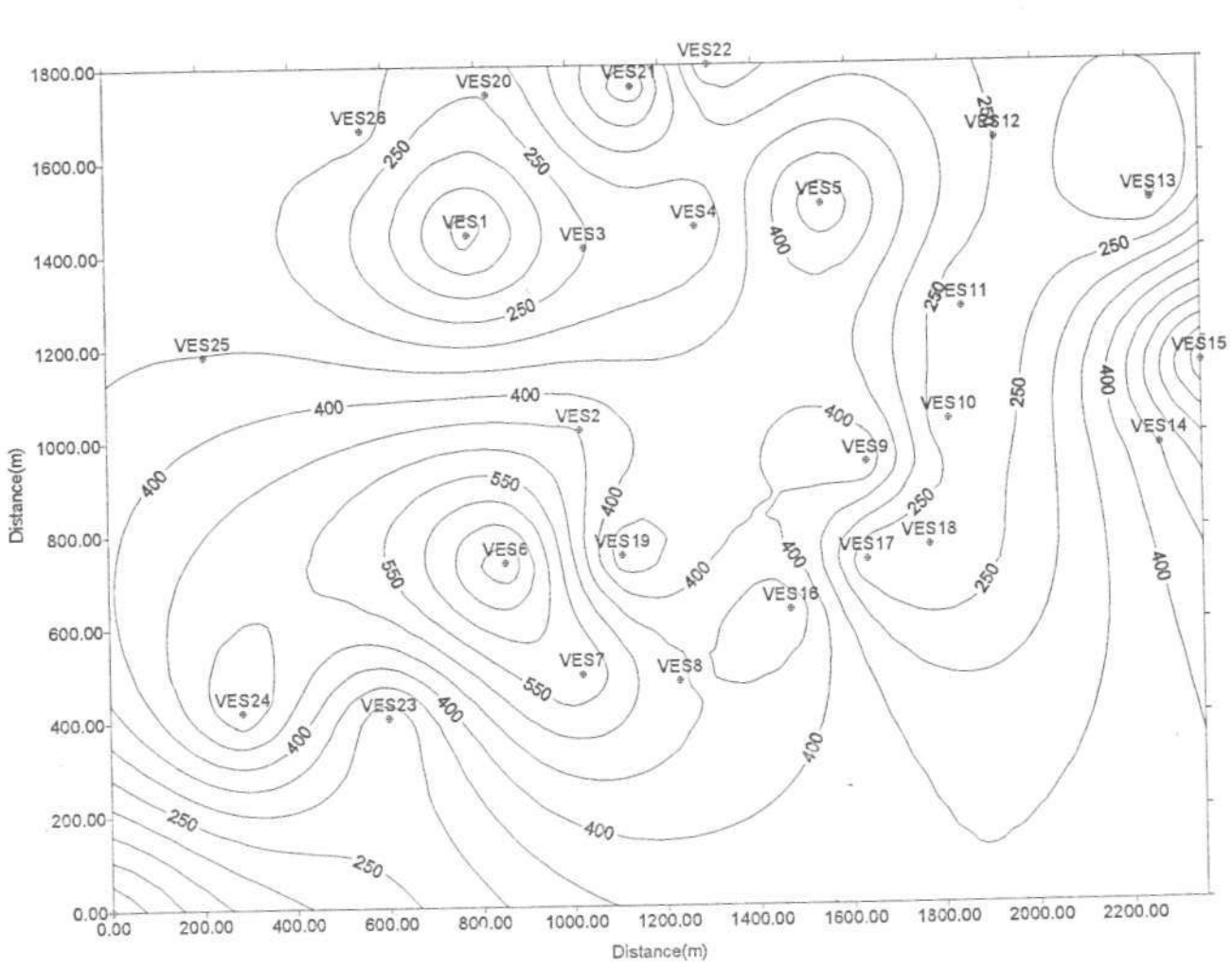


Fig. 5.14f: Isoresistivity Contour Map at 20 m Depth.

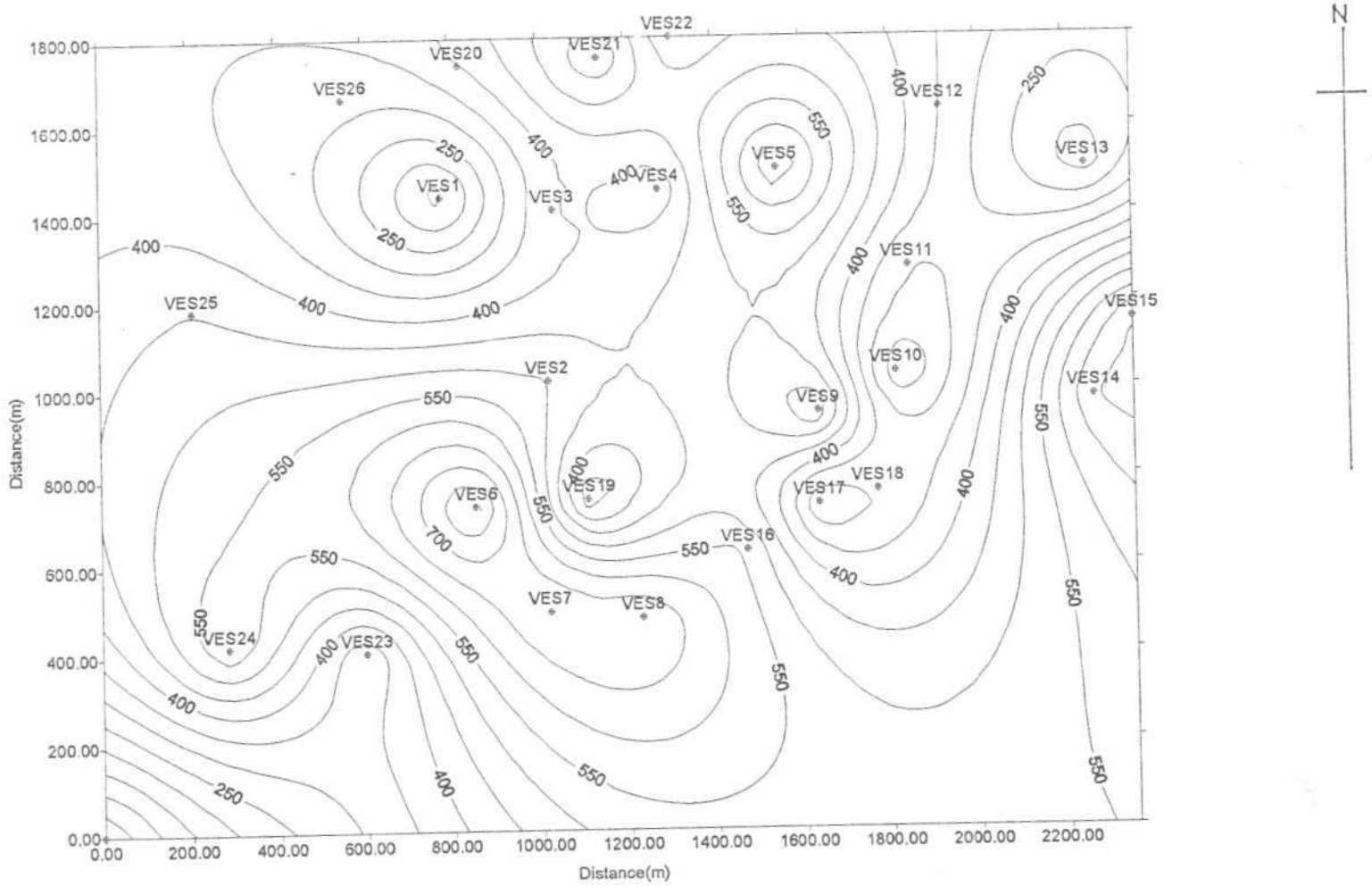


Fig. 5.14g: Isoresistivity Contour Map at 25 m Depth.

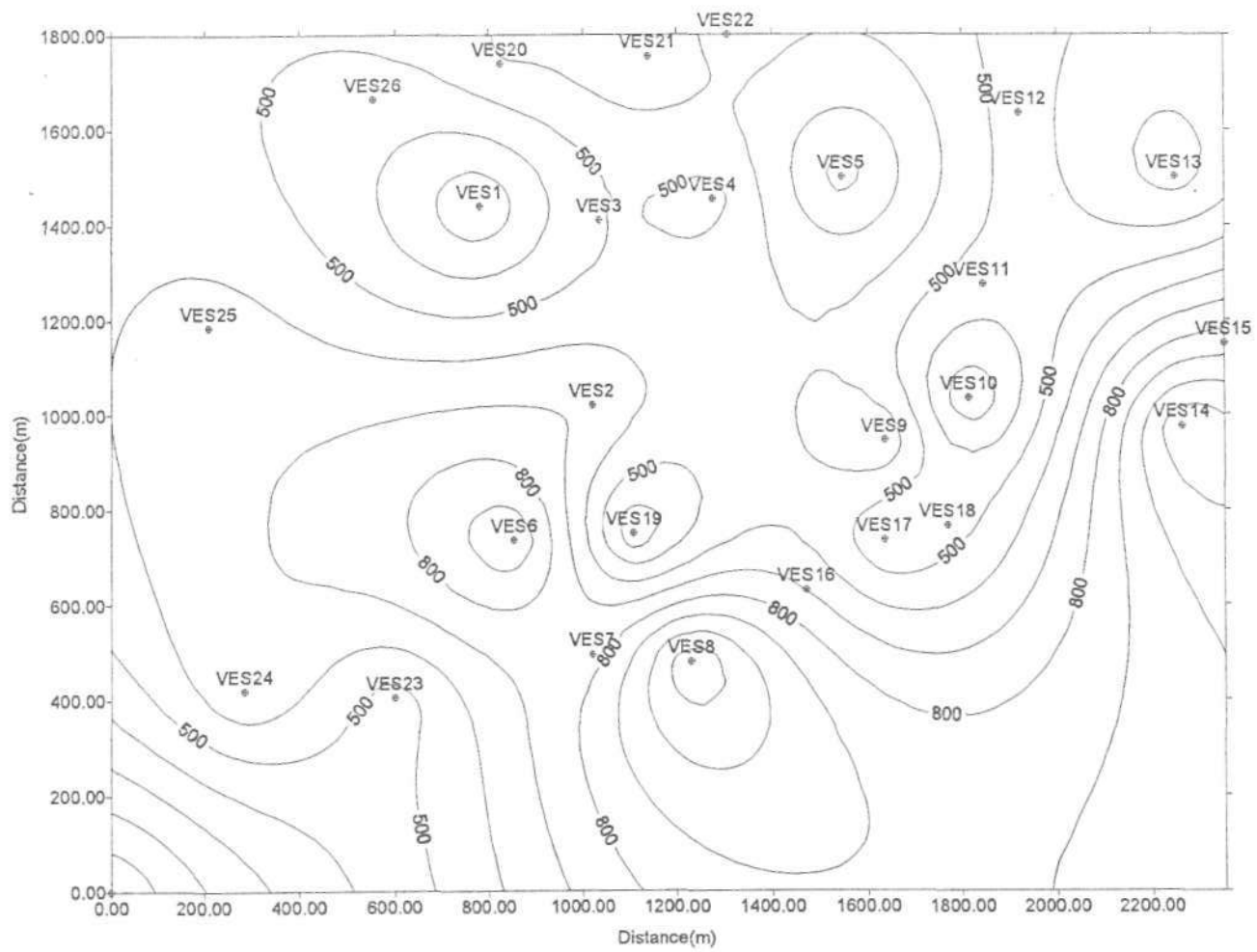


Fig. 5.14h: Isoresistivity Contour Map at 30 m Depth.

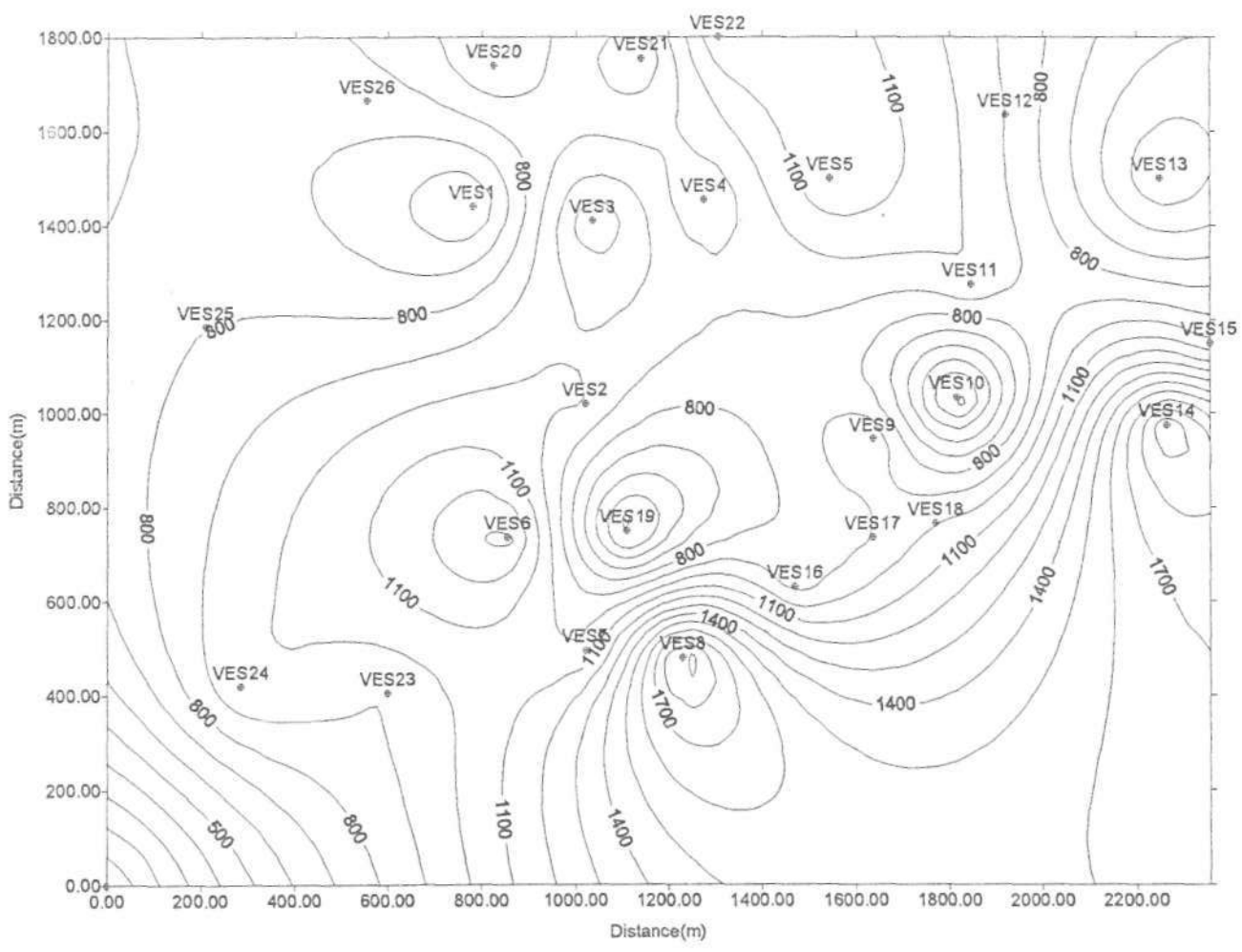


Fig. 5.14i: Isoresistivity Contour Map at 40 m Depth.

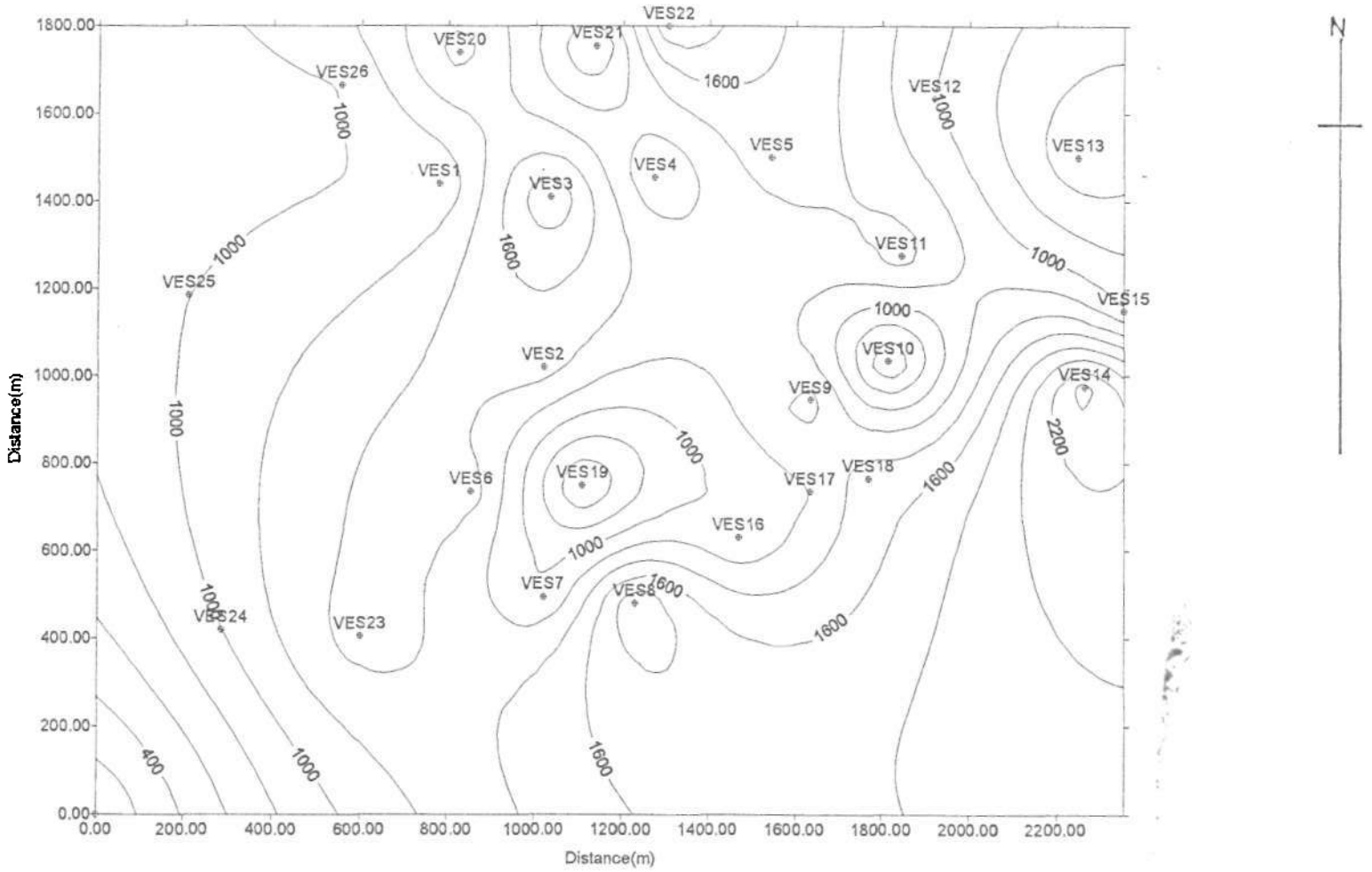


Fig. 5.14j: Isoresistivity Contour Map at 50 m Depth.

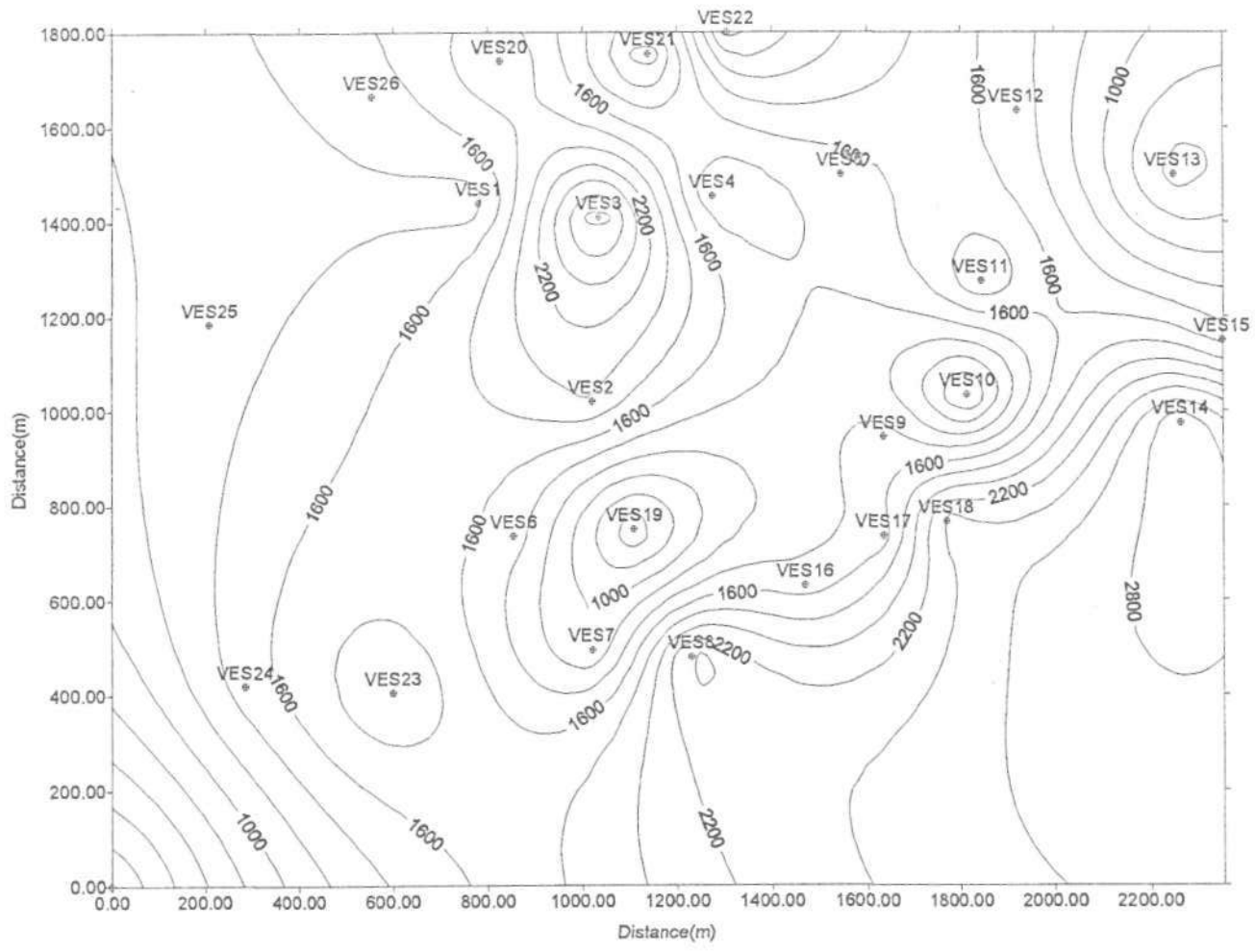


Fig. 5.14k: Isoresistivity Contour Map at 60 m Depth.

5.7.3 DEPTH TO BASEMENT MAP

The depth to basement contour map for the study area is shown in fig. 5.15. The map was produced from the interpreted depth to the fresh basement at each VES station. This depth to the fresh basement beneath each of the 26 soundings was plotted at the corresponding location on the base map and contoured at an interval of 5 m. This map gave a good picture of the basement topography in the area. The map shows that the basement topography is rugged or undulating being deeper at some points and shallower at other points. The depth to basement ranges from 30 m around VES 8 to 66 m around VES 19. The map also reveals a linear structure (VES 23, 19, 10 and VES 13) which trends in the NE – SW direction. This structure suggests a basement depression at these points. Generally, the depth to basement increases from south to north towards the river Dilimi. Furthermore, the contour map suggests that the course of Dilimi river is structurally controlled.

5.7.4 AQUIFER THICKNESS MAP.

Fig. 5.16 shows the map of the aquifer thickness (Finely weathered basement) produced for the study area. The map was produced using the thickness of the finely weathered basement (see geologic sections) obtained at each VES station. However, this does not rule out the possibility of the partially weathered basement contributing to the aquifer system, especially where its thickness is appreciably large. The weathered basement was taken to be the aquifer in the

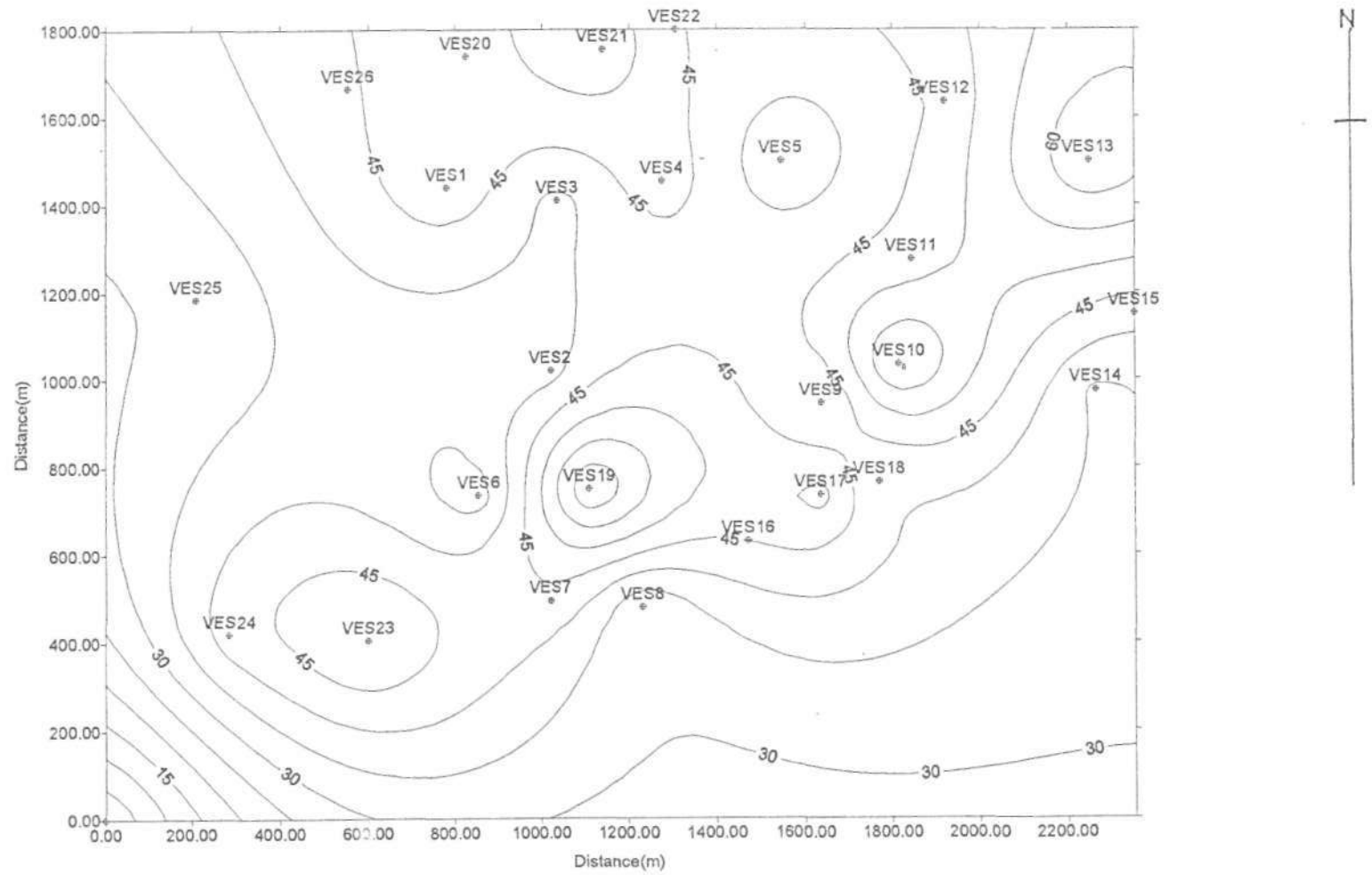


Fig. 5.15: Depth to Basement Contour Map.

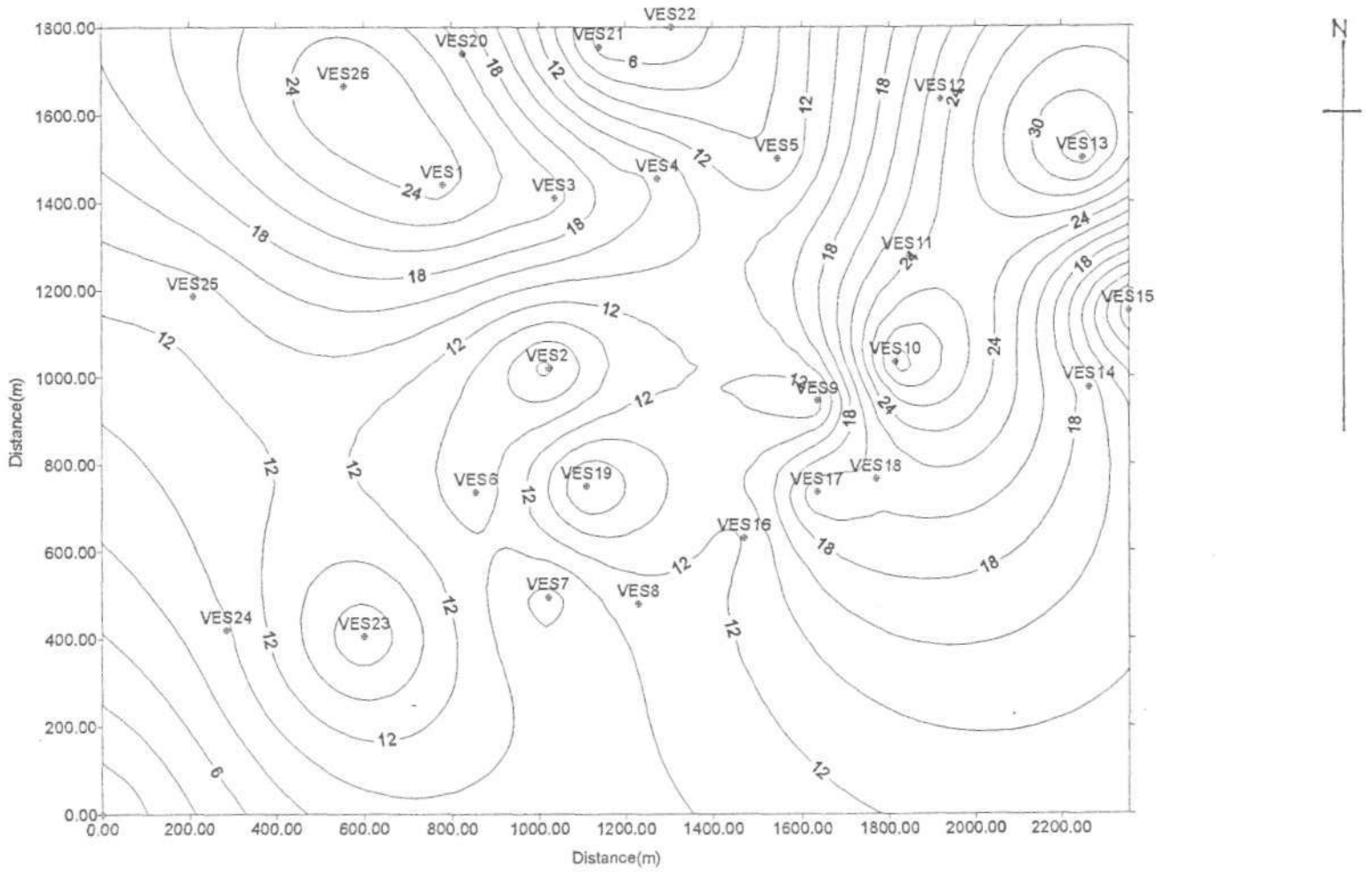


Fig. 5.16: Aquifer Thickness Contour Map.

study area since it constitutes the major component of the aquifer system in the Basement Complex areas. This map was produced to see how the thickness of this finely weathered layer varies from place to place within the study area.

The map shows that the thickness varies from 3.9 to 34 m. As expected, a comparison of the aquifer thickness and the depth to basement maps show that the low thickness values correlate well with the areas of shallow basement while larger thickness values correlate with basement depressions. Such large aquifer thicknesses are more likely to retain a good quantity of water, and such areas are of prime importance in groundwater exploration.

CHAPTER 6

DISCUSSIONS, CONCLUSIONS AND RECOMMENDATIONS.

6.1 Discussion Of Results

The interpretation of the resistivity (VES and Profiling) as well as the EM data presented in chapter five, provides the basis for which certain deductions and recommendation are made , especially, on the aquifer system and the basement topography underlying the study area.

Results of the resistivity profiling and those of the EM are in fairly good agreement. Interpretation of the resistivity profiling data reveal a weathered basement (though of varying degrees) within the depths of 10 and 20 m probed. This was evident from the low resistivity values obtained along the occupied Profiles. On the other hand, the EM method which probed up to 30 m depth yielded some conductivity anomalies that were interpreted to be as a result of varying weathering thicknesses. Furthermore, the method gave some negative anomalies (fig 5.7a) along certain profiles. Such negative anomalies are usually associated with dipping fractures, or fracture zones generally.

Thus, results of both profiling methods suggest the presence of a weathered/fractured basement, whose thicknesses vary from place to place within the study area.

Owing to the fact that the components of aquifer in basement areas are generally classified into weathered basement fractures and alluvial deposits (Ajayi and Hassan, 1990; Amadi and Nurudeen, 1990), the weathered basement and of

course, the fractured basement are believed to be the major components of the aquifer system in the study area. The fractured basement could contribute to the aquifer system where the fracture density is high, and its thickness is considerably large. The fractured layer delineated in the study area at all the VES stations is unconfined.

In line with the above discussion, the finely weathered basement thickness(shown on the geologic sections) is taken to be the aquifer thickness map for the study area shown in fig 5.16.

The interpretation of the VES data led to the final determination of the regions within the study area that are considered to have the greatest groudwater potential. To arrive at these, the geoelectric as well as the deduced geologic sections were carefully examined to see the regions where extensive weathering occurs along fractures (see fig 5.11). These together with information obtained from such maps as; depth to basement (fig 5.15) and the aquifer thickness (fig 5.16) map led to the conclusion that: VES 13, VES 10, VES 19, VES 23, and VES 1,(in order of preference) have the greatest groundwater potentials in the study area. VES 13, 10, 19 and 23 fall on the linear region of the basement depression shown in fig. 5.15. Also, the thickness of the weathered/fractured basement beneath these regions were found to be considerably large. Moreover, the weathered basement resistivity values in those zones fall within the accepted range for water saturation(30 - 200 ohm - m).

The depth to basement map (fig 5.15) shows that the fresh basement in the study

area lies in the range of 30.0 - 66.0 m depth with an average value of 44.5 m. This suggests that the fresh basement rock possesses an undulating configuration, being deeper towards the Northern end and shallower towards the southern end. The map also suggests a basement depression of large lateral extent in a NE – SW direction.

Thus, generally, results of the different geoelectrical methods correlate well with each other.

6.2 LIMITATIONS

A few problems were encountered during the course of this study.

(1) It was mentioned earlier that one of the aims of using the EM survey in this study area was to help resolve the problem of equivalence and suppression often encountered in the interpretation of resistivity sounding curves. However, EM sounding could not be carried out as planned due to the non-availability of the 40 m connecting cable. As a result, only the EM profiling was carried out and as such, the problem, of equivalence could not be resolved.

(2) Outcrops and buildings encountered at some points in the area made it impossible to carry out resistivity sounding at such positions. Moreover, the rugged topography coupled with gullying and erosion made data collection at some points a very difficult task.

(3) Some of the boundaries of the borehole lithology do not correspond

to the interpreted layers. This could be due to the fact that the iterative computer program (Zohdy) used provides a multi-layered curve, and as such, layer compression had to be done in order to obtain an equivalent 3 or four layer model. It is obvious that there may be some slight errors in the layer compressions, leading to some ambiguity in the interpretation.

(4) Another limitation could be in the application of the Zohdy program. The program assumes that the incremental value per decade during each sounding is very small for isotropic and homogeneity conditions to hold for the different layers. However, this assumption is violated as the increamental value becomes large at higher decades, this imposes some limitations on the use of Zohdy's method for very large current electrode separations.

6.3 CONCLUSIONS

This survey is a preliminary investigation of the basement structure as well as the groundwater potential of the University of Jos permanent site.

Despite the limitations mentioned above, the following conclusions are drawn:

1. The geologic sections deduced for Profiles AA', BB', CC', DD' respectively, suggests that the study area is underlain by 3 - 5 layers of different lithological units

2. The resistivity profiles in Figures 5.2 - 5.5 suggests that the

subsurface is extensively weathered within the depths probed. The EM profiles presented in Figures 5.6 - 5.8 also support this fact. They also reveal the occurrence of dipping fractures as discussed in chapter five.

3. The geologic sections as well as the depth to the basement map suggests that the overburden thickness in the study area ranges from 30 m to 66 m.

4. The depth to basement (fig. 5.15) map of the study area suggests that the bedrock is undulating being deeper in the northern part of the area.

5. The aquifer thickness map for the study area (Fig.5.16) suggests that the thickness of the aquifer layer varies between 3.9 m and 34 m.

6. The depth to basement(Fig 5.15) and the aquifer thickness(Fig.5.16) maps produced for the study area seem to suggest that the drainage pattern in the river Dilimi is controlled by the basement topography.

6.4 RECOMMENDATIONS

As mentioned earlier in chapter one, there is no record of previous geophysical work done in the study area which would have served as a guide in the interpretation of the data generated in this study. As a result, the conclusions reached in this work cannot be compared with any other previous result(s). It is,

therefore, important to mention that further geophysical and geological investigations need be carried out in the area, especially, seismic refraction. It is equally important to emphasize that no single geophysical method can single handedly give a complete and unique information about the parameters of interest in a given survey area. As such, the geoelectric method used here cannot provide all the information required about the subsurface of the study area to the expected degree of accuracy.

The use of other geophysical methods will further affirm the authenticity of the conclusions drawn from this study.

The following are specific recommendations for further investigations in the study area.

1. There is need to follow up the vertical electrical sounding (VES) carried out in this study with the EM sounding. This will more or less confirm results of the VES interpretation. Moreover, the EM sounding will help resolve the problem of equivalence and suppression often accompanying VES interpretation.
2. In further works, it will be necessary to determine other electrical parameters for the aquiferous zones. These include; hydraulic conductivity, aquifer transmissivity, coefficient of resistivity anisotropy as well as the coefficient of storage.
3. The area covered by this study is very small compared with the entire area that was originally allocated to the university for its development, thus the

study is more or less localized. There is need to carry out a regional resistivity survey so as to delineate all the possible subsurface structures(and structural trends) found within the study area.

REFERENCES

Abdel-Aziz, I.K. (1987): Ground water engineering.Mc Graw-Hill International, Singapore.

Ajaegbu, H.I; Adepetu, A.A.; Ajakpo, J.E,; Ihemegbulem, V.C; Jumbo, S.E.; Olaniyan,J.A.; Okechukwu,G.C.; and Schoeneich, K. (1992): Jos Plateau Environmental excursion guide. Unpublished document of Department of Geography and Planning, University of Jos.

Ajakaiye, D. E. (1976): A gravity survey over the Nigerian Younger Granite province. In Kogbe, C.A.(Ed). Geology of Nigeria. pp 207-224.

Ajayi, O; and Adegoke-Anthony, C.W. (1988): Groundwater Prospects in the Basement Complex rocks of Southern Nigeria. Journal of African Earth Sciences, 7 (1) PP 227-235.

Ajayi,C.O. and Hassan, M.(1990) The Delineation of the Aquifer Overlying the Basement Complex in the Western Part of Kubanni Basin of Zaria (Nigeria). Joural of Mining and Geology Vol,26, NO.1 pp117 - 125

Ako, B.D (1982); Geophysical Prospecting for groundwate in an area without adequate geological database. Journal of Min. & Geology 18 (2), PP 88-105.

Ako B.D.; T.R. Ajayi: A.O. Alabi (1978):A geoelectrical study of the Ifewara area.Journal of Mining and Geology, Vol.. 15 (2), pp. 84-89.

Amadi, U.M.P and Nurudeen, S.I. (1990) Electromagnetic Survey and the Search for ground water in the crystalline basement complex of Nigeria. Journal Mining and Geology, Vol. 26 PP.45-53

Amadi, U.M.P. and Amadi, P.A. (1990); Saltwater Migration in the Coastal aquifers of southern Nigeria, Nig. Journal of Min. And Geology 26 (1) pp 35-44

Alfano,L(1959): Introduction to the interpretation of resistivity measurements for complicated structural conditions: Geophysical Prosp.Vol. 7 pp. 311 - 366.

Atlas Copco, ABEM (1981): Geophysical Instrument Manual (Terameter SAS 300B) ABEM,Sweden.

Barongo, J.O(1983): Geophysical investigation for Kimberlite pipes in the greenstone belt of western Kenya. Journal of African earth Sciences vol.1, no.3/4; pp235-253.

Beck, A.E.(1981)Physical Principles of Exploration Methods: The Macmillan press limited, London.

Beeson, S and Jones, C.R.C.(1988): The Combined EMT/VES geophysical methods for citing boreholes.Groundwater journal, Vol, 26(1) pp 54-63.

Bowen, R.(1986): Groundwater. Elseiver Applied Sciences Publishers, New York.

Dar Al handassah Consultants (1979): Preliminary Design report on the University of Jos infrastructure, Jos. Unpublished document No. 22 of the Physical Planning Unit, University of Jos

Carel de Rooy & Mohammed, K. (1993): Electromagnetic prospecting for water in Nigeria; Waterfront, Issue 4. A Bi-annual publication of the water and sanitation cluster, Unicef, pp 14-18

Du Preez, J.W. and Barber, W (1965): The distribution and chemical quality of groundwater in Northern Nigeria. Geological survey of Nigeria, Bulletin No. 36.

Egboka, B.E.C.(1988): The hydrogeological provinces of Nigeria. I.A.H.S. Publication No. 1454, pp. 117-125.

Ekine, A.S. and Osobonye, G.T(1996): Surface Geoelectric Sounding for the determination of aquifer characteristics in parts of Bonny local Government Area, Rivers State, Nigeria. Nig. Journal of Phys. Vol. 85, pp.93-99.

Etu-Efeotor,J.O.; Alabo, E.H. and Michalski, A.(1989): Geophysical investigation for groundwater in parts of Eastern Niger Delta: Nigerian Journal of Mining and Geology; 25 (1,2) pp 51-54.

Etu-efeotor, J.O. and E.G. Akpokodje, (1990): Aquifer systems of the Niger Delta. Nigeria Journal of Mining and Geology, 26 (2) pp 279-284.

Gosh. D.P. (1971): The application of Linear filter theory to the direct interpretation of geoelectrical resistivity sounding measurements: Geophys. Prosp. Vol. 19, pp 192-217.

Grant, F.S. and West, G.F.(1965): Interpretation theory in applied Geophysics. Mc Graw-Hill Book Company, New York.

Hassan, M; Ajayi, C.O. and Ojo, S.B.(1991): A Basement structuredetermined from Geoelectric mapping of the Kubanni River Basin, Zaria: Nigerian Journal of Physics, Vol. 3 pp 166-173.

Hazell, J: Cratchley, C and Preston, A (1988): The location of aquifers in Crystalline rocks and alluvium in Northern Nigeria using combined electromagnetic and resistivity techniques: Quarterly Journal of Engineering Geology, London, Vol. 21, pp 159-175.

Koefoed, O (1971): Geosounding principles, 1, measurements, methods in Geo-Chemistry and Geophysics: Elsevier, New York.

Kunetz, G. (1966): Principles of direct current resistivity prospecting:Gebruder-Brontraeger.

MacLeod, W.N.; Turner, D.C. and Wright, E.P. (1971): The Geology of the Jos Plateau. Geological survey of Nigeria Bulletin No. 32, Vols 1 and 2.

Masson-Smith, S.H. (1965): Geophysical prospecting for bassalt covered alluvial Casseterite on the Jos Plateau, Northern Nigeria. Overseas geol. surv.,London. Geophys. rev. no. 27.

Mbipom, E.M. and Archibong, J.E. (1989): Vertical electric sounding of Coastal aquifers near Qua-Iboe Estuary .Journ. Of min. and geol. Vol.25, pp151-154.

Maclean, A.C. and Gribble, C.D. (1979): Geology for Civil Engineers. Mc Graw Hill,London.

McNeill, J.D. (1980): Electromagnetic terrain conductivity at low induction numbers; Technical note TN-6, Geonics Ltd, Ontario, Canada.

McNeill,J.D.(1980): EM 34-3 Survey interpretation techniques. Technical note TN-8, Geonics Ltd, Ontario, Canada.

Obiakor, I.P. and Chukwudebelu, J.U.(1992): Geophysical Investigation for groundwater in the Nanka Sands of the Anambra Sedimentary basin: Nigerian Journal of Physics, Vol. 43, pp. 135-1432.

Ogezi, A.E; Litko, V. And Pospisil, P.(1983): Preliminary assessment of a small Damsite within the permanent site of the University of Jos.(Unpublished).

Ojo, J.S; Olorunfemi, M.O. and Loremikan, O.K.(1995): Crossed square array resistivity response curves over conductive and resistive dyke models.Jornal of Mining and geology,vol.31 no 125,pp155-159.

Ojo, J.S; and Olorunfemi, M.O.(1995): Geoelectric Mapping of a near vertical contact: A case study arround Erusu,Ikare area, Southwestern Nigeria. Journal of Mining and Geology vol.31,pp 151-153.

Okwueze, E.E. and Ezeanyim, V.E.(1985): The Vertical electrical sounding (Ves) method in laterite regions and in iron-rich glaciated areas. Nig. Journal of Mining and Geology, Vol. 22 Nos. 1 and 2 pp.193-198.

Olatinwo, M.O(1994): Geoelectrical investigation in the northern part of Kaduna state,Nigeria. Unpublished ph.D thesis, A.B.U Zaria.

Olayinka, A.I.(1990): Electromagnetic profiling and resistivity soundings in groundwater investigation near Egbeda-Kabba, Kogi State. Journal Mining Geology 26, pp243-250.

Olorunfemi, M.O and Fasuyi, S.(1993): Aquifer types and the geoelectric hydrogeologic characteristics of part of the central basement terrain of Nigeria (Niger State): Journal of African Earth Sciences Vol.. 16(3), pp. 309-317.

Olorunfemi, M.O.; Dan-hassan, M.A and Ojo, J.S.(1995): On the scope and limitations of the electromagnetic method in groundwater prospecting in a precambrain basement terrain - a Nigerian case study. Journal of African Earth Sciences, Vol. 20 No 2, pp 151-160

Onu, N.N. and Ajakaiye, D.E. (1990): Geoelectric soundings for groundwater in the semi-Arid area of Nigeria - A case study. The internal Hydrological program (IHP) document, UNESCO.

Oteri, A.U.(1982): Electrical resistivity survey of Dungeness south east Egland. An example of resistivity measurement in difficulty terrain. Journal of Mining and Geology 18 (2) pp 81-87.

Oteri, A.U(1990) Delineation of seawater intrusion in a coastal beach ridge of Forcadoes. Nig. Journal of Mining and Geology 26 (2), pp. 225-229.

Palacky, C.J. and Kiyoshi, K. K. (1979): Effect of tropical weathering on electrical and electromagnetic measurements: Geophysics, Vol. 44, pp 69-88.

Palacky, G.J; Ritsema, I.L. and Dejong, S. J. (1981); Elecgtromagnetic prospecting for groundwater in the precambrian terrains in the Republic of Upper Volta: Geophysical Prospecting, Vol. 29, pp 932-955.

Pekeris, C.L.(1940) Direct Method of Interpretation in Resistivity Prospecting: Geophysics Vol. 5, pp 31 - 36.

Rijo, L.; Pelton,W.H; Feitosa,E.C and Ward,S.H(1977): Interpretation of apparent resistivity from Apodi Valley, Rio Grande Do Norte, Brazil. Geophysics, Vol. 42 (4), pp 811-822.

Sarma, V.V. and Rao, V.B. (1962):Variation Electrical resistivity of river sands, Calcite and quartz powders with water content. Geophysics Vol. 27, pp70-479.

Shaw, S. H. (1951): The use of the electrical resistivity method for prospecting deep - leads in the Jos Plateau Tin field. Geol. Survey, Nigeria.

Shemang, E.M.(1990) Electrical Depth Soundings at Selected Well Sites within the Kubani River Basin, Zaria. Unpublished M.Sc thesis, Dept. Of Physics, A. B. U Zaria.

Telford, W.M; Geldart, L.P.; Sheriff, R.E.and Keys, D.A. (1976): Applied geophysics. Cambridge University press, New York.

Todd,K.D;(1980): Groundwater hydrology; John Wiley and sons.

Zohdy,A.A.R and Bisdorf, R.j.(1989) A New Iterative Program for the Automatic interpretation of Wenner and Schlumberger Sounding Curves. Software.

Zohdy, A.A.R and Jacson, D.B(1969): Application of deep electric sounding for groundwater exploration in Hawaii: Geophysics 34(4), pp. 584-600.

Zohdy, A.A.R. Anderson, L.A. and Muffler, I.J.P. (1973): Resistivity,Self-potential, and induced polarization surveys of a vapor dominated geothermal system: Geophysics vol. 38, pp 1130-1144.

Palacky, C.J. and Kiyoshi, K. K. (1979): Effect of tropical weathering on electrical and electromagnetic measurements: Geophysics, Vol. 44, pp 69-88.

Palacky, G.J; Ritsema, I.L. and Dejong, S. J. (1981); Elecgtromagnetic prospecting for groundwater in the precambrian terrains in the Republic of Upper Volta: Geophysical Prospecting, Vol. 29, pp 932-955.

Pekeris, C.L.(1940) Direct Method of Interpretation in Resistivity Prospecting: Geophysics Vol. 5, pp 31 - 36.

Rijo, L.; Pelton,W.H; Feitosa,E.C and Ward,S.H(1977): Interpretation of apparent resistivity from Apodi Valley, Rio Grande Do Norte, Brazil. Geophysics, Vol. 42 (4), pp 811-822.

Sarma, V.V. and Rao, V.B. (1962):Variation Electrical resistivity of river sands, Calcite and quartz powders with water content. Geophysics Vol. 27, pp70-479.

Shaw, S. H. (1951): The use of the electrical resistivity method for prospecting deep - leads in the Jos Plateau Tin field. Geol. Survey, Nigeria.

Shemang, E.M.(1990) Electrical Depth Soundings at Selected Well Sites within the Kubani River Basin, Zaria. Unpublished M.Sc thesis, Dept. Of Physics, A. B. U Zaria.

Telford, W.M; Geldart, L.P.; Sheriff, R.E.and Keys, D.A. (1976): Applied geophysics. Cambridge University press, New York.

Todd,K.D;(1980): Groundwater hydrology; John Wiley and sons.

Zohdy,A.A.R and Bisdorf, R.j.(1989) A New Iterative Program for the Automatic interpretation of Wenner and Schlumberger Sounding Curves. Software.

Zohdy, A.A.R and Jacson, D.B(1969): Application of deep electric sounding for groundwater exploration in Hawaii: Geophysics 34(4), pp. 584-600.

Zohdy, A.A.R. Anderson, L.A. and Muffler, I.J.P. (1973): Resistivity,Self-potential, and induced polarization surveys of a vapor dominated geothermal system: Geophysics vol. 38, pp 1130-1144.

Zohdy, A.A.R. (1975): Automatic interpretation of Schlumberger Sounding curves,using modified Dar Zarrouk function: U.S.G.S. Geophysics Vol. 42(4) pp 811-822.

Zohdy, A.A.R. (1989): A new method for the automatic interpretation of Schlumberger and Wenner sounding curves: Geophysics Vol. 4(2), pp245-253.

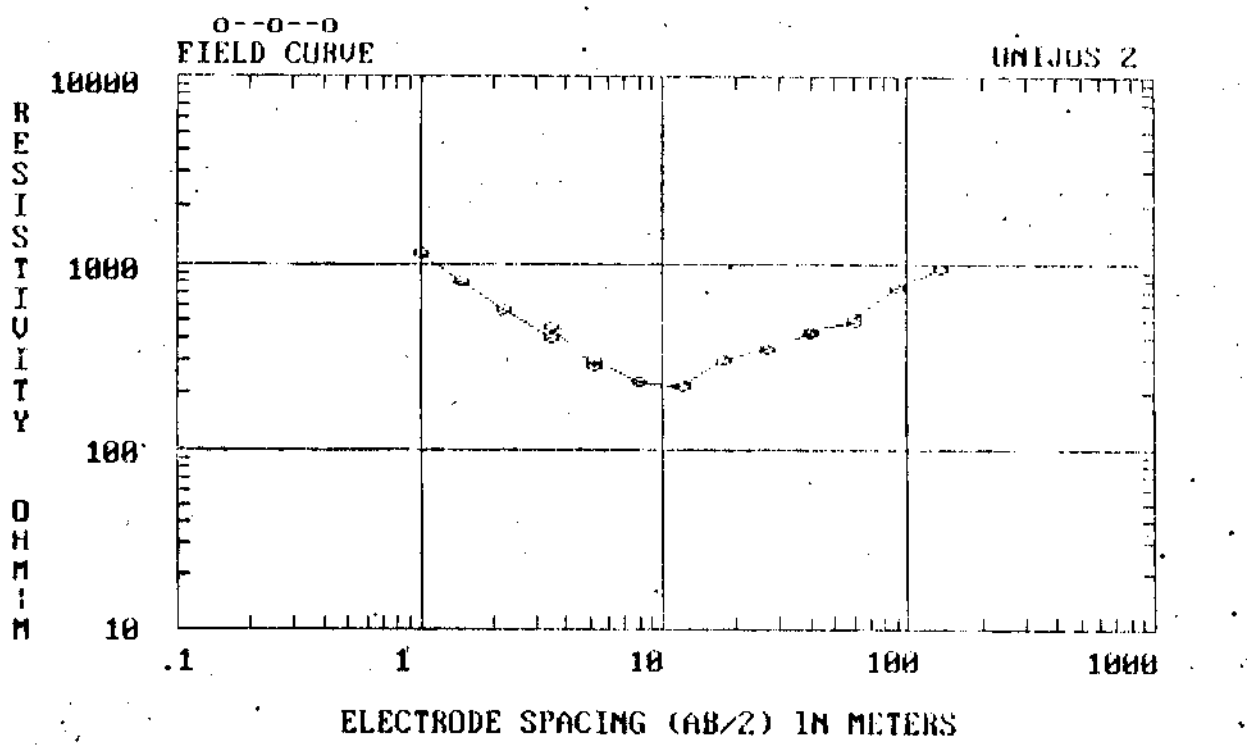
APPENDIX A

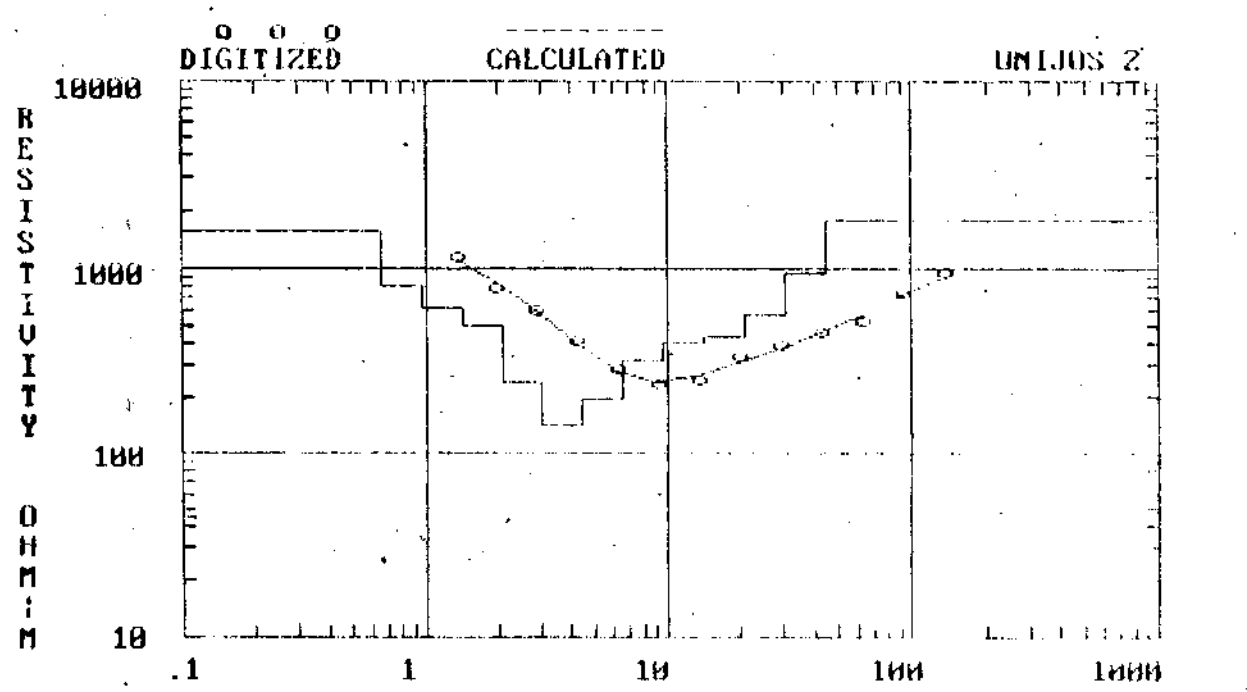
SUMMARY OF VES INTERPRETATION

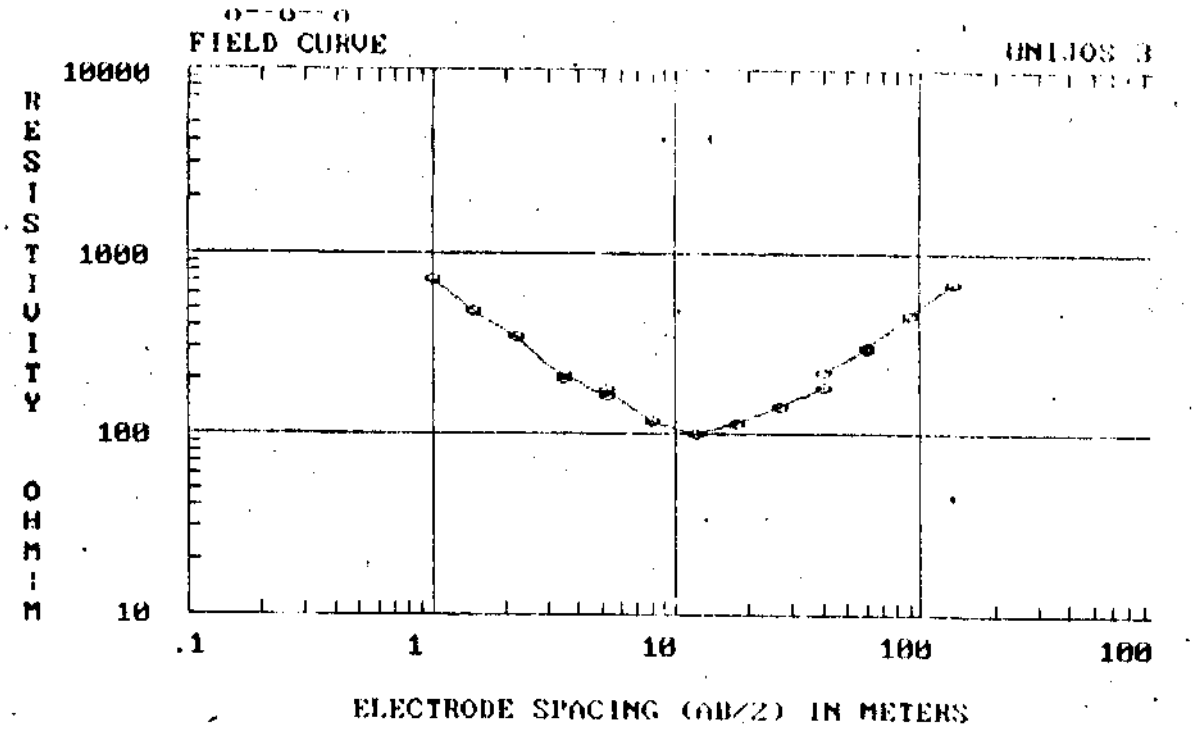
VES Station Number	No. of Layers	Resistivity of Layers (Ohm-m)					Thickness of Layers (m)				
		ρ1	ρ2	ρ3	ρ4	ρ5	T1	T2	T3	T4	T5
1	5	520	68.5	321.2	576	1385.2	2.0	25	12.0	9.0	∞
2	5	1000	122	175	612	1250	2.5	5.0	21.0	11.0	∞
3	5	612	191	300	1000	3000	2.0	21.0	11.0	6.0	∞
4	5	450	150	450	775.2	1350	2.5	16.0	16.0	11.5	∞
5	5	320	70	376	531	1230	0.7	10.0	18.5	11.0	∞
6	5	483	183	172	851	1500	1.1	8.9	8.7	15.3	∞
7	5	1200	200	304.2	700	1092	1.0	7.0	20.5	14.0	∞
8	5	121	113	325	613	1750	2.0	11.1	9.0	12.0	∞
9	4	215	91.5	375	850	-	2.3	10.0	16.5	14.2	∞
10	3	32.5	105	317.6	-	-	7.0	31.5	∞		
11	5	125	82.7	375	850	1500	1.0	23.7	10.7	11.7	∞
12	3	150	97.1	612.5	-	-	0.8	23.1	∞		
13	3	100	91.4	501.6	-	-	2.5	33.4	∞		
14	5	100	111	422.2	961.2	3.21	1.0	17.1	16.0	∞	
15	5	6125	175	613	1000	1150	1.9	5.7	22.0	12.5	∞
16	5	300	115	421.5	802	1067	1.0	11.5	17.0	16.0	∞
17	5	251	181	315	856.3	1500	0.8	22.0	10.5	12.0	∞
18	5	350	45	223	718	2200	0.8	20.0	9.0	11.5	∞
19	4	450	200	350.2	693.5	-	2.0	19.0	8.0	∞	
20	5	483	93.7	307	775	1750	1.5	20.2	11.0	15.4	∞
21	4	700	75	475	1092	-	1.5	5.0	27.0	∞	
22	5	716.7	178	97.1	612.5	1750	0.7	3.9	18.4	22.0	∞
23	5	650	95	480	750	1500	1.5	18.0	12.0	11.5	∞
24	4	250	156	375	850	-	0.8	9.7	18.3	∞	
25		1050	213	485	920	1100	0.8	13.0	12.5	16.2	∞
26		1180	271	450	815	1500	5.1	2.6	13.2	0.5	∞

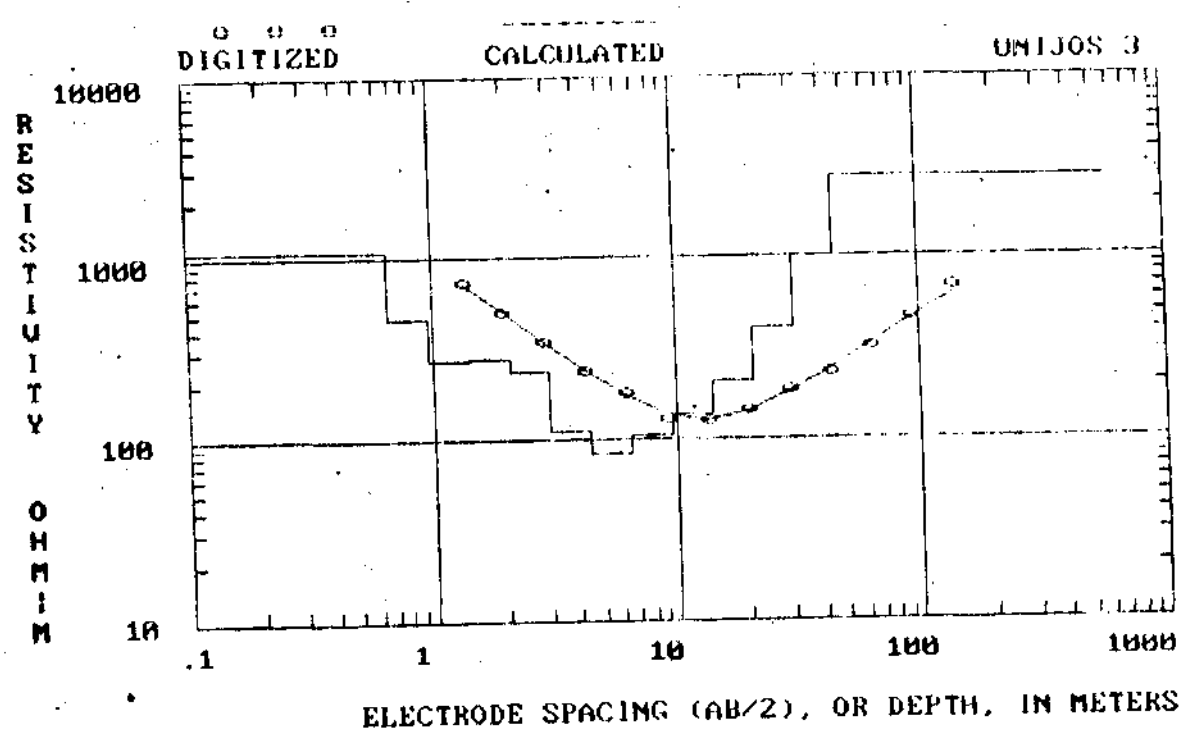
APPENDIX B

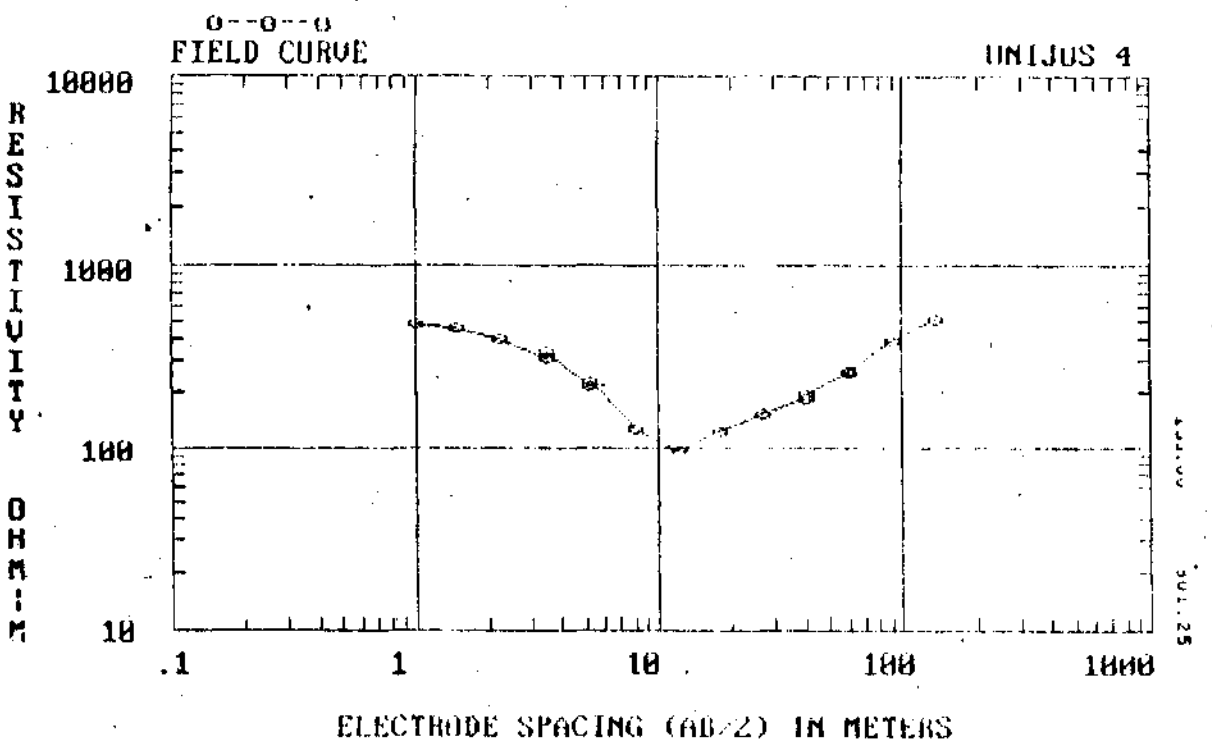
Field Curves and Interpreted True Resistivity Layer Models for the VES Measurements.

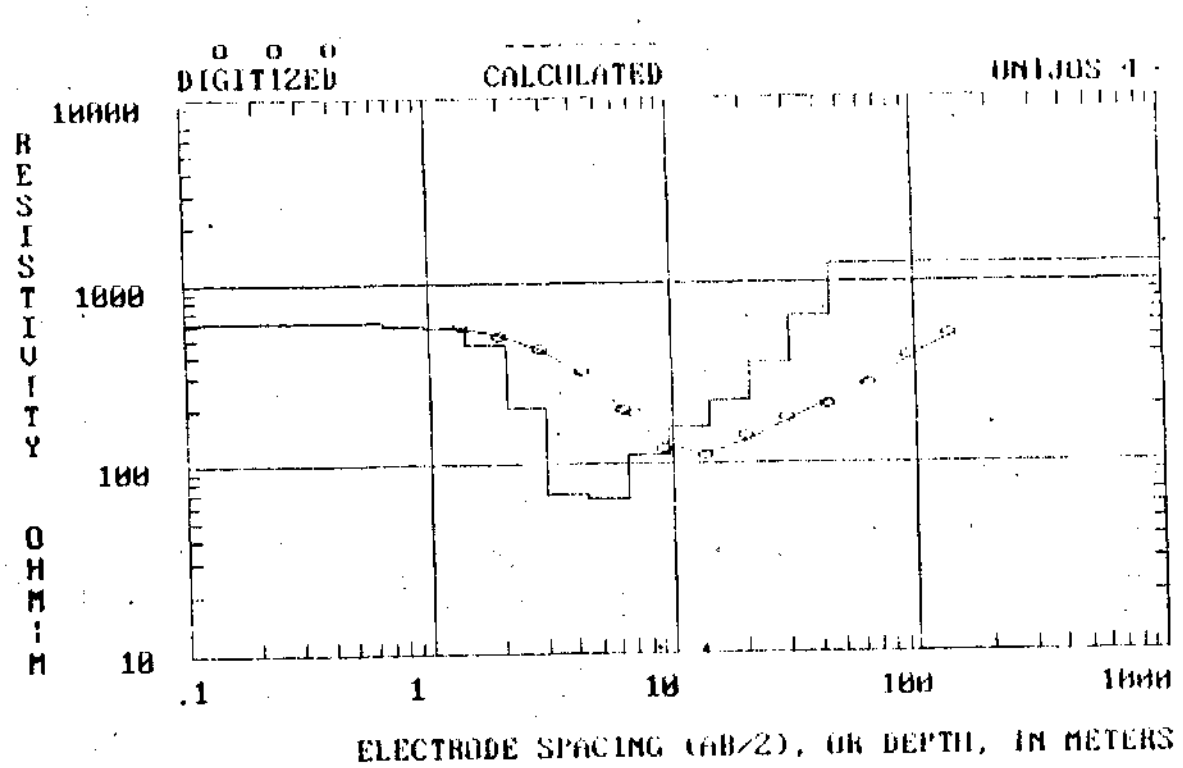

o--o--o
FIELD CURVE
UNIJOS 2
RESISTIVITY OHM-M
10000
1000
100
10
.1
1
10
100
1000
ELECTRODE SPACING (AB/2) IN METERS

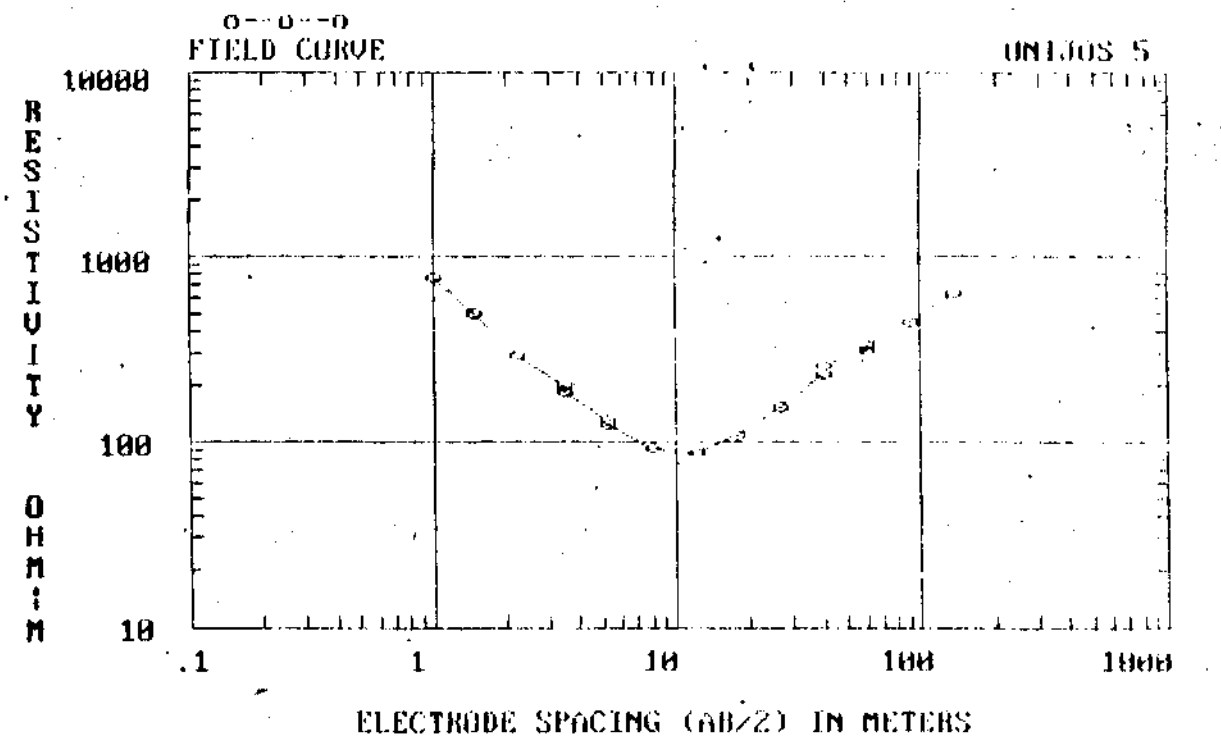

o o o
DIGITIZED
CALCULATED
UNIJOS 2
RESISTIVITY OHM-M
10000
1000
100
10
.1
1
10
100
1000
ELECTRODE SPACING (AB/2), OR DEPTH, IN METERS

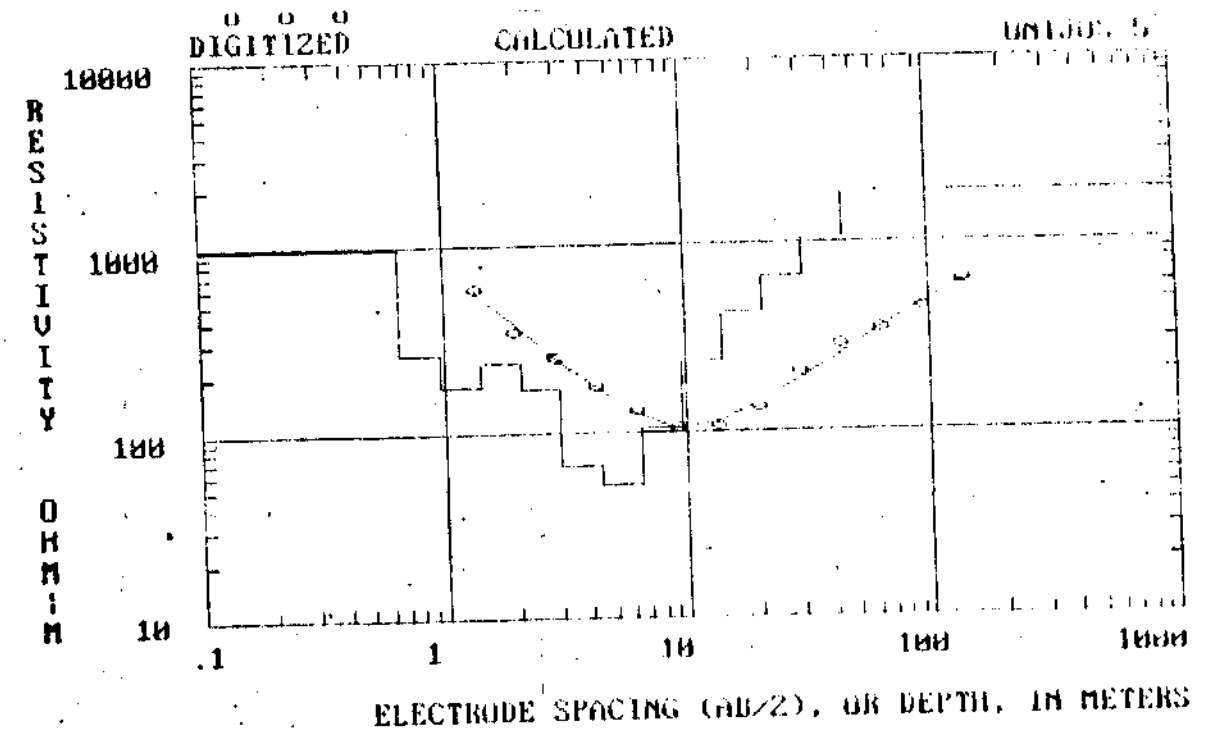

FIELD CURVE
UNIJOS 3
RESISTIVITY OHMM
10000
1000
100
10
.1
1
10
100
100
ELECTRODE SPACING (AB/2) IN METERS

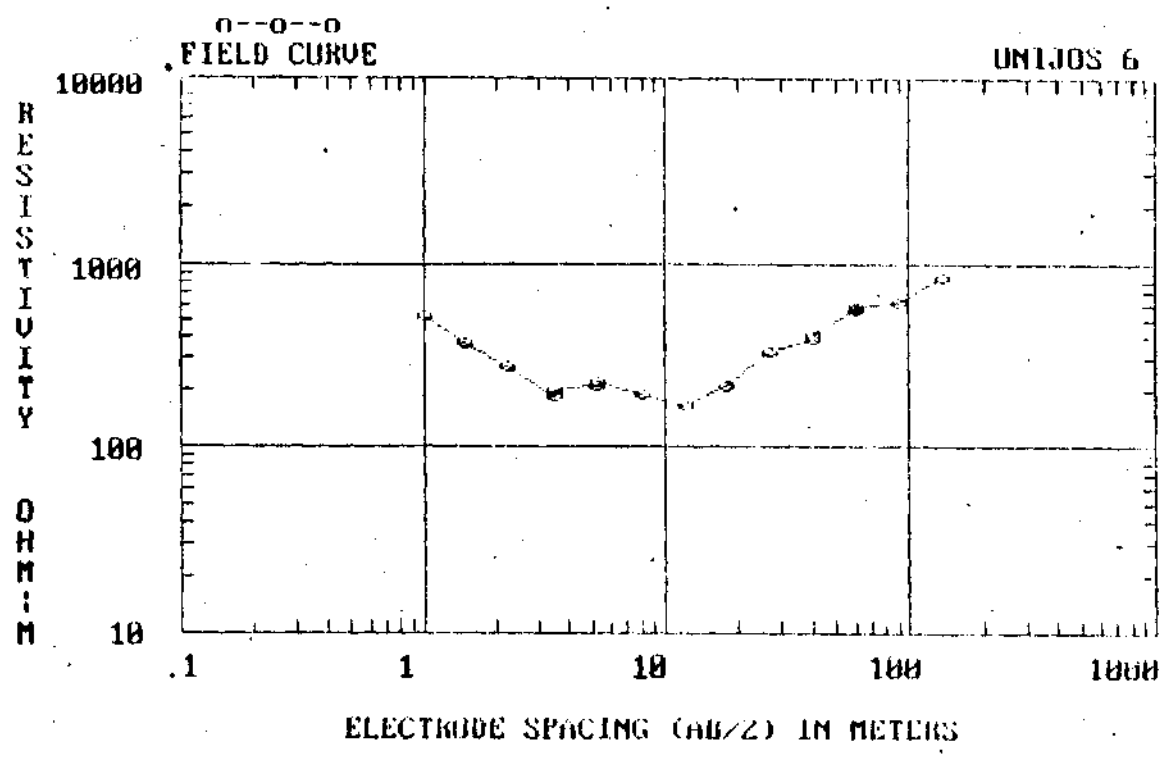

DIGITIZED
CALCULATED
UNIJOS 3
RESISTIVITY OHMM
10000
1000
100
10
.1
1
10
100
1000
ELECTRODE SPACING (AB/2), OR DEPTH, IN METERS

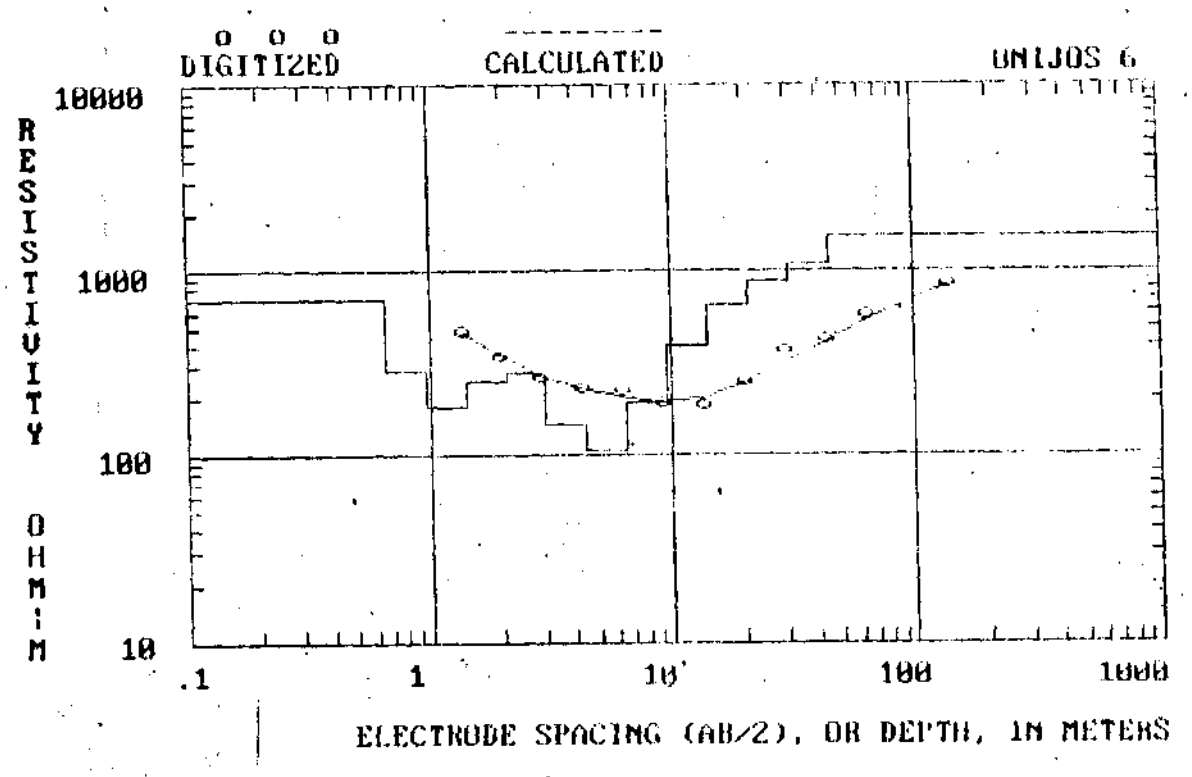

o--o--o
FIELD CURVE
UNIJUS 4
RESISTIVITY OHM--M
10000
1000
100
10
.1
1
10
100
1000
ELECTRODE SPACING (AB/2) IN METERS

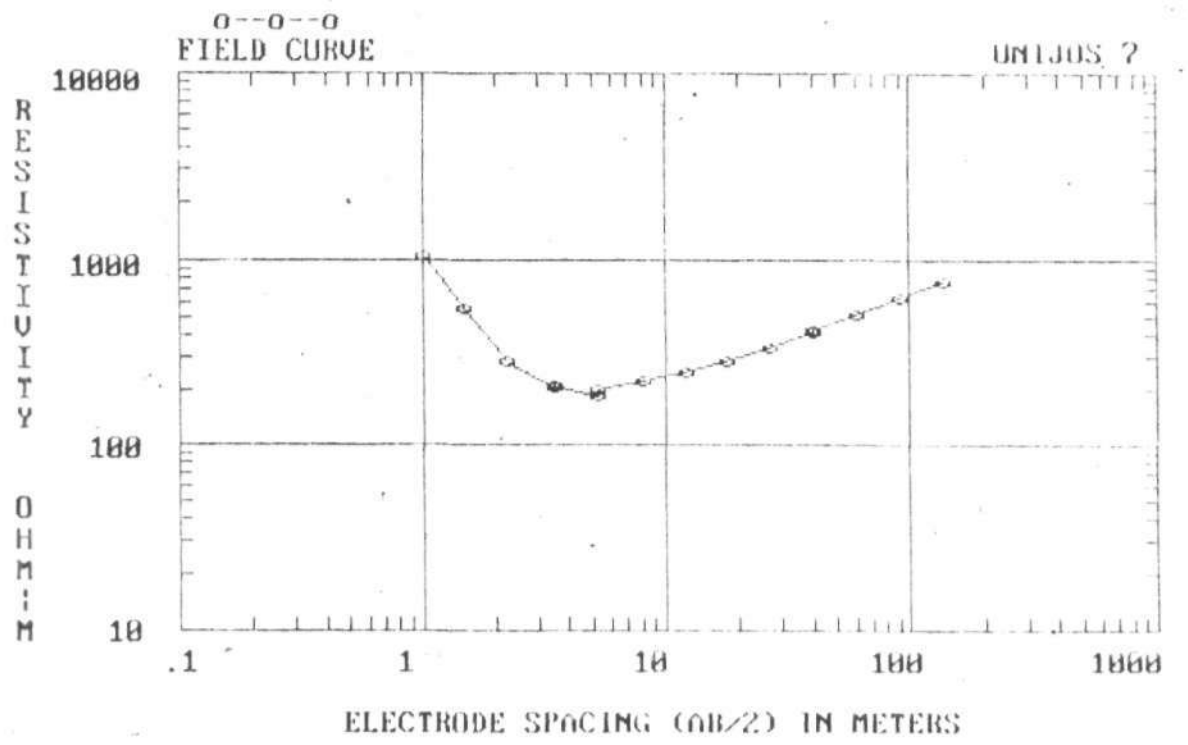

o o o
DIGITIZED
CALCULATED
UNIJUS 4
RESISTIVITY OHM-M
10000
1000
100
10
.1
1
10
100
1000
ELECTRODE SPACING (AB/2), OR DEPTH, IN METERS

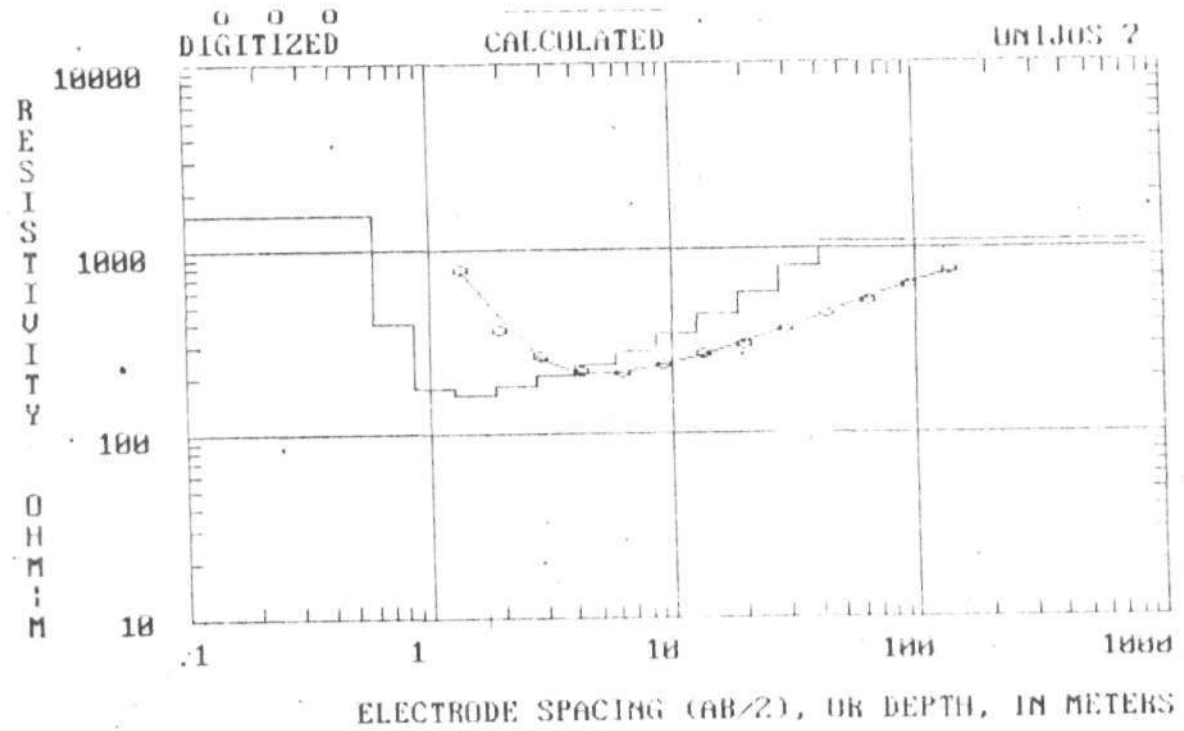

o--o--o
FIELD CURVE
UNIJOS 5
RESISTIVITY OHM-M
10000
1000
100
10
.1
1
10
100
1000
ELECTRODE SPACING (AB/2) IN METERS

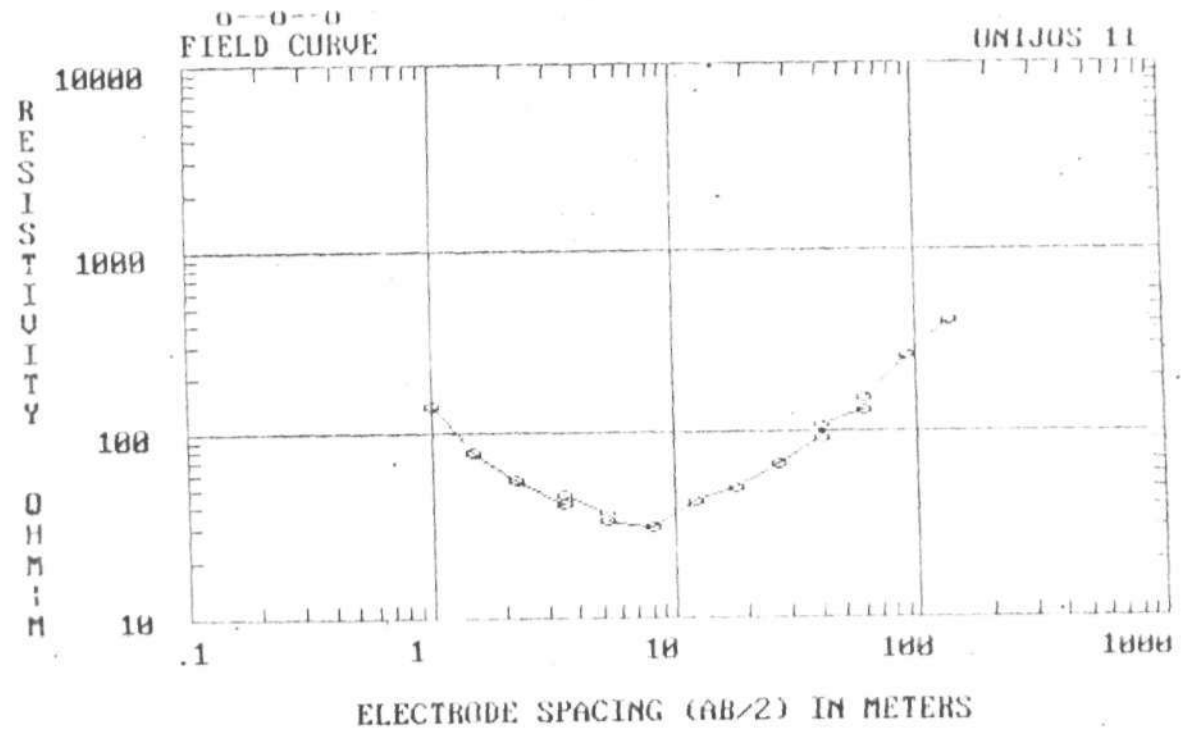

o o o
DIGITIZED
CALCULATED
UNIJOS 5
RESISTIVITY OHM-M
10000
1000
100
10
.1
1
10
100
1000
ELECTRODE SPACING (AB/2), OR DEPTH, IN METERS

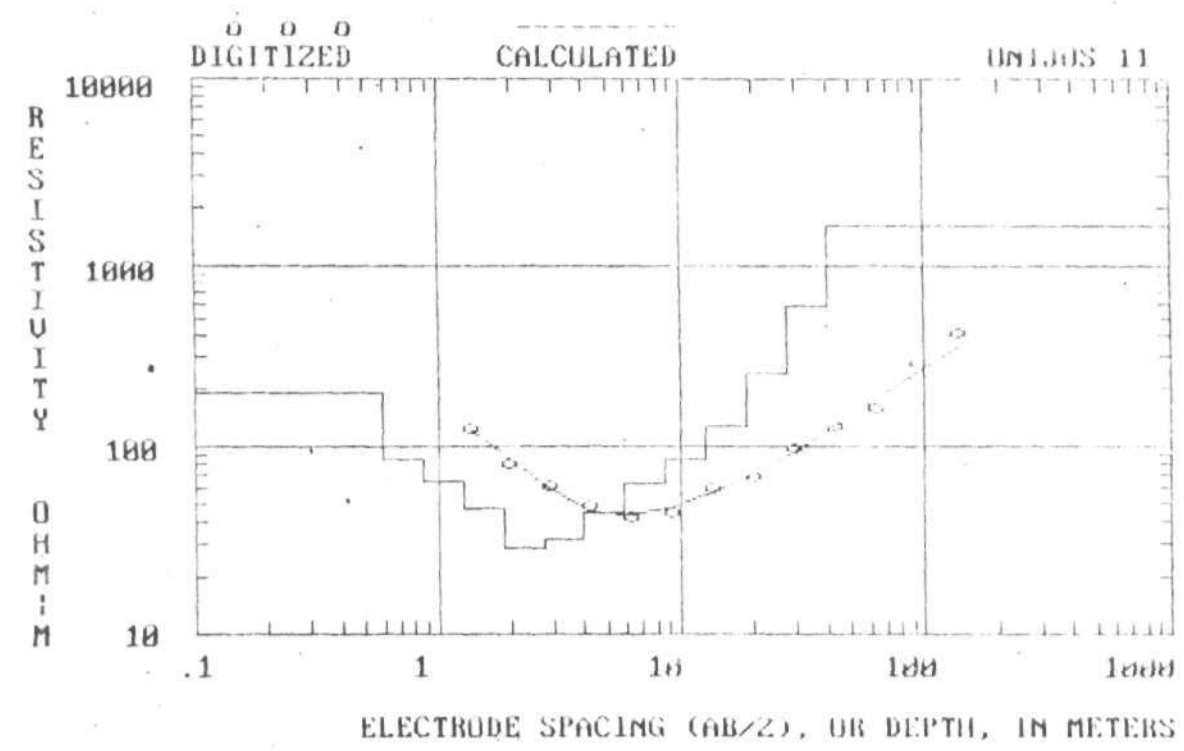

o--o--o
FIELD CURVE
UNIJOS 6
RESISTIVITY OHM-M
10000
1000
100
10
.1
1
10
100
1000
ELECTRODE SPACING (AB/2) IN METERS

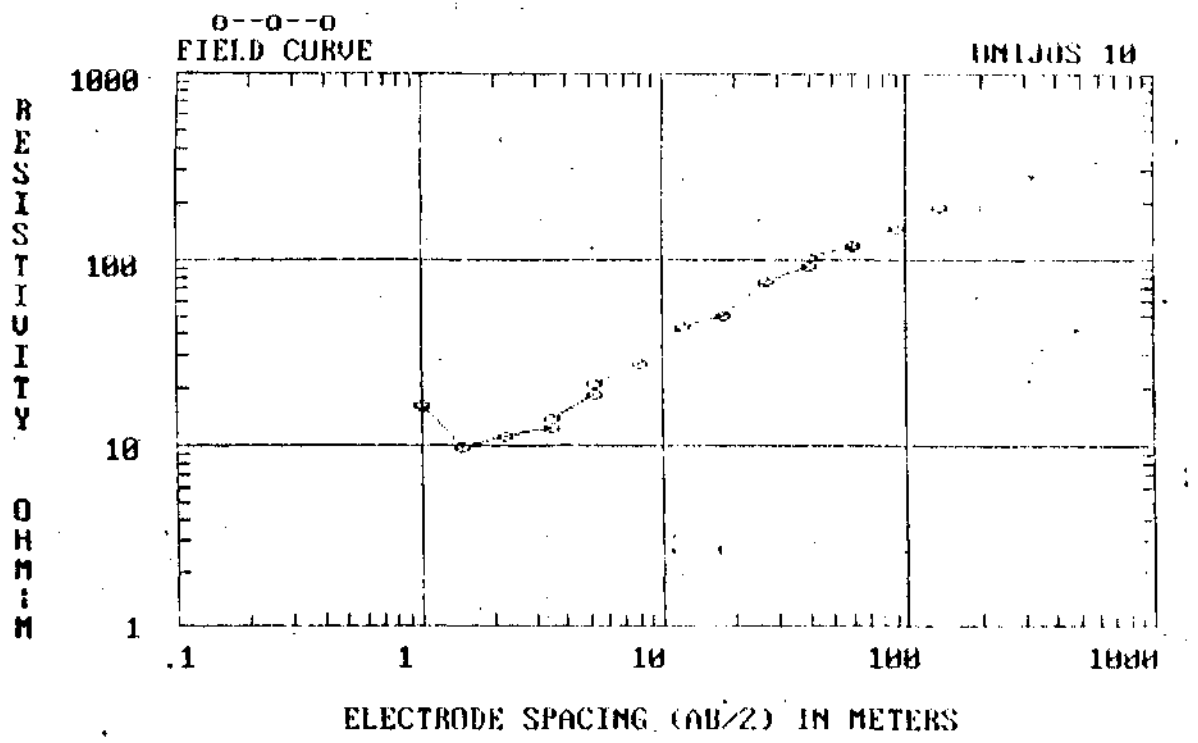

o o o
DIGITIZED
CALCULATED
UNIJOS 6
RESISTIVITY OHM-M
10000
1000
100
10
.1
1
10
100
1000
ELECTRODE SPACING (AB/2), OR DEPTH, IN METERS

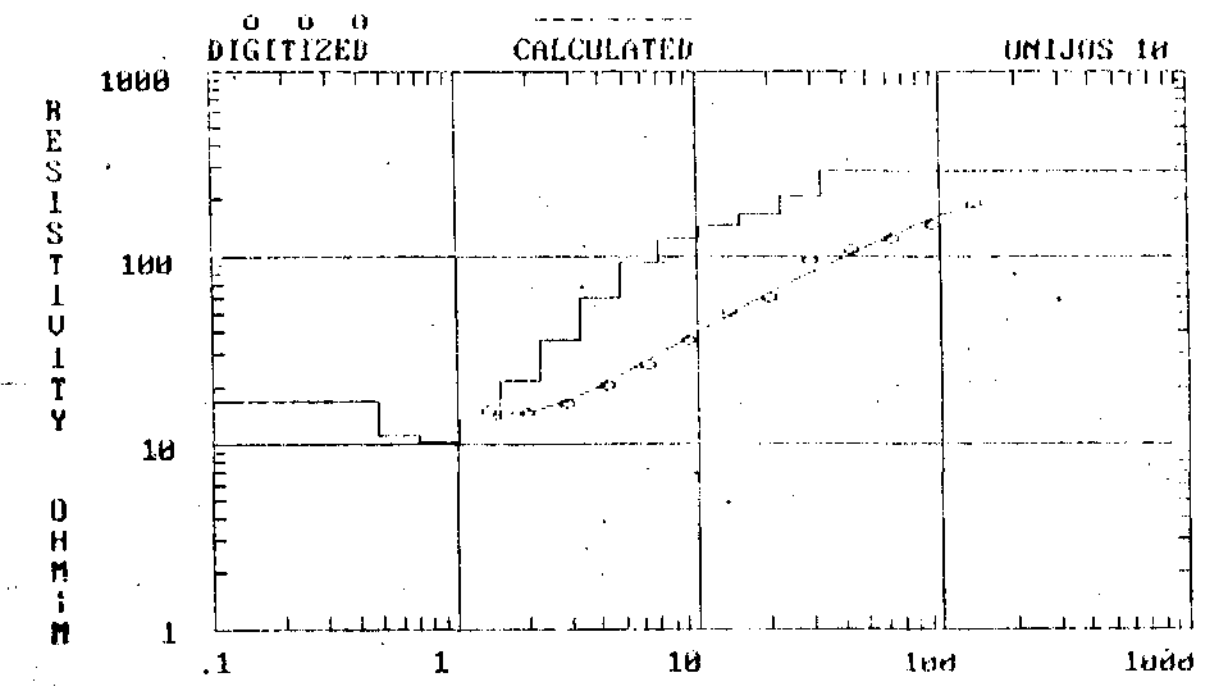

o--o--o
FIELD CURVE
UNIJOS ?
10000
1000
100
10
RESISTIVITY OHM-M
.1
1
10
100
1000
ELECTRODE SPACING (AB/2) IN METERS

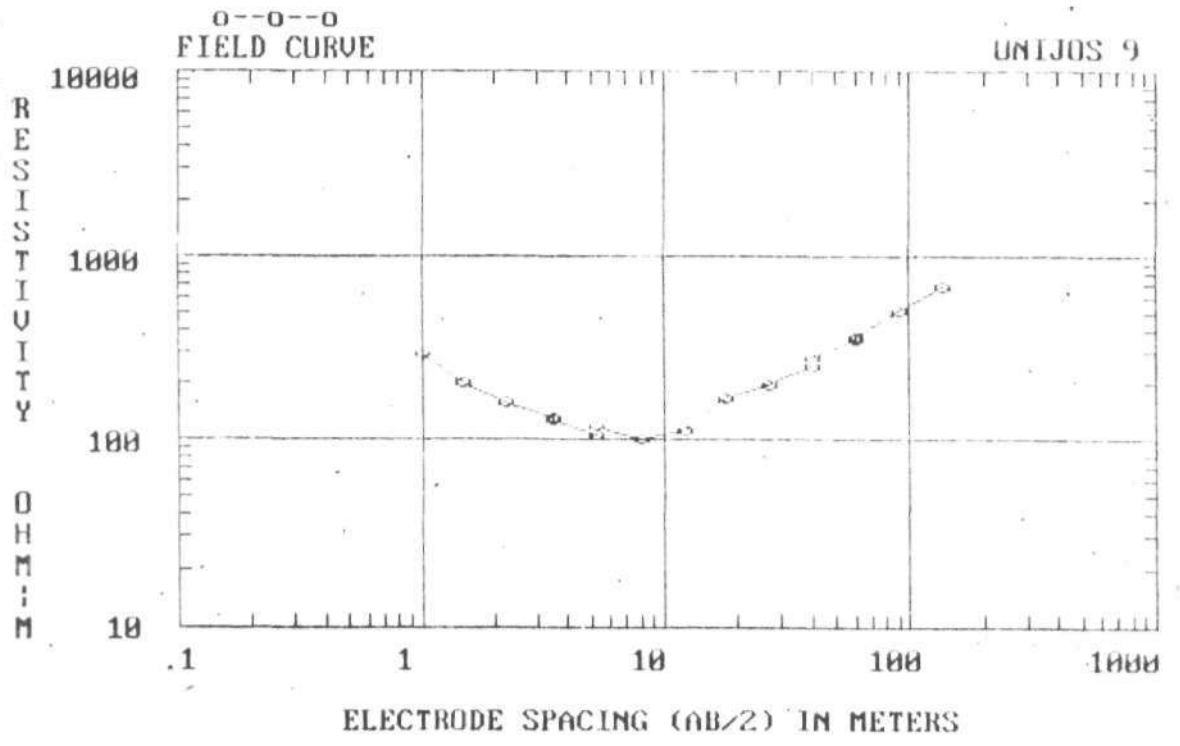

o o o
DIGITIZED
CALCULATED
UNIJOS ?
10000
1000
100
10
RESISTIVITY OHM-M
.1
1
10
100
1000
ELECTRODE SPACING (AB/2), OR DEPTH, IN METERS

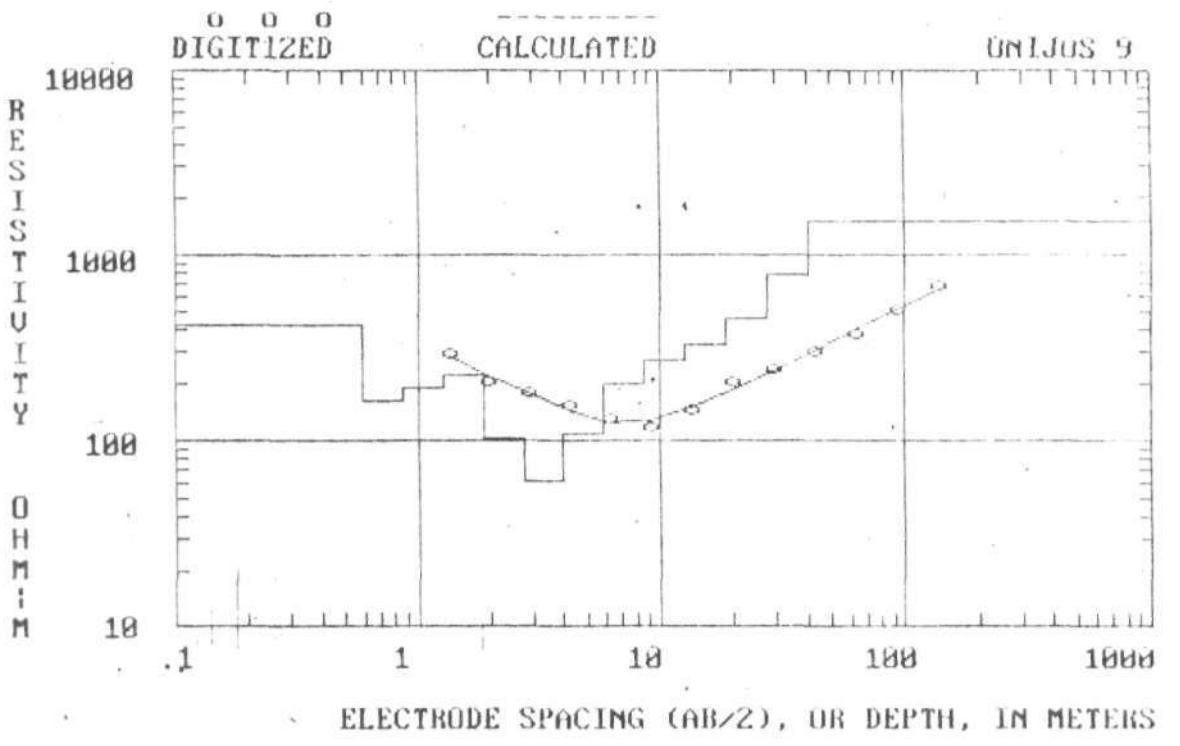

FIELD CURVE
UNIJOS 11
10000
1000
100
10
RESISTIVITY OHM-M
.1
1
10
100
1000
ELECTRODE SPACING (AB/2) IN METERS

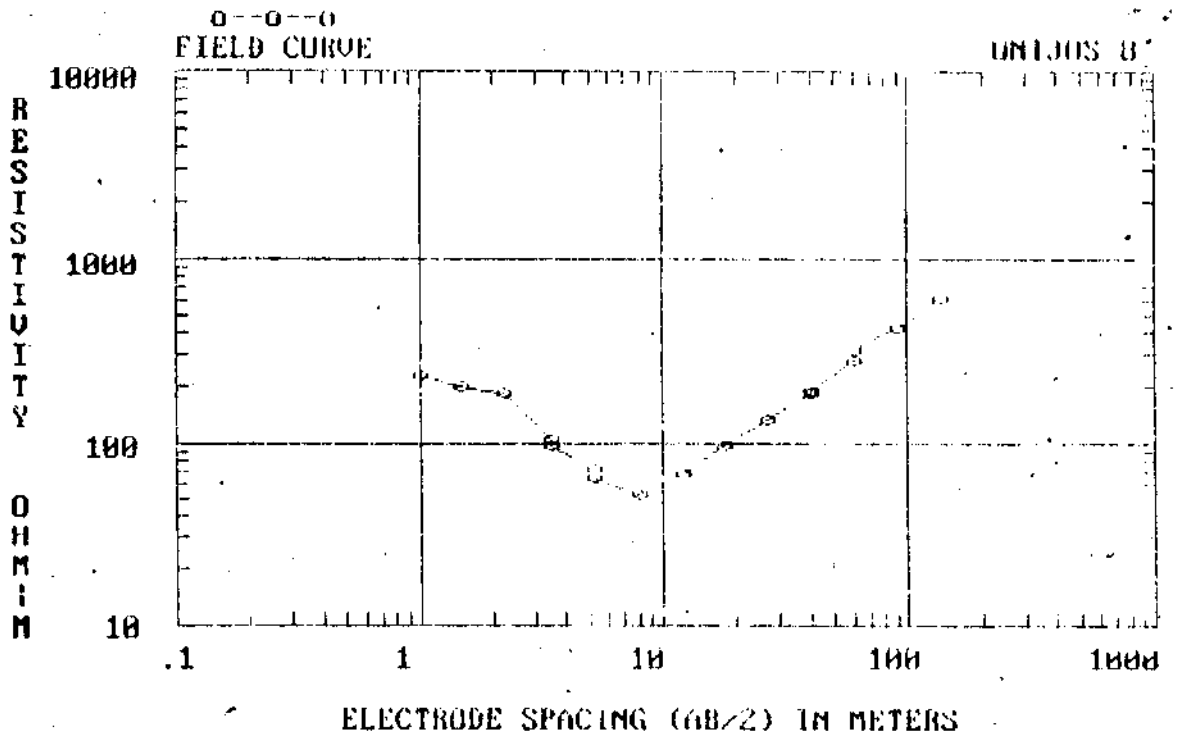

DIGITIZED
CALCULATED
UNIJOS 11
10000
1000
100
10
RESISTIVITY OHM-M
.1
1
10
100
1000
ELECTRODE SPACING (AB/2), OR DEPTH, IN METERS

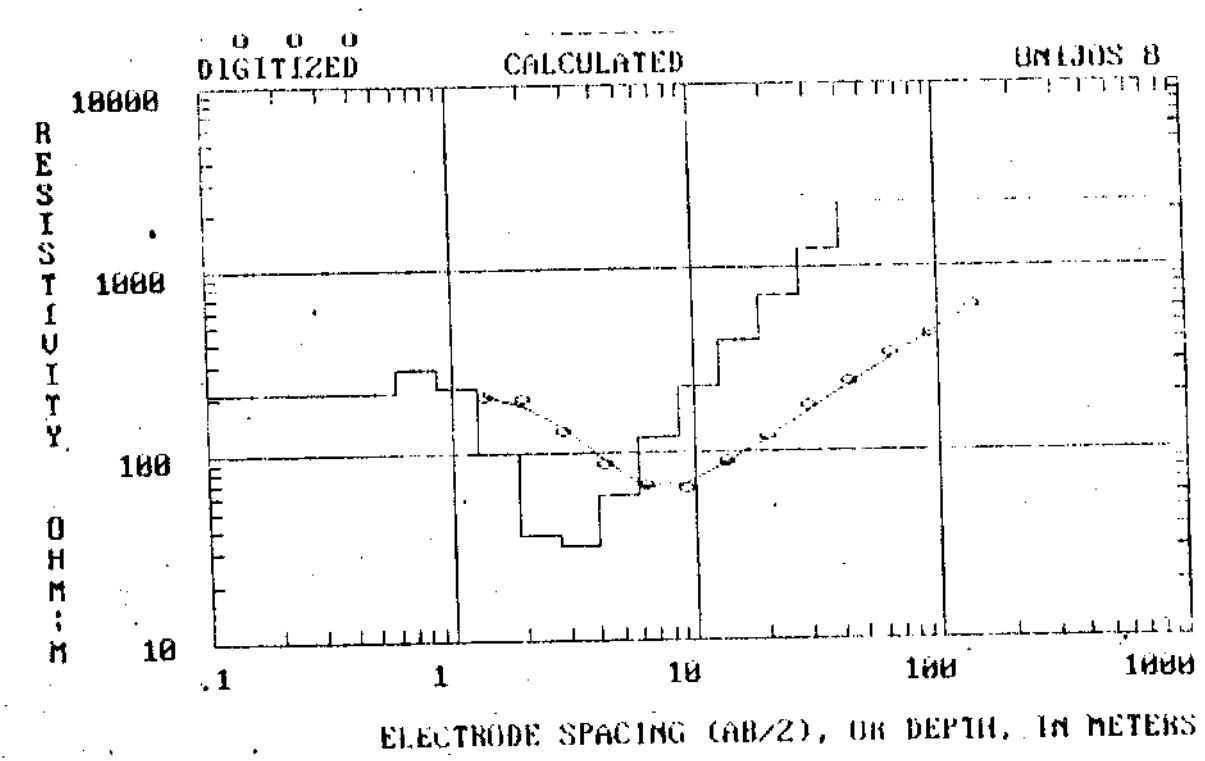

o--o--o
FIELD CURVE
UNIJOS 10
RESISTIVITY OHM-M
1000
100
10
1
.1
1
10
100
1000
ELECTRODE SPACING (AB/2) IN METERS

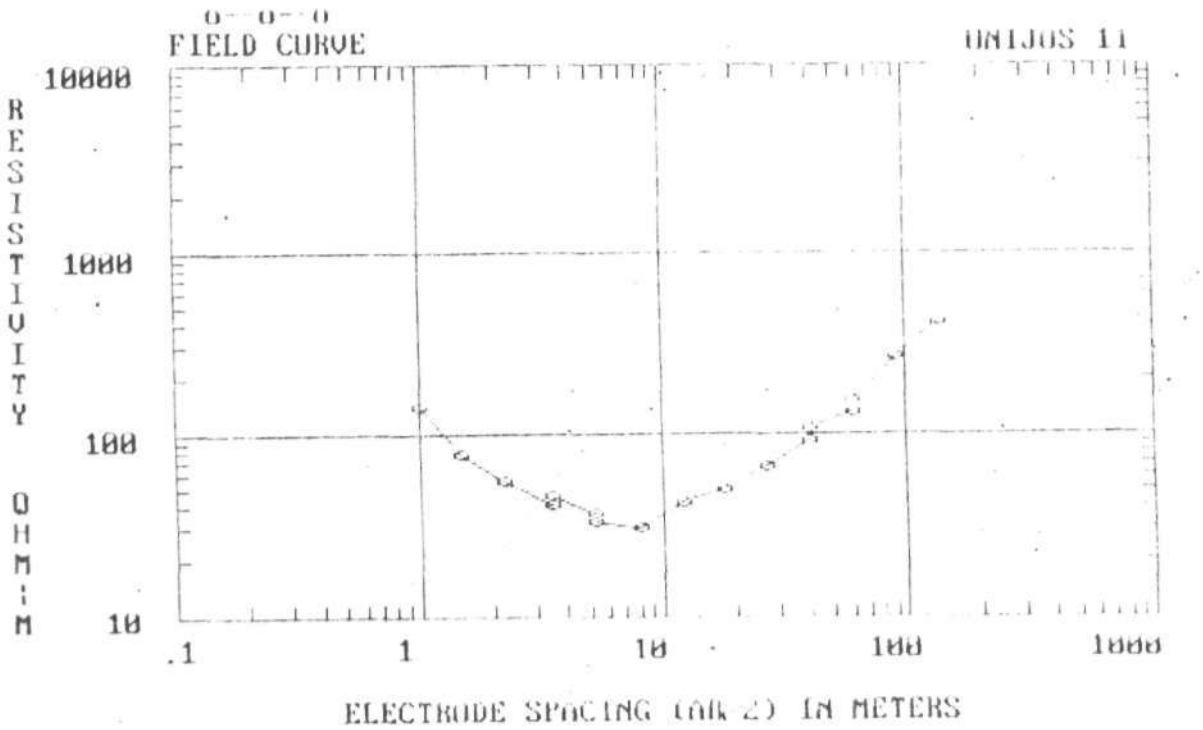

o o o
DIGITIZED
CALCULATED
UNIJOS 10
RESISTIVITY OHM-M
1000
100
10
1
.1
1
10
100
1000
ELECTRODE SPACING (AB/2), OR DEPTH, IN METERS

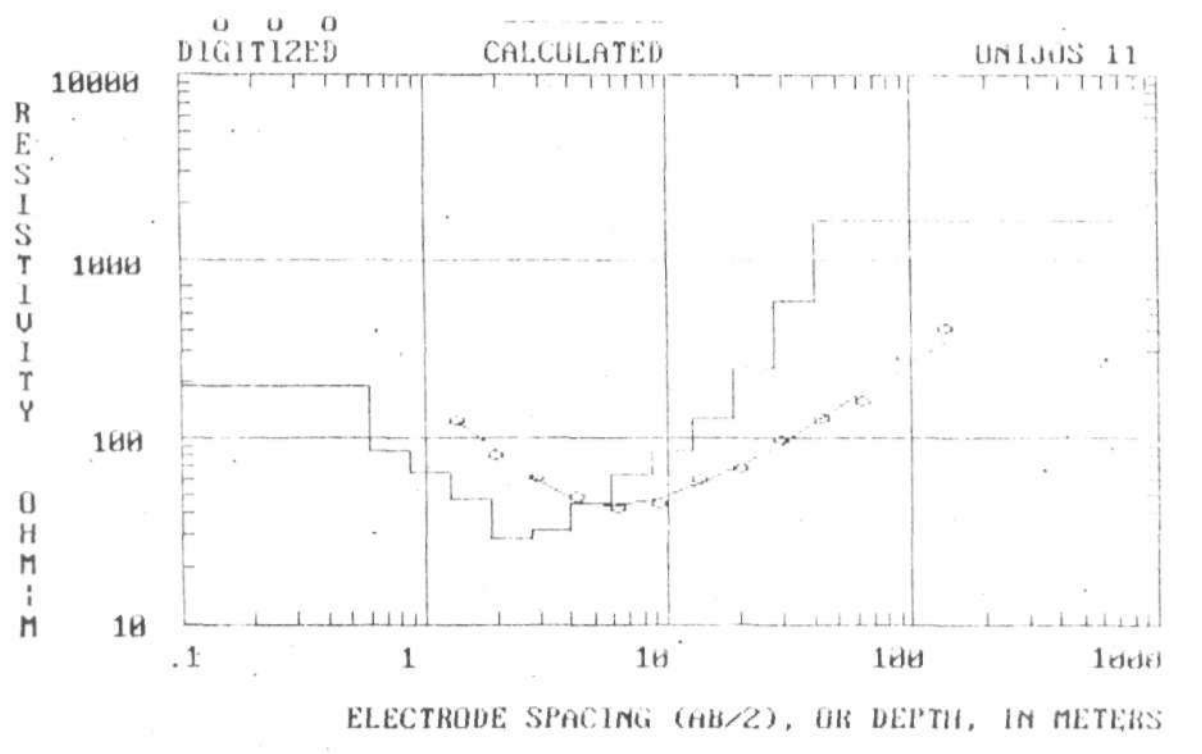

o--o--o
FIELD CURVE
UNIJOS 9
RESISTIVITY OHM-M
10000
1000
100
10
.1
1
10
100
1000
ELECTRODE SPACING (AB/2) IN METERS

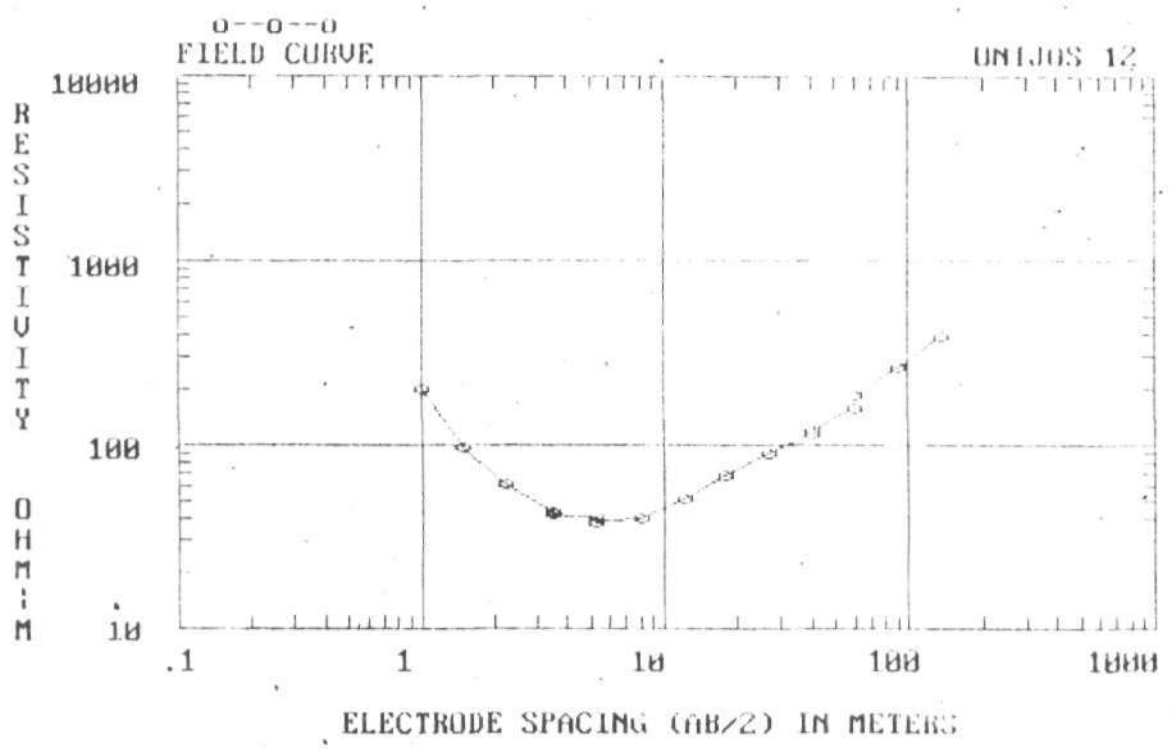

o o o
DIGITIZED
CALCULATED
UNIJOS 9
RESISTIVITY OHM-M
10000
1000
100
10
.1
1
10
100
1000
ELECTRODE SPACING (AB/2), OR DEPTH, IN METERS

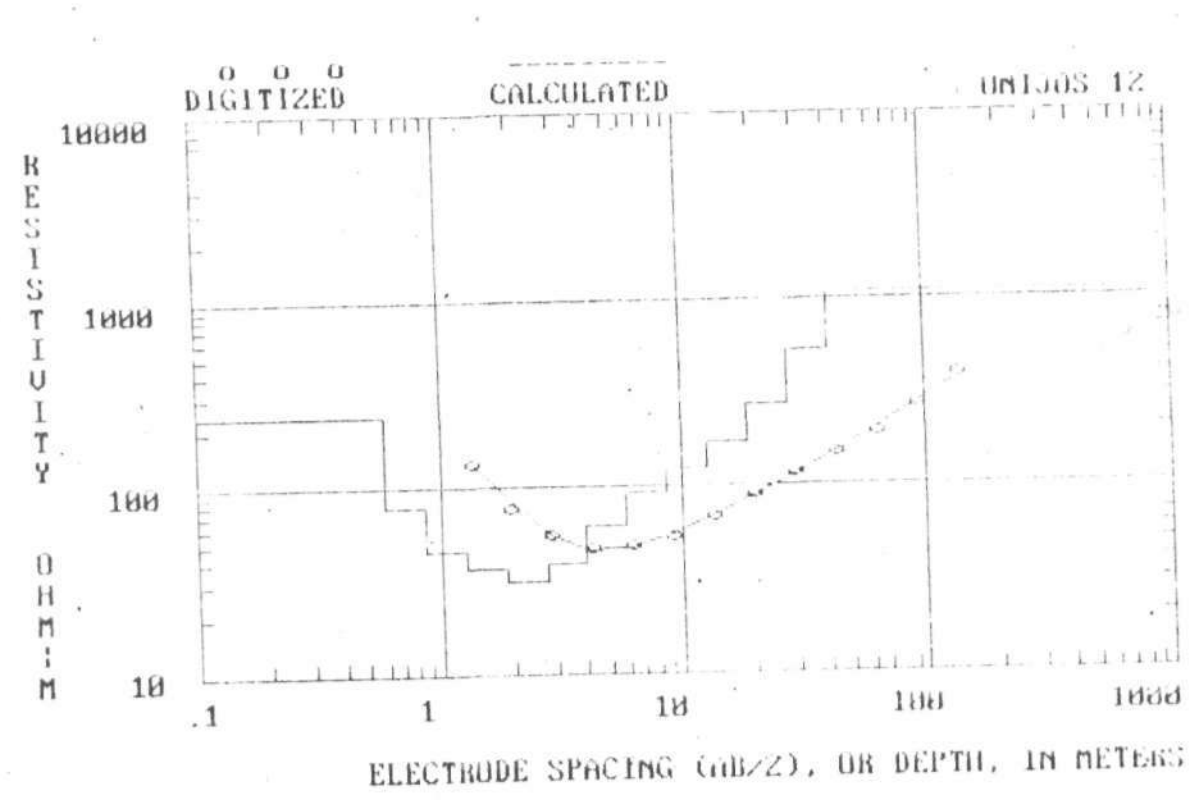

o--o--o
FIELD CURVE
UNIJOS 8
RESISTIVITY OHM-M
10000
1000
100
10
.1
1
10
100
1000
ELECTRODE SPACING (AB/2) IN METERS

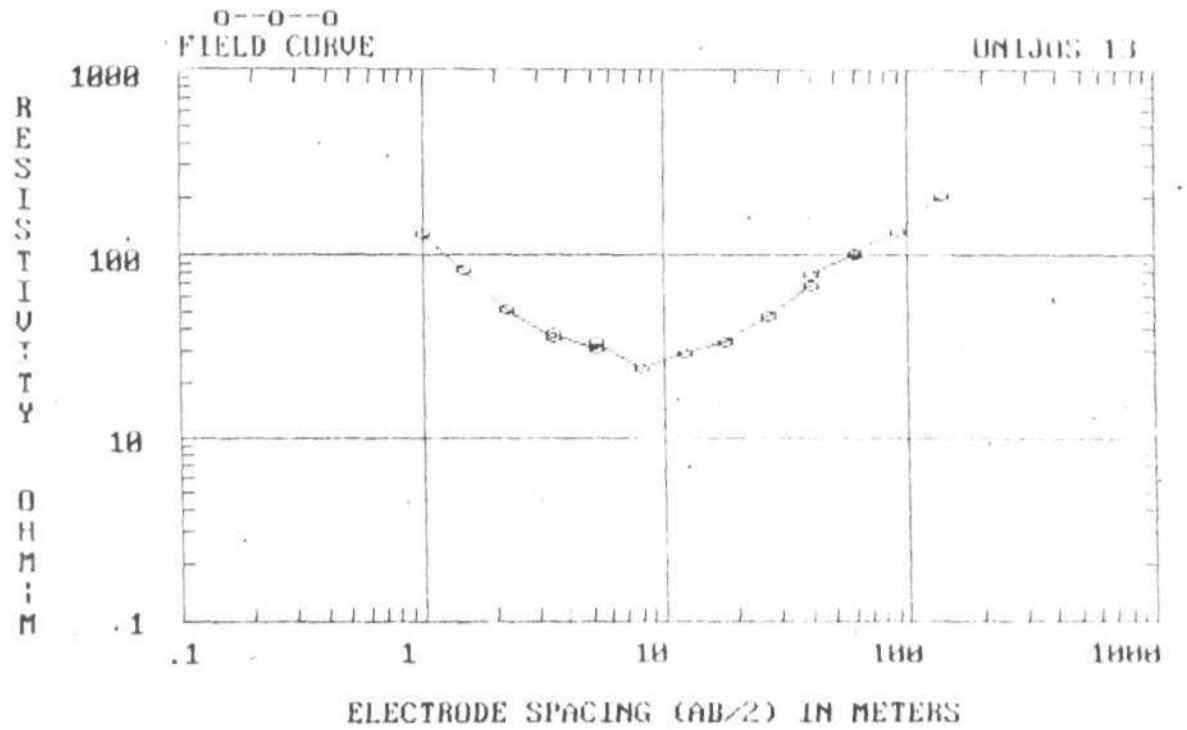

o o o
DIGITIZED
CALCULATED
UNIJOS 8
RESISTIVITY OHM-M
10000
1000
100
10
.1
1
10
100
1000
ELECTRODE SPACING (AB/2), OR DEPTH, IN METERS

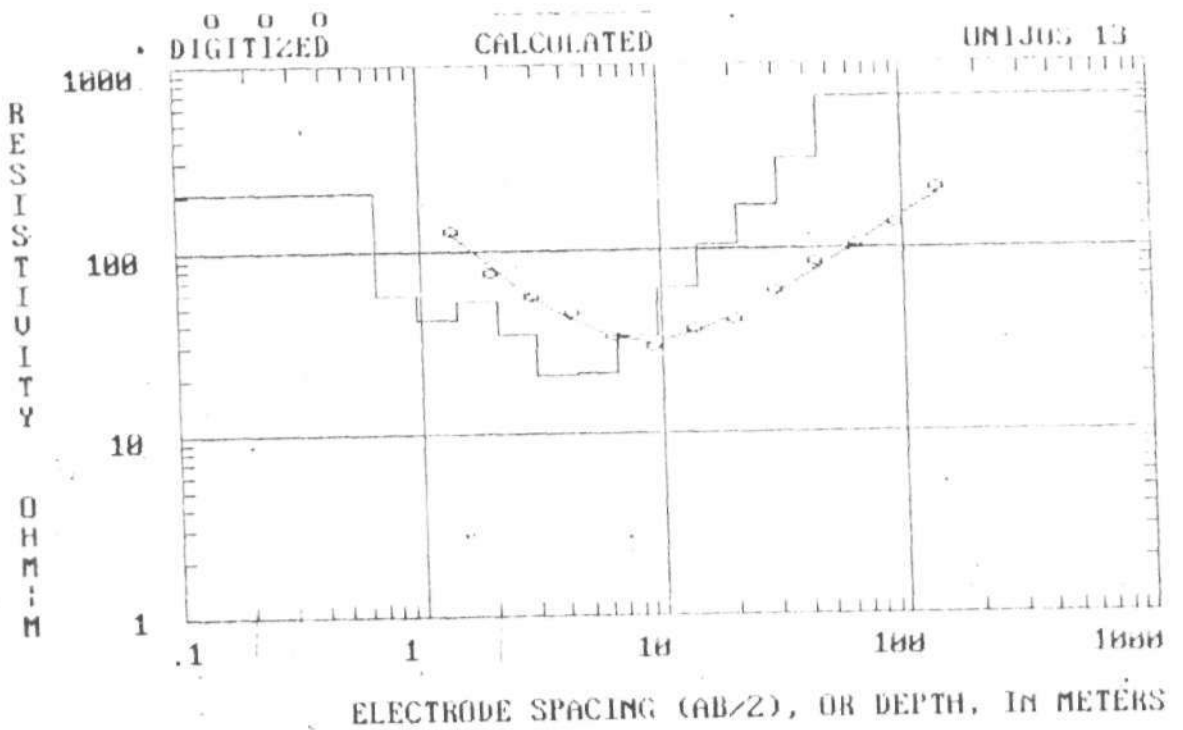

FIELD CURVE
UNIJOS 11
RESISTIVITY OHM-M
10000
1000
100
10
.1
1
10
100
1000
ELECTRODE SPACING (AB/2) IN METERS

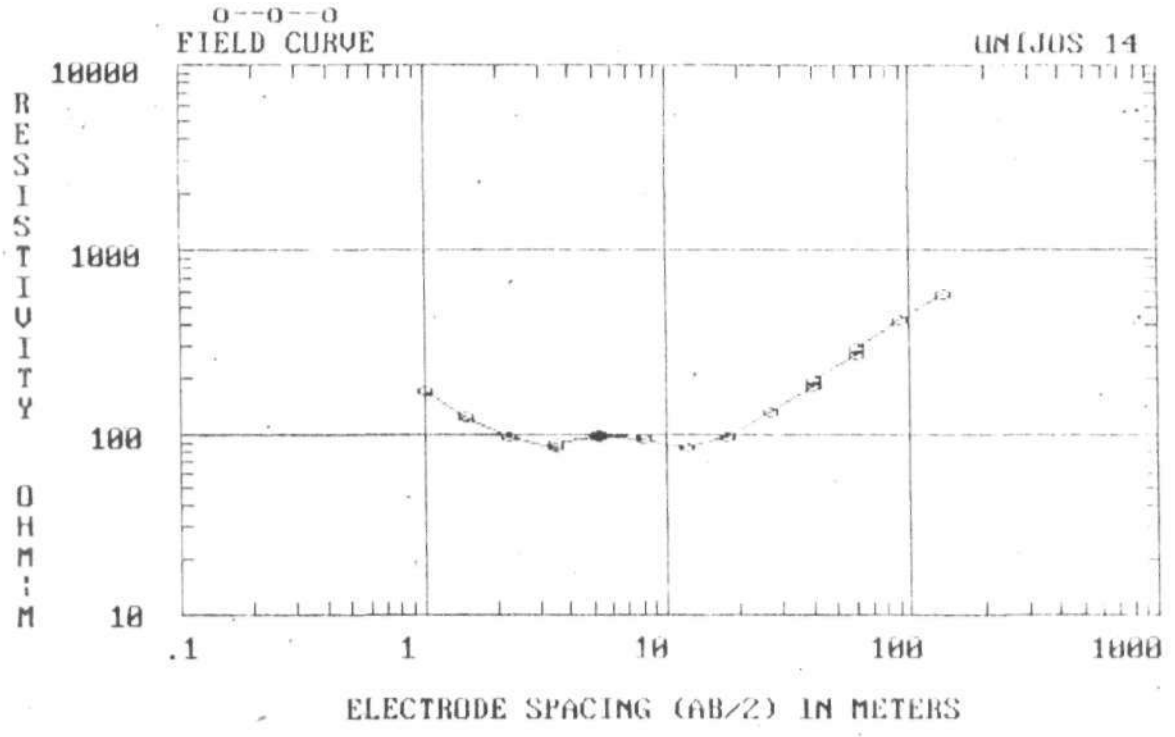

DIGITIZED
CALCULATED
UNIJOS 11
RESISTIVITY OHM-M
10000
1000
100
10
.1
1
10
100
1000
ELECTRODE SPACING (AB/2), OR DEPTH, IN METERS

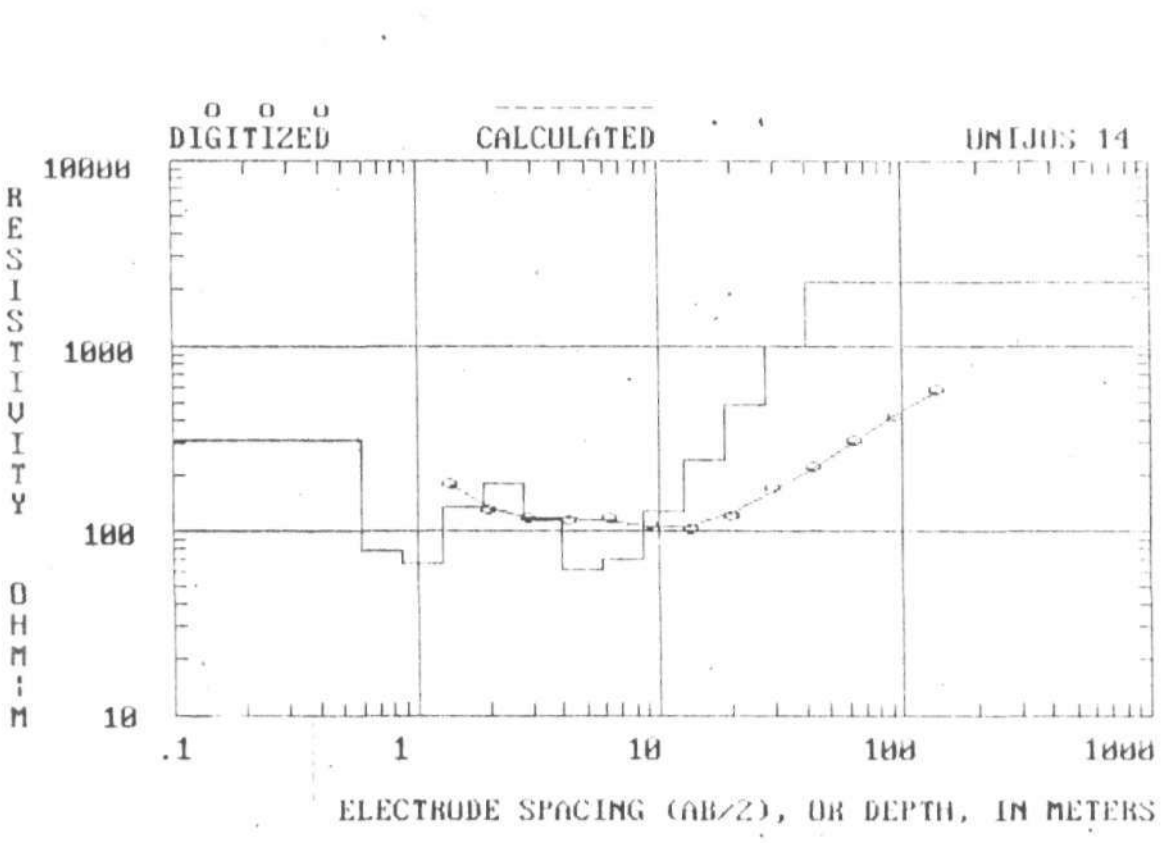

o--o--o
FIELD CURVE
UNIJOS 12
RESISTIVITY OHM-M
10000
1000
100
10
.1
1
10
100
1000
ELECTRODE SPACING (AB/2) IN METERS

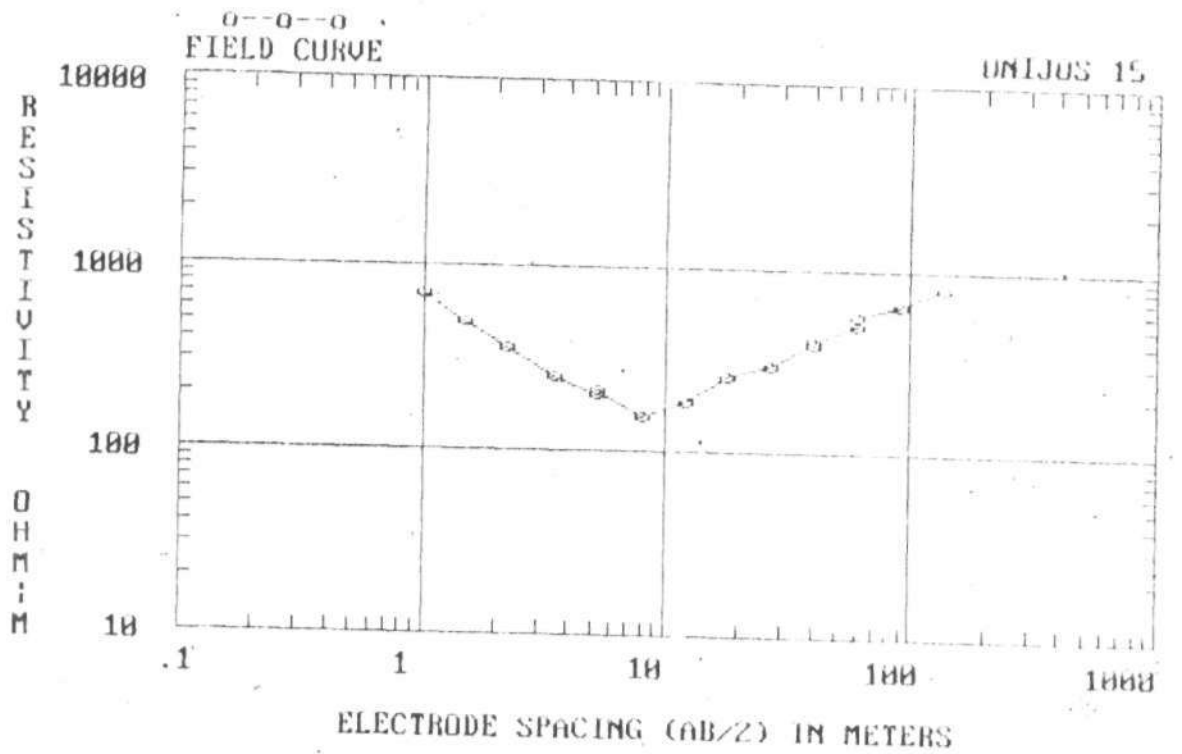

o o o
DIGITIZED
CALCULATED
UNIJOS 12
RESISTIVITY OHM-M
10000
1000
100
10
.1
1
10
100
1000
ELECTRODE SPACING (AB/2), OR DEPTH, IN METERS

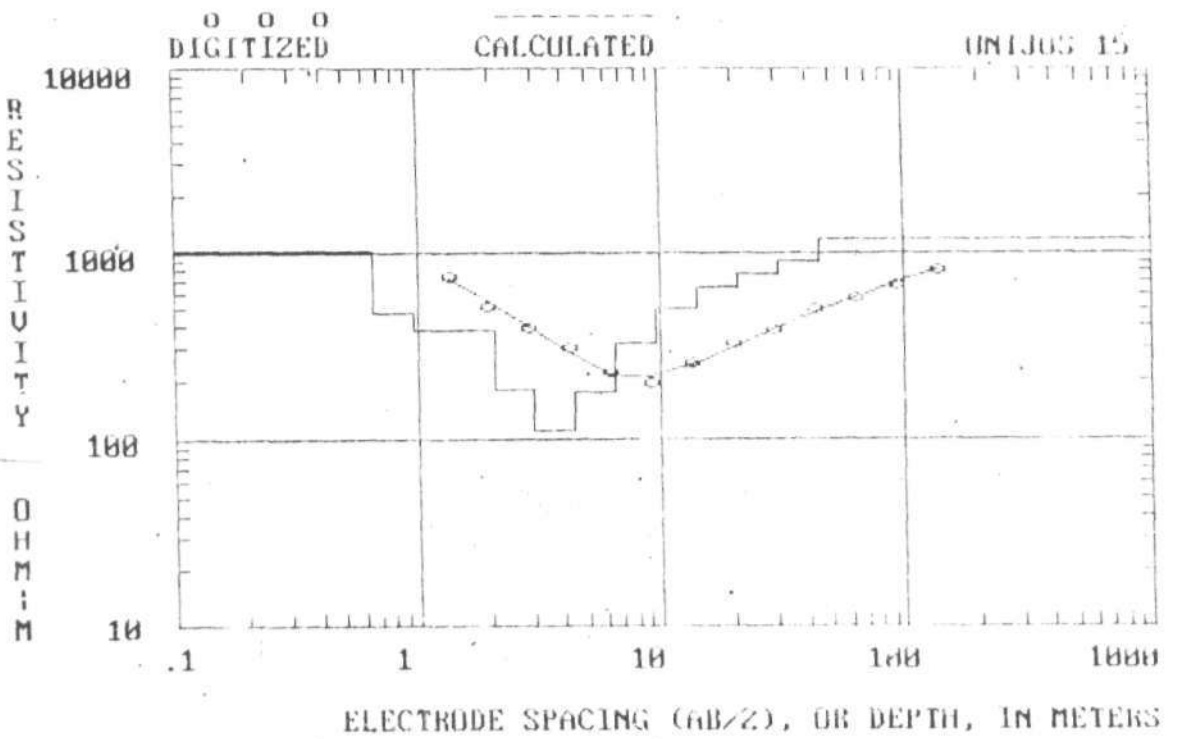

o--o--o
FIELD CURVE
UNIJOB 13
1000
100
10
.1
RESISTIVITY OHM-M
.1
1
10
100
1000
ELECTRODE SPACING (AB/2) IN METERS

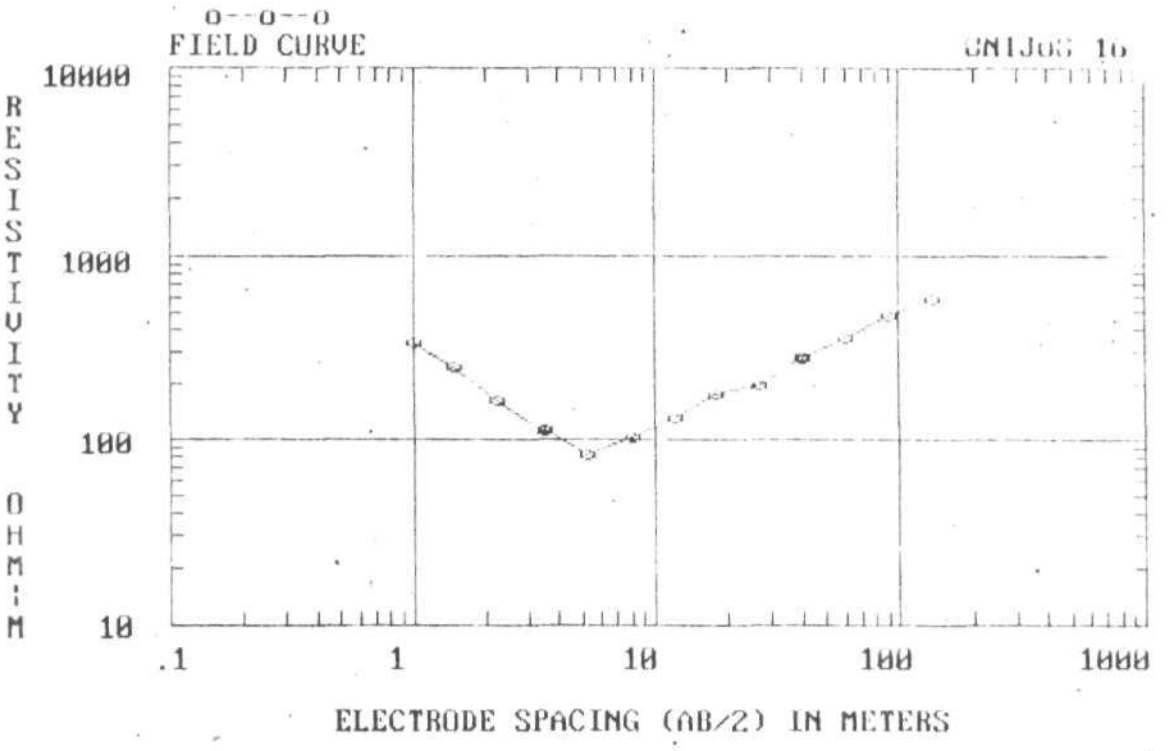

o o o
DIGITIZED
CALCULATED
UNIJOB 13
1000
100
10
1
.1
RESISTIVITY OHM-M
.1
1
10
100
1000
ELECTRODE SPACING (AB/2), OR DEPTH, IN METERS

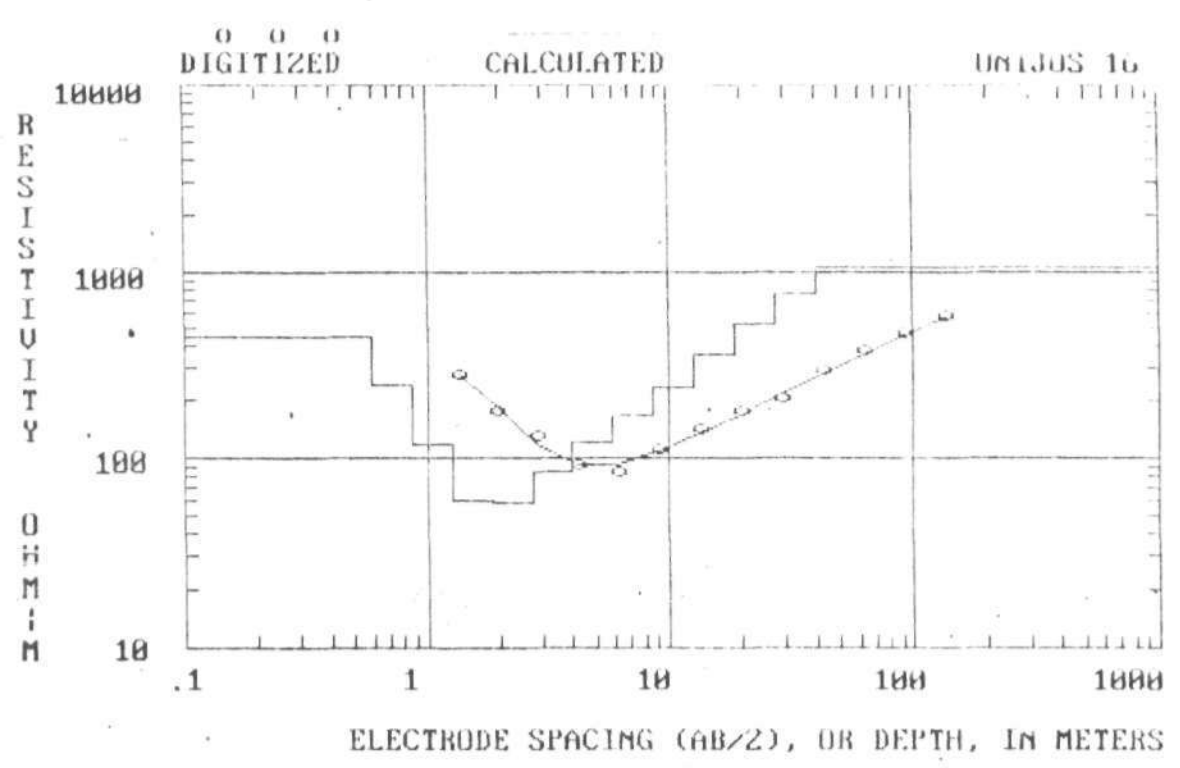

o--o--o
FIELD CURVE
UNIJOS 14
RESISTIVITY OHM-M
10000
1000
100
10
.1
1
10
100
1000
ELECTRODE SPACING (AB/2) IN METERS

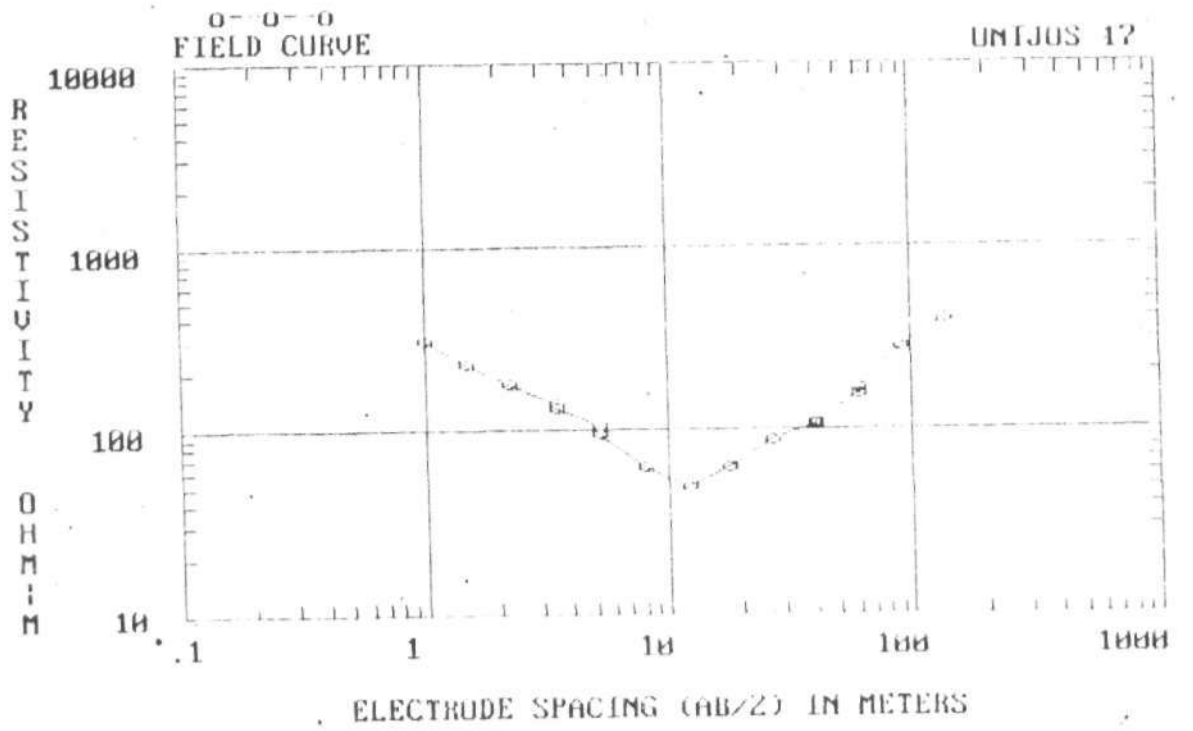

o o o
DIGITIZED
CALCULATED
UNIJOS 14
RESISTIVITY OHM-M
10000
1000
100
10
.1
1
10
100
1000
ELECTRODE SPACING (AB/2), OR DEPTH, IN METERS

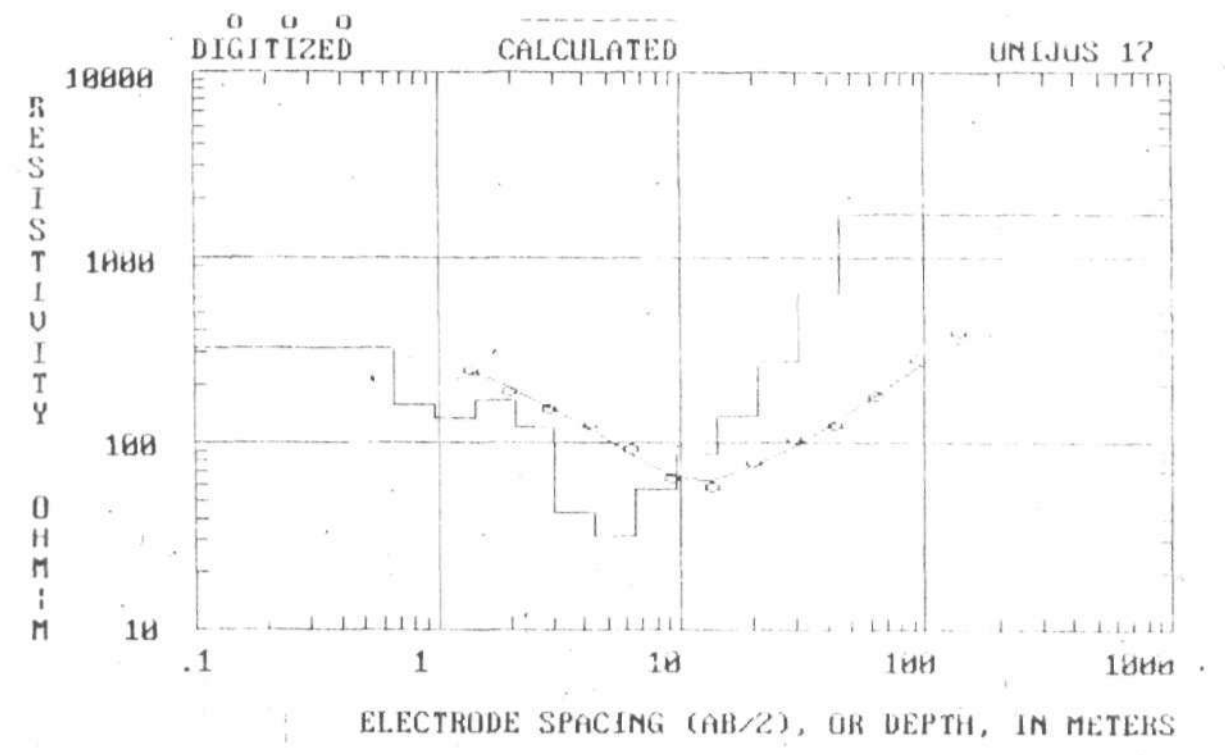

o--o--o
FIELD CURVE
UNIJOS 15
RESISTIVITY OHM-M
10000
1000
100
10
.1
1
10
100
1000
ELECTRODE SPACING (AB/2) IN METERS

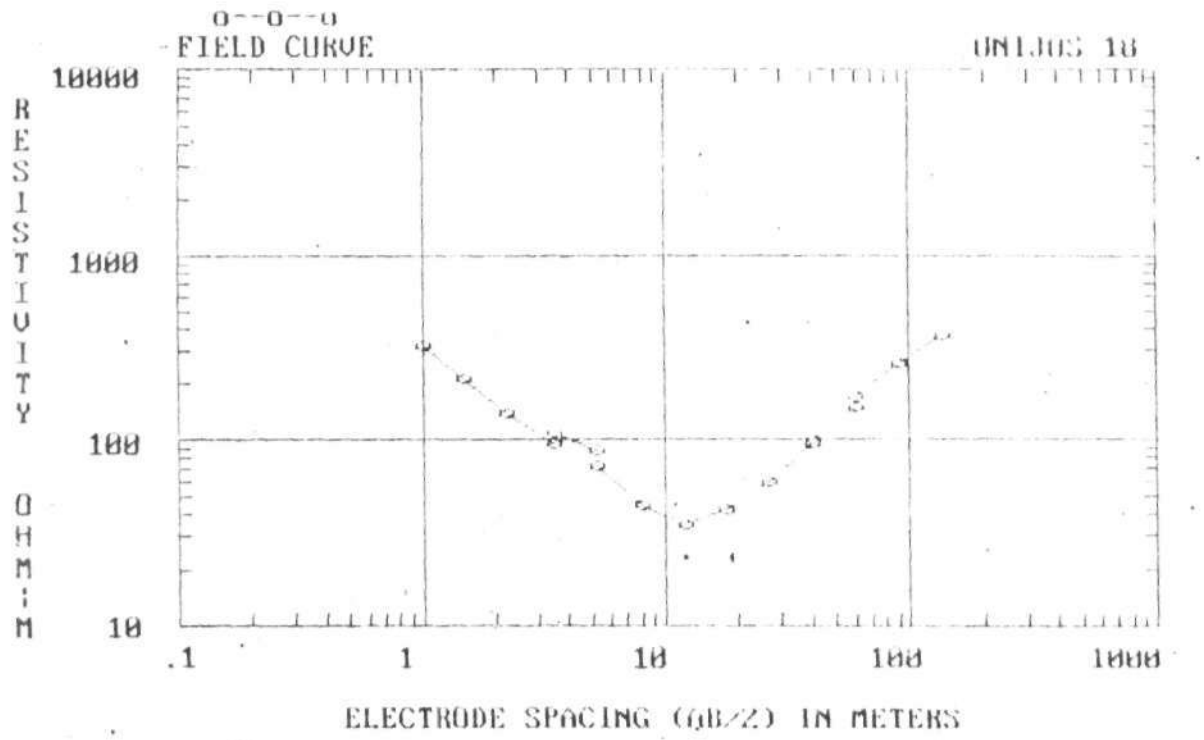

o o o
DIGITIZED
CALCULATED
UNIJOS 15
RESISTIVITY OHM-M
10000
1000
100
10
.1
1
10
100
1000
ELECTRODE SPACING (AB/2), OR DEPTH, IN METERS

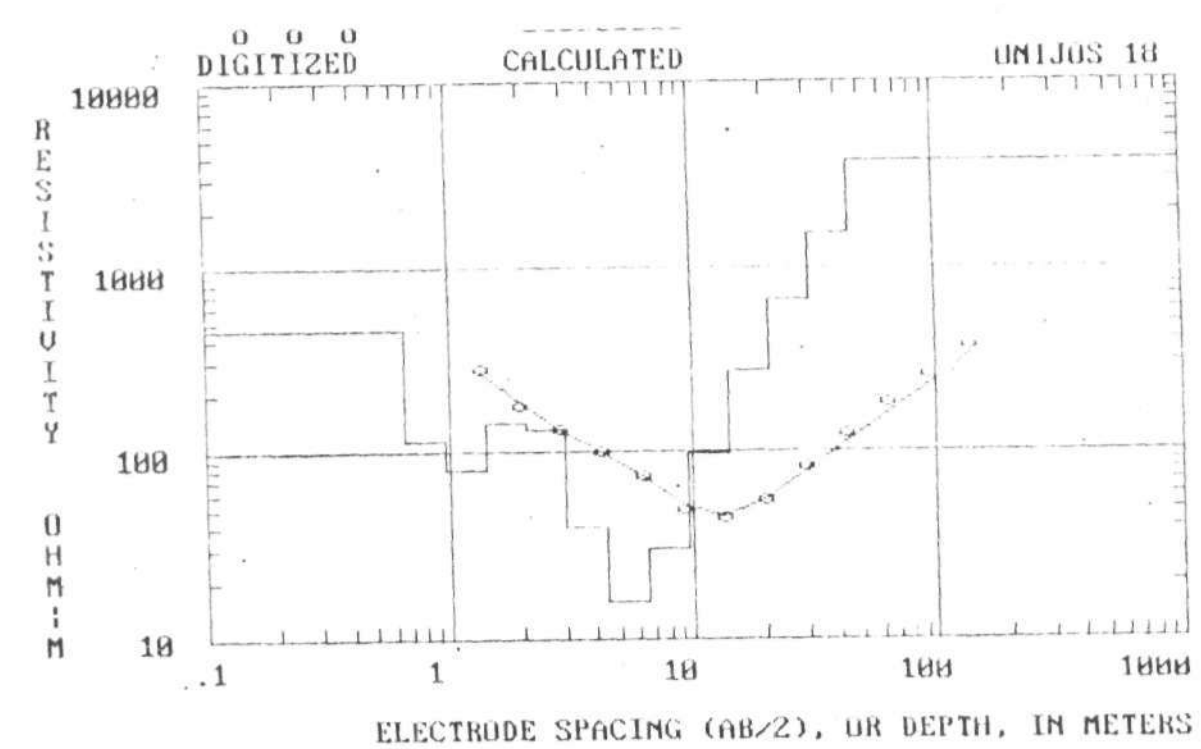

o--o--o
FIELD CURVE
UNIJOB 16
RESISTIVITY OHM-M
10000
1000
100
10
.1
1
10
100
1000
ELECTRODE SPACING (AB/2) IN METERS

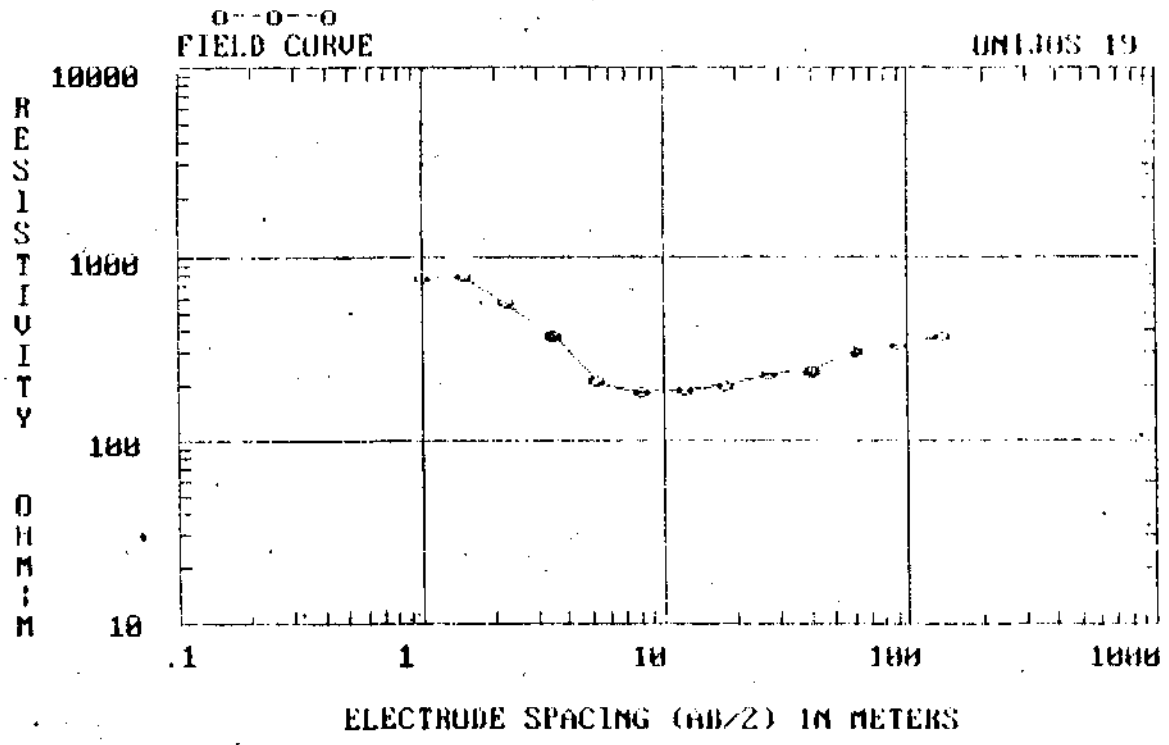

o o o
DIGITIZED
CALCULATED
UNIJOB 16
RESISTIVITY OHM-M
10000
1000
100
10
.1
1
10
100
1000
ELECTRODE SPACING (AB/2), OR DEPTH, IN METERS

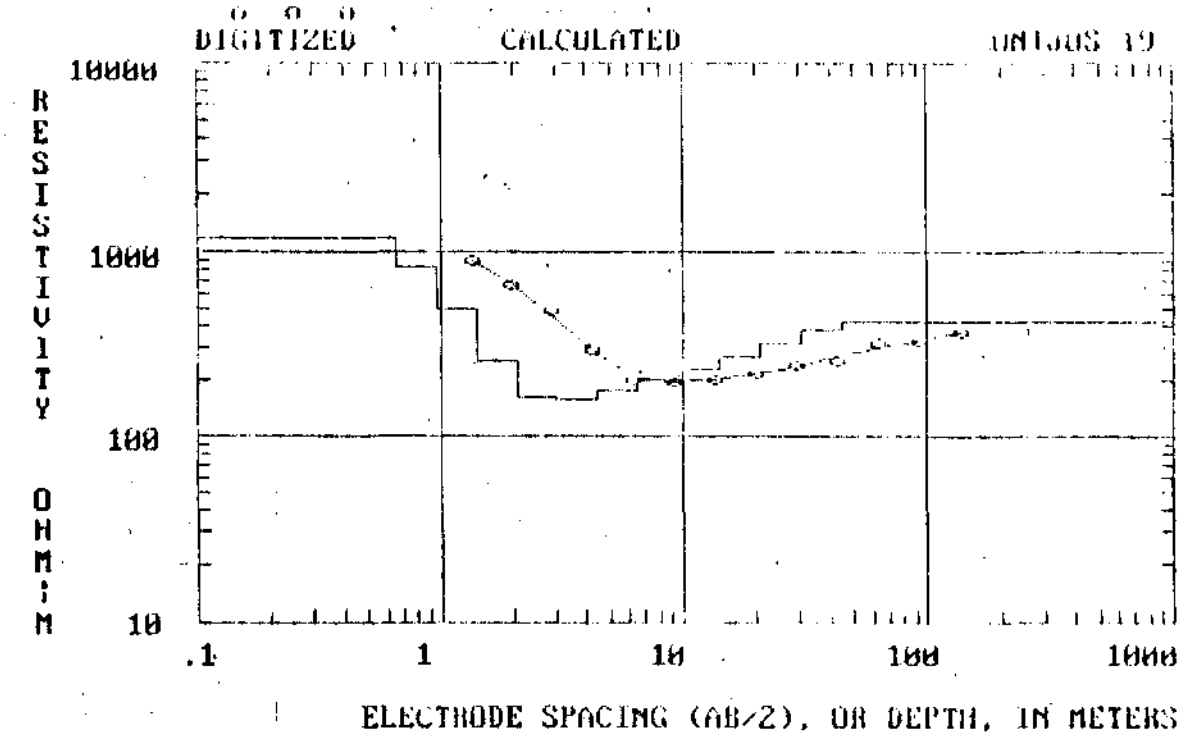

o- o- o
FIELD CURVE
UNIJUS 17
RESISTIVITY OHM-M
10000
1000
100
10
.1
1
10
100
1000
ELECTRODE SPACING (AB/2) IN METERS

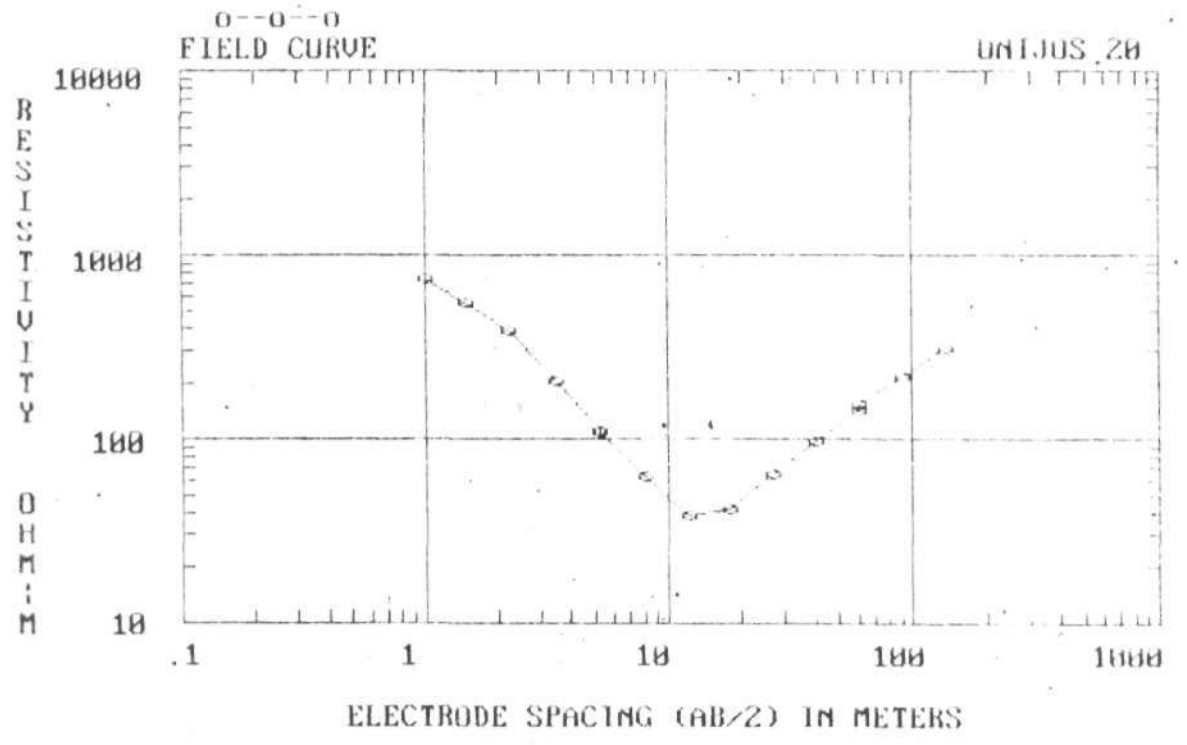

o o o
DIGITIZED
CALCULATED
UNIJUS 17
RESISTIVITY OHM-M
10000
1000
100
10
.1
1
10
100
1000
ELECTRODE SPACING (AB/2), OR DEPTH, IN METERS

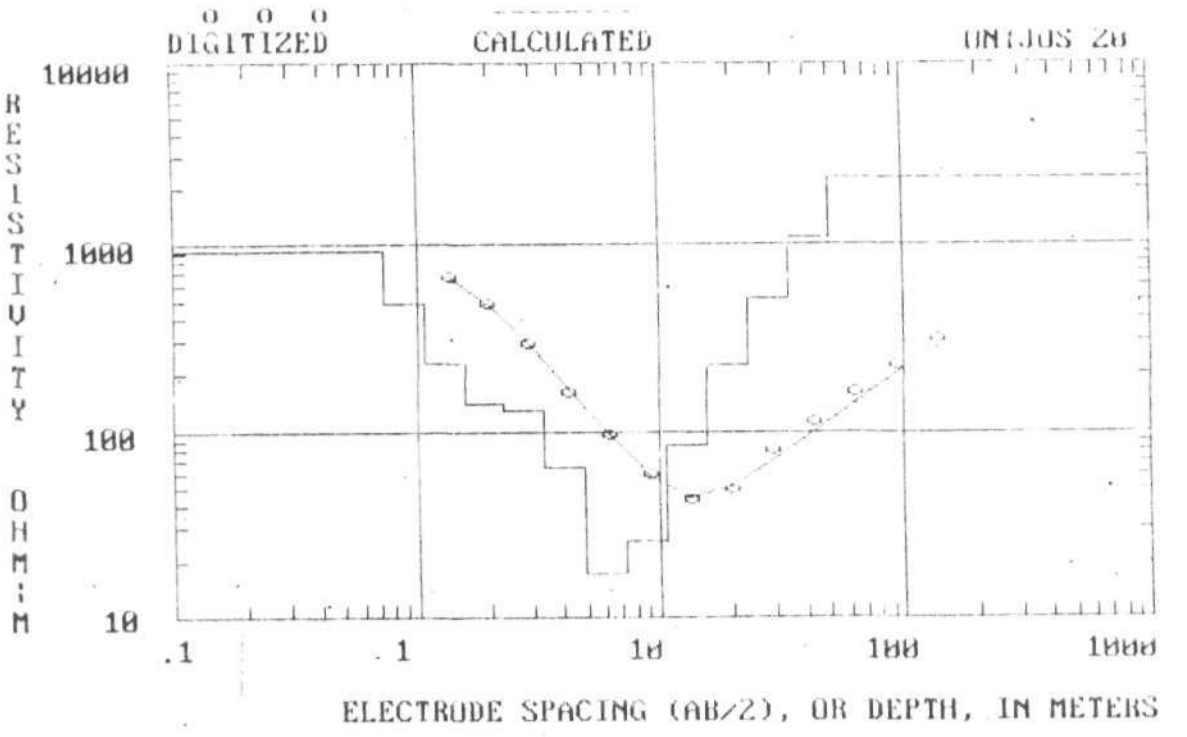

o--o--o
FIELD CURVE
UNIJOS 18
RESISTIVITY OHM-M
10000
1000
100
10
.1
1
10
100
1000
ELECTRODE SPACING (AB/2) IN METERS

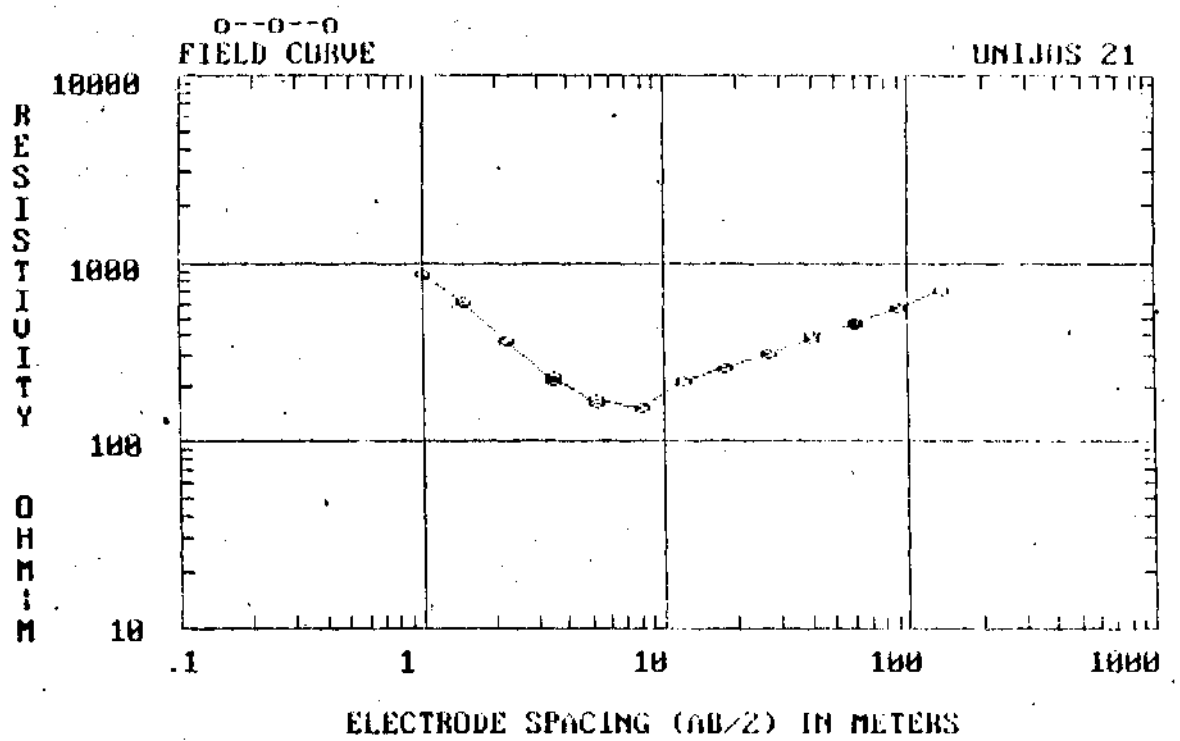

o o o
DIGITIZED
CALCULATED
UNIJOS 18
RESISTIVITY OHM-M
10000
1000
100
10
.1
1
10
100
1000
ELECTRODE SPACING (AB/2), OR DEPTH, IN METERS

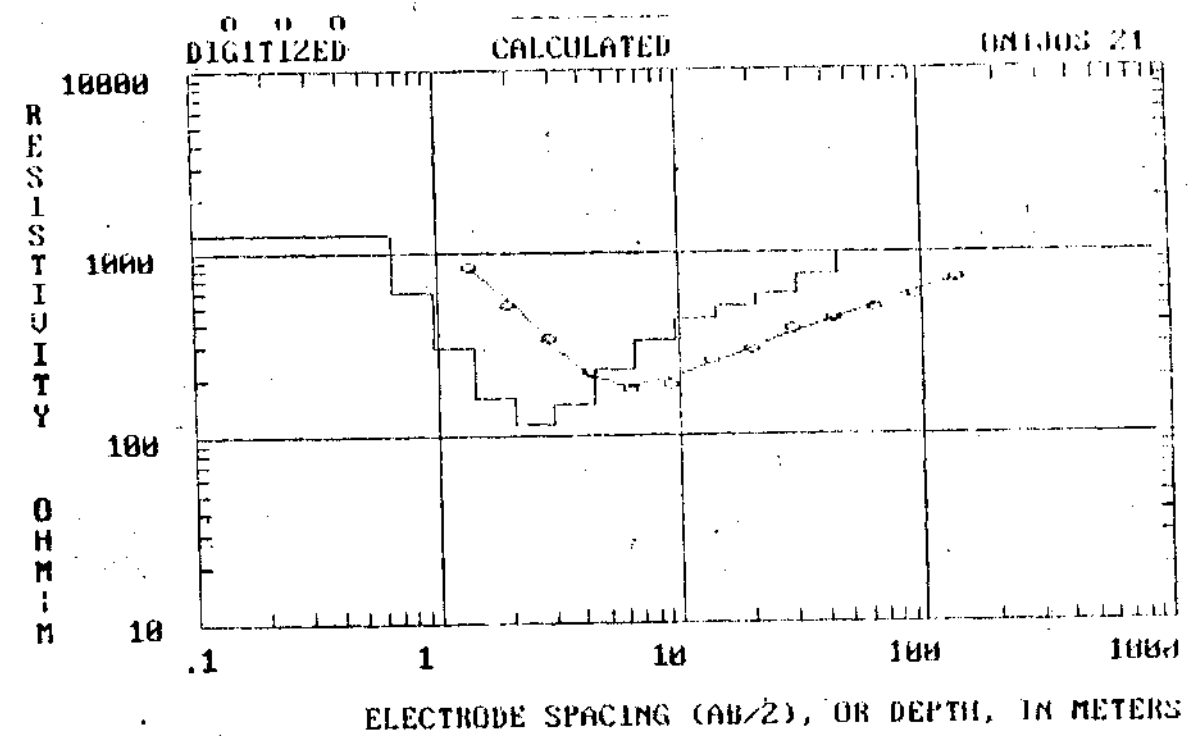

o--o--o
FIELD CURVE
UNIJOS 19
10000
1000
100
10
RESISTIVITY OHM-M
.1
1
10
100
1000
ELECTRODE SPACING (AB/2) IN METERS

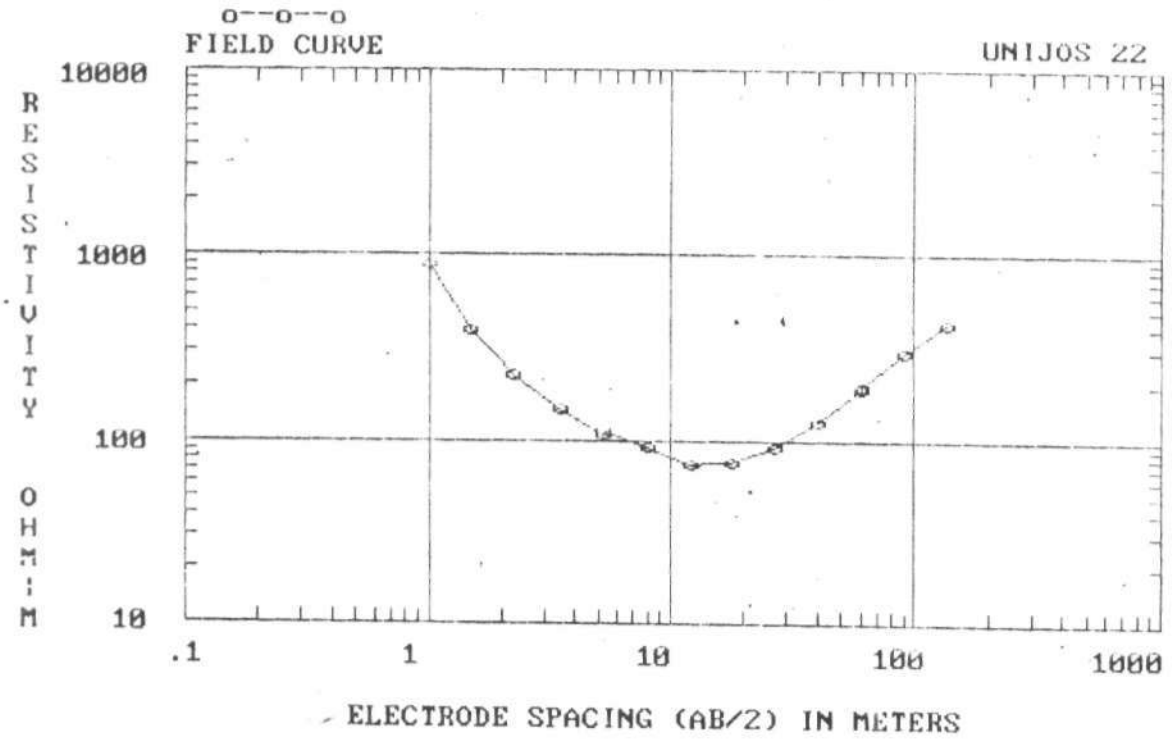

o o o
DIGITIZED
CALCULATED
UNIJOS 19
10000
1000
100
10
RESISTIVITY OHM-M
.1
1
10
100
1000
ELECTRODE SPACING (AB/2), OR DEPTH, IN METERS

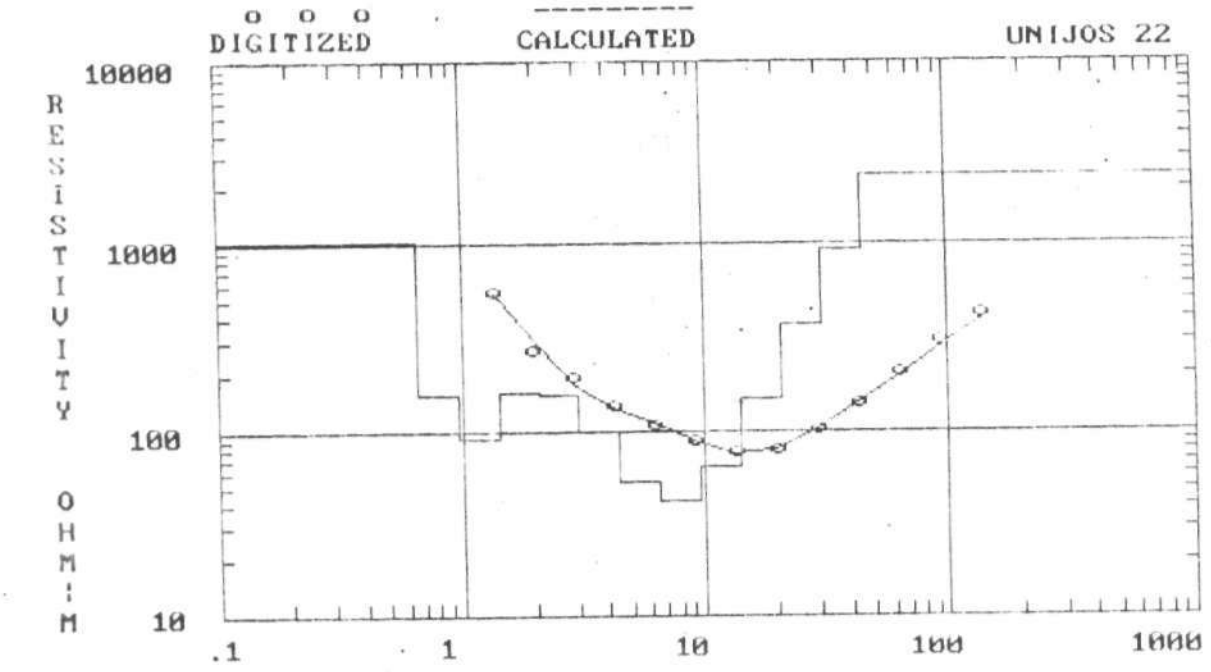

o--o--o
FIELD CURVE
UNIJOS 20
10000
1000
100
10
RESISTIVITY OHM-M
.1
1
10
100
1000
ELECTRODE SPACING (AB/2) IN METERS

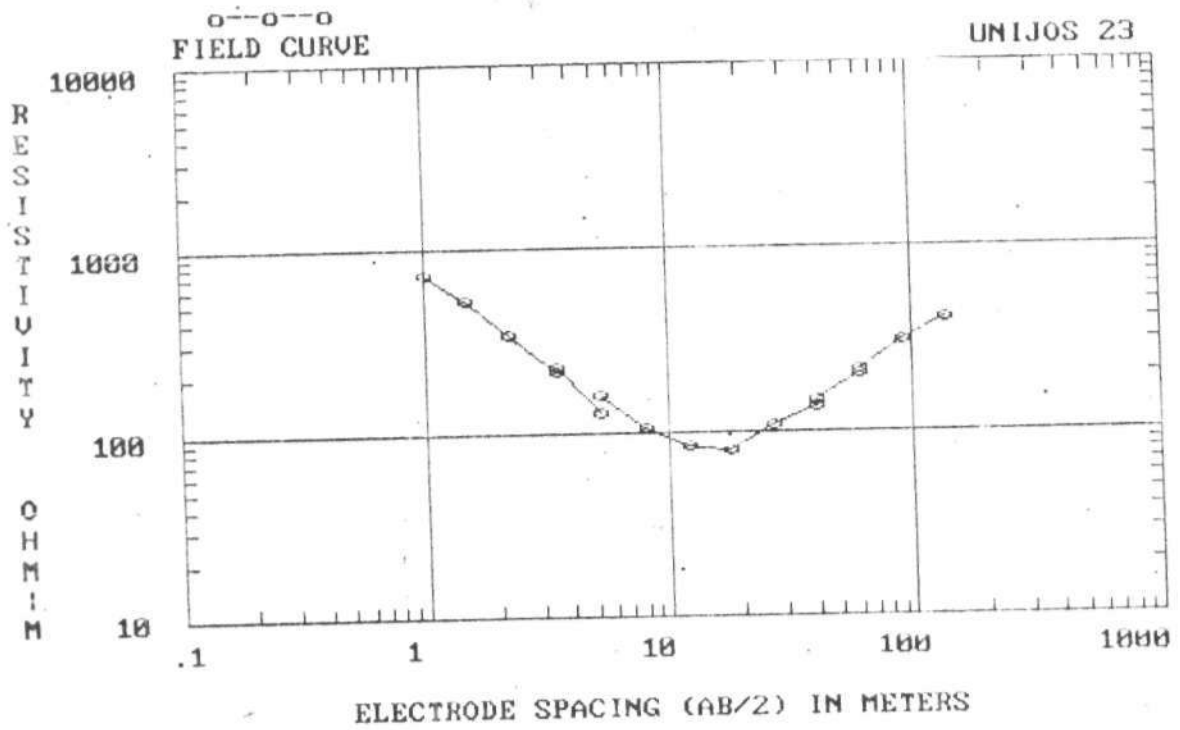

o o o
DIGITIZED
CALCULATED
UNIJOS 20
10000
1000
100
10
RESISTIVITY OHM-M
.1
1
10
100
1000
ELECTRODE SPACING (AB/2), OR DEPTH, IN METERS

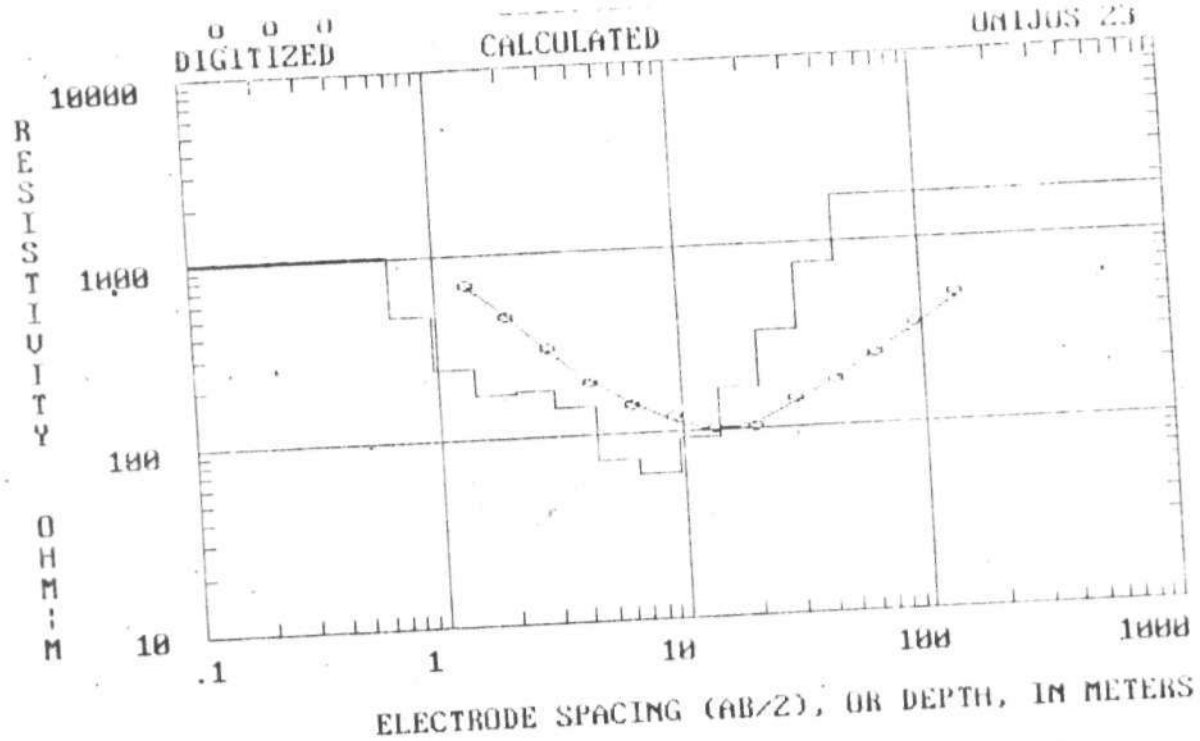

o--o--o
FIELD CURVE
UNIJOS 21
10000
1000
100
10
RESISTIVITY OHM-M
.1
1
10
100
1000
ELECTRODE SPACING (AB/2) IN METERS

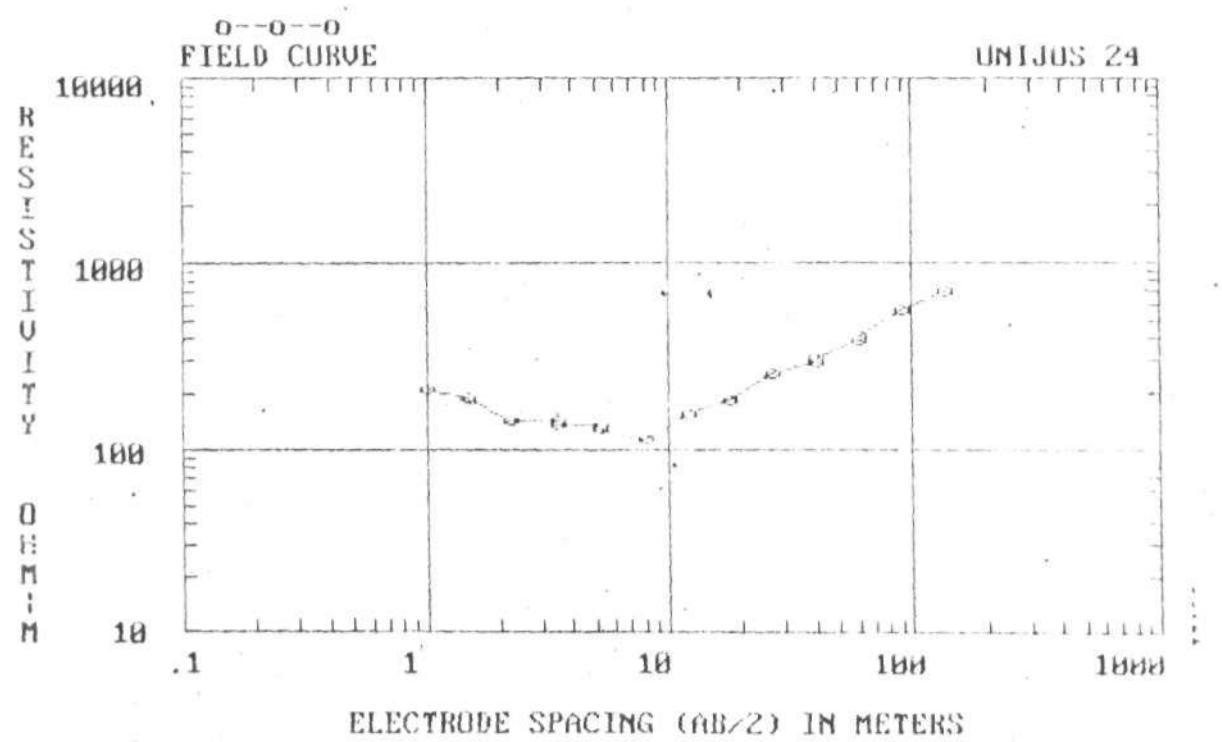

o o o
DIGITIZED
CALCULATED
UNIJOS 21
10000
1000
100
10
RESISTIVITY OHM-M
.1
1
10
100
1000
ELECTRODE SPACING (AB/2), OR DEPTH, IN METERS

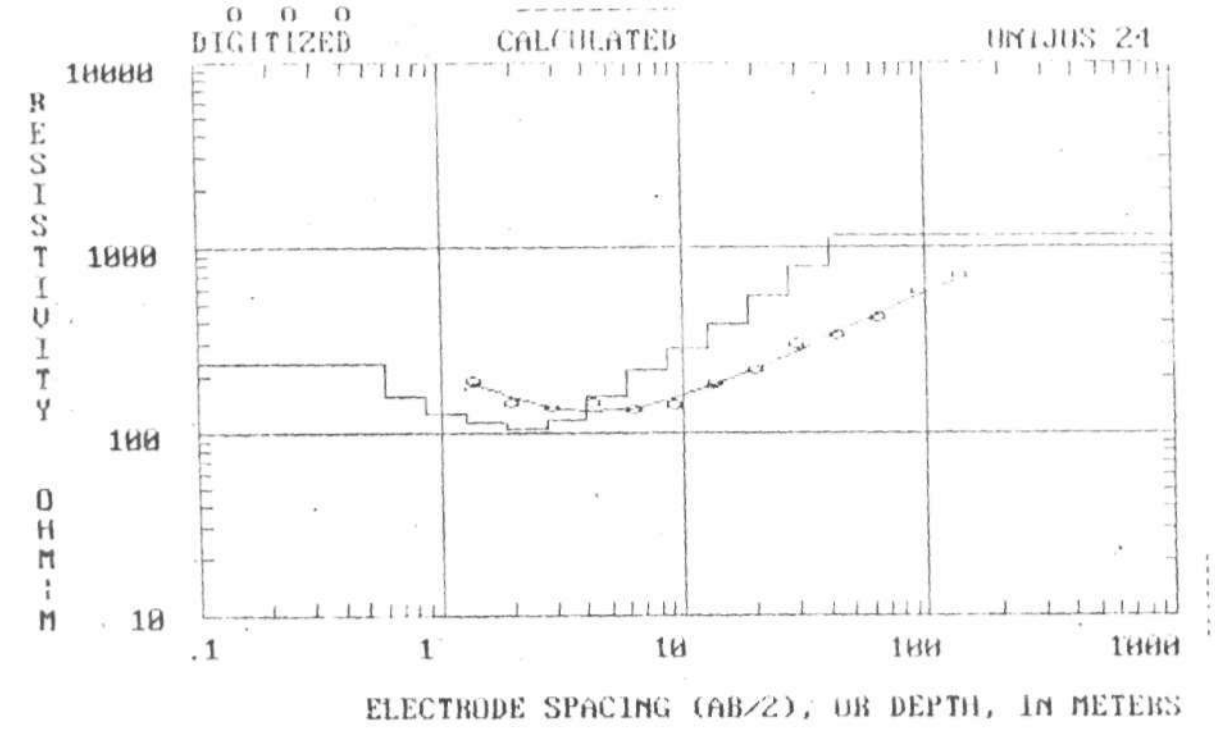

o--o--o
FIELD CURVE
UNIJOS 22
RESISTIVITY OHM-M
10000
1000
100
10
.1
1
10
100
1000
ELECTRODE SPACING (AB/2) IN METERS

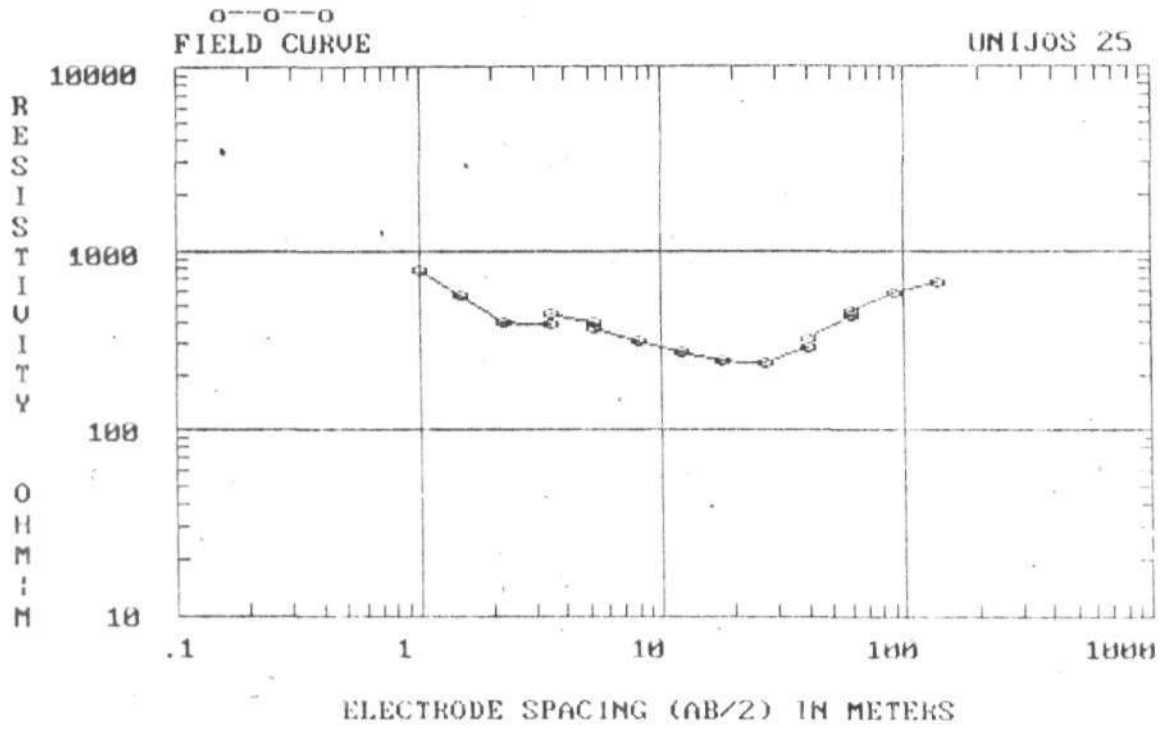

o o o
DIGITIZED
CALCULATED
UNIJOS 22
RESISTIVITY OHM-M
10000
1000
100
10
.1
1
10
100
1000
ELECTRODE SPACING (AB/2), OR DEPTH, IN METERS

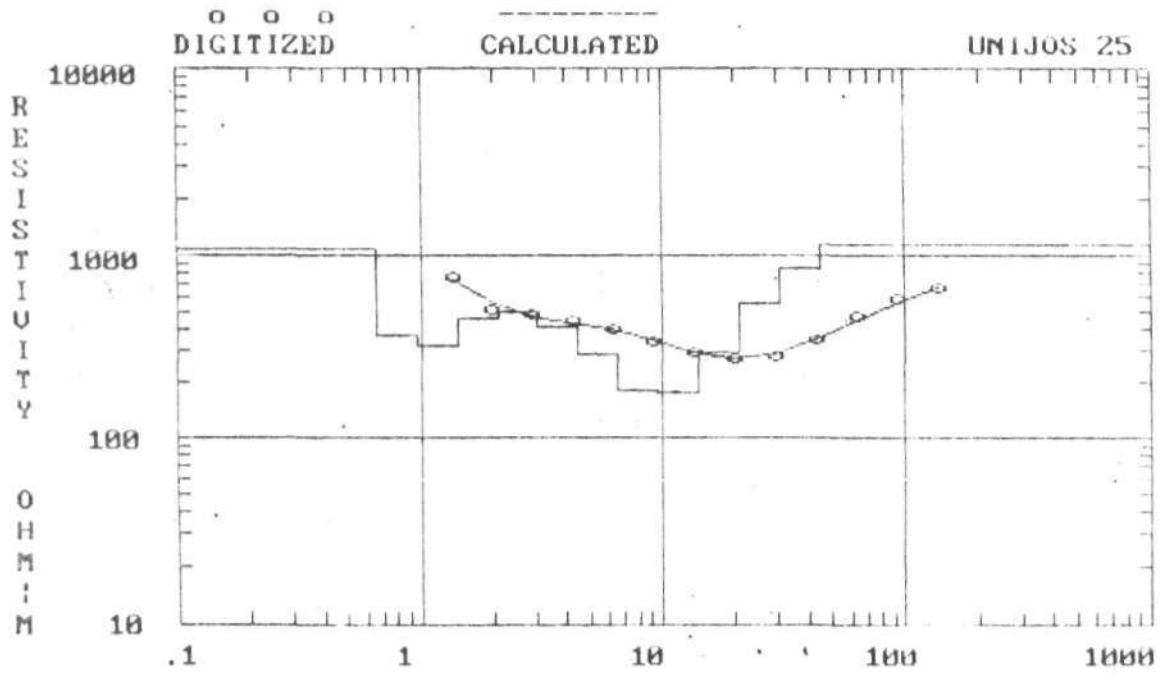

o--o--o
FIELD CURVE
UNIJOS 23
10000
1000
100
10
RESISTIVITY OHM:M
.1
1
10
100
1000
ELECTRODE SPACING (AB/2) IN METERS

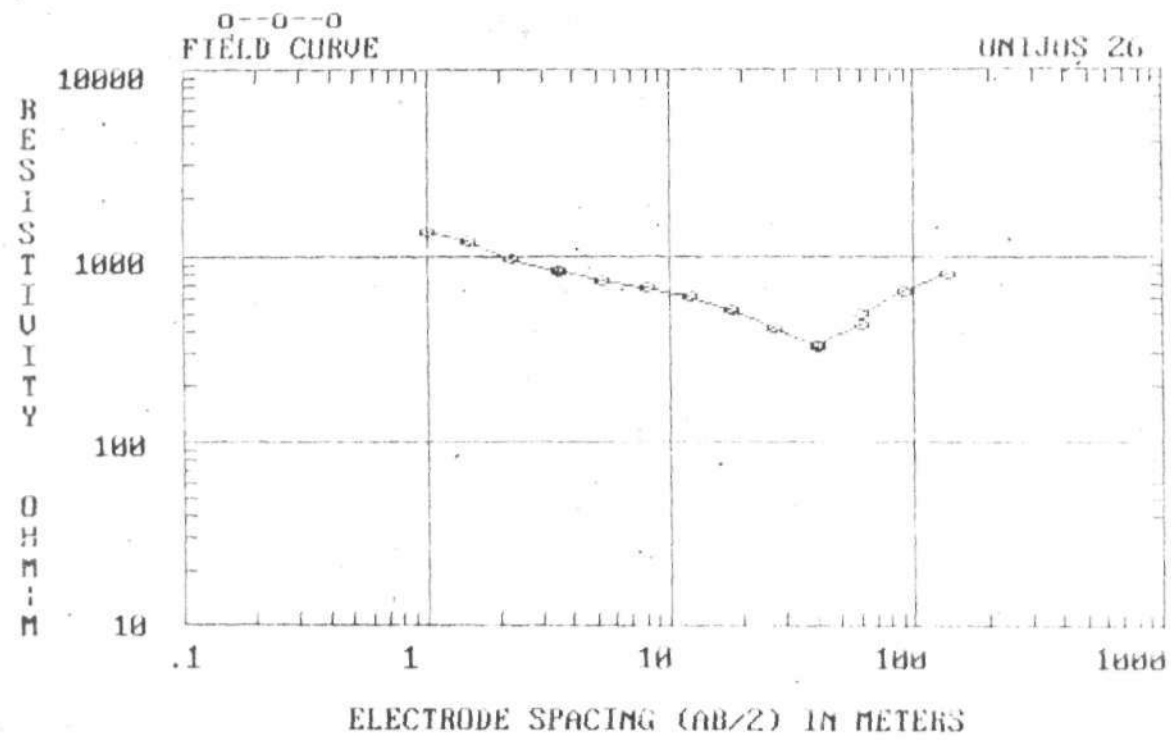

o o o
DIGITIZED
CALCULATED
UNIJOS 23
10000
1000
100
10
RESISTIVITY OHM:M
.1
1
10
100
1000
ELECTRODE SPACING (AB/2), OR DEPTH, IN METERS

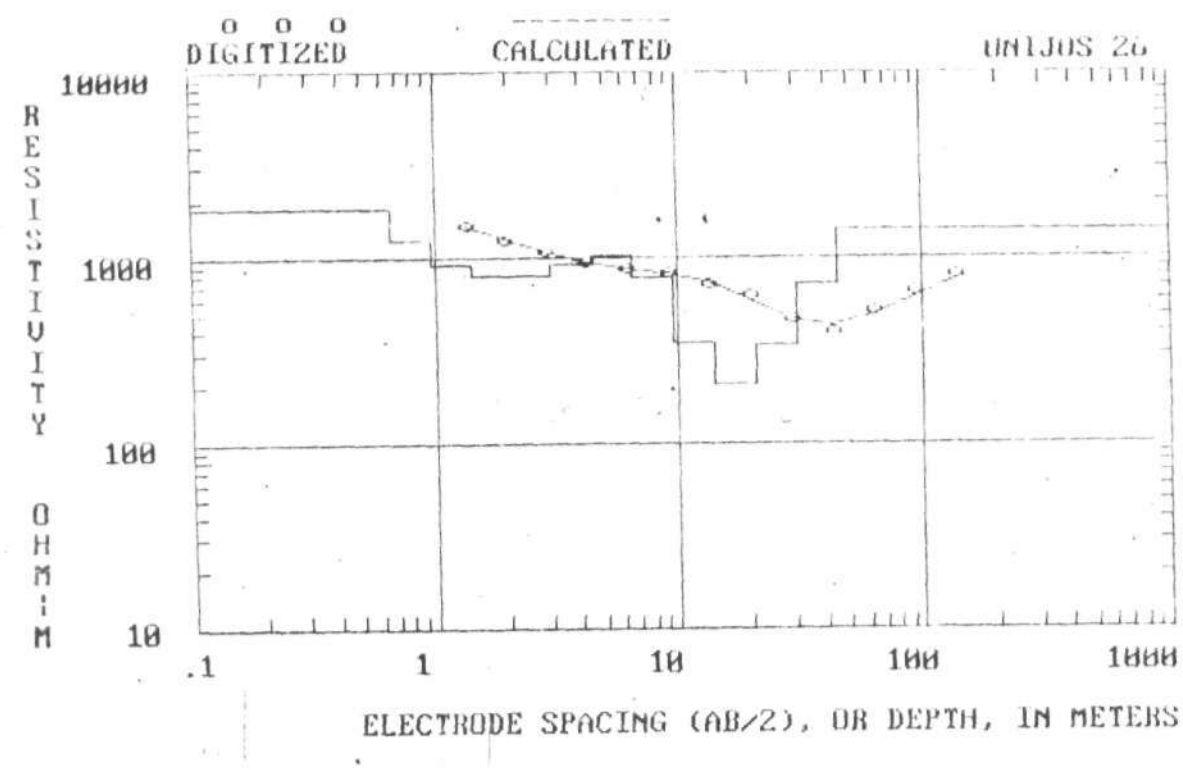

o--o--o
FIELD CURVE
UNIJOS 24
RESISTIVITY OHM-M
10000
1000
100
10
.1
1
10
100
1000
ELECTRODE SPACING (AB/2) IN METERS


o o o
DIGITIZED
CALCULATED
UNIJOS 24
RESISTIVITY OHM-M
10000
1000
100
10
.1
1
10
100
1000
ELECTRODE SPACING (AB/2), OR DEPTH, IN METERS


o--o--o
FIELD CURVE
UNIJOS 25
RESISTIVITY OHM-M
10000
1000
100
10
.1
1
10
100
1000
ELECTRODE SPACING (AB/2) IN METERS


o o o
DIGITIZED
CALCULATED
UNIJOS 25
RESISTIVITY OHM-M
10000
1000
100
10
.1
1
10
100
1000
ELECTRODE SPACING (AB/2), OR DEPTH, IN METERS


o--o--o
FIELD CURVE
UNIJOS 26
10000
1000
100
10
RESISTIVITY OHM-M
.1
1
10
100
1000
ELECTRODE SPACING (AB/2) IN METERS


o o o
DIGITIZED
CALCULATED
UNIJOS 26
10000
1000
100
10
RESISTIVITY OHM-M
.1
1
10
100
1000
ELECTRODE SPACING (AB/2), OR DEPTH, IN METERS